https://doi.org/10.1070/RCR5032

Topological methods for analysis and design of coordination polymers

Eugeny V. Alexandrov, Alexander P. Shevchenko, Nadezhda A. Nekrasova, Vladislav A. Blatov

Samara State Technical University,
ul. Molodogvardeyskaya 244, 443011 Samara, Russian Federation

A comprehensive review of the methods for topological analysis of crystalline compounds as applied to the structures of coordination polymers is presented for the first time. The basic concepts of reticular chemistry, a new branch of science, which combines methods of synthetic chemistry with methods for topological design of polymer compounds, are considered. Reticular chemistry methods are illustrated with examples of the analysis and design of coordination polymers. The most complete classification of coordination polymers, which are similar in terms of various compositional and topological parameters, is given. This review describes and integrates information on the topological analysis tools, such as computer software and electronic databases. A special attention is paid to the application of topological methods in the machine analysis and the prediction of structures and properties of coordination polymers, in particular to the establishment of chemical composition – structure – property relationships and the development of knowledge bases and artificial intelligence systems. A procedure for the search for the general crystal-chemical features using automatic heuristic analysis of large sets of structural data is discussed. It is shown how this analysis can be used to determine the limits of applicability of reticular chemistry and the possibility of its extension to coordination polymers containing structurally, chemically and topologically complex building units with high conformational flexibility. Approaches of reticular chemistry are considered in detail in relation to the design of proton-conductive coordination polymers, which have received considerable attention in the past decade. The specific features of the topological structures of this class of compounds are described in a systematic way. The relationships between the chemical composition, structure and conductive properties of these compounds and the applicability of targeted design are discussed.
The bibliography includes 303 references.

Contents

1. Introduction 1
2. Terminology, methods and tools of reticular chemistry 3
2.1. Terminology of periodic chemical graphs 3
2.2. Topological structure simplification 4
2.3. Isoreticular series, topological isomerism, polymorphism, reconstruction and relationship 5
2.4. Computer programs for topological analysis 7
2.5. Topological databases 8
2.6. Topological descriptors, knowledge bases and elements of artificial intelligence 10
3. Topological structural patterns of coordination polymers 12
3.1. Classification of topological motifs 12
3.1.1. Framework coordination polymers 12
3.1.2. Layered coordination polymers 13
3.1.3. Chain coordination polymers 14
3.2. Relationships between local and overall topology 14
3.3. Composition – topology – property relationships 15
3.3.1. Porosity 15
3.3.2. Mechanical properties 16
3.3.3. Proton conductivity 16
4. Reticular design 18
4.1. Topological design principles 19
4.1.1. Decoration and expansion of the underlying net 19
4.1.2. Principles for the selection of building units for decoration 19
4.1.3. Reconstruction 20
4.2. Examples of the design of coordination polymers and metal-organic frameworks 20
4.2.1. Design of coordination polymers and metal-organic frameworks with a given network topology 20
4.2.2. Design of proton-conducting metal-organic frameworks 22
5. Conclusion 25
6. List of abbreviations and designations 25
7. References 25

1. Introduction

In the 21st century, the design of new chemical compounds and materials was no longer a prerogative of synthetic chemists. The mathematical modeling by quantum chemical calculations, molecular dynamics simulations and the Monte-Carlo method enables high-precision calculations of the structures and properties of hypothetical compounds and the prediction of the conditions of their synthesis.[1] However, the concept of chemical bonding is either ignored or used in a restricted way in all these approaches, and the conclusions about the stability and properties of compounds are drawn by solving systems of equations for an ensemble of atoms in a certain model force field. This drawback is particularly severe in studies of crystalline compounds. Until recently, structural chemistry, which

Received 3 July 2021
© 2022 Uspekhi Khimii, ZIOC RAS, Russian Academy of Sciences and IOP Publishing Limited

proved to be efficient in the description of molecules and molecular complexes, was rarely used as a tool for considering the complete crystal structures and the latter were represented as their fragments or structural groups (local coordination of atoms, molecules or clusters). Crystal-chemical models, such as hard-sphere close-packing models,[2] cation templates[3] or molecular packing models,[4] based on the analysis of the arrangement of atoms and so-called building units (blocks) in space are also used to analyze only the direct binding in terms of coordination, or contact, numbers. This limitation was due to the difficulties of description of infinite periodic systems of chemical bonds, the lack of a relevant theory, which is still under development, and the lack of software, which is required to perform the full analysis of complex structures.

The treatment of chemical bonding inevitably leads to the concept of topology of crystal structures. Therefore, topological methods can be considered as a reasonable chemical supplement to physical-based modeling of rigid-body systems. Modern program packages for the topological description allow the visualization and analysis of objects of any complexity in a short time. However, the topological description makes it possible to draw conclusions only at a qualitative or semiquantitative level, while a combination of this approach with mathematical modeling methods is required for accurate calculations of the crystal properties. Such hybrid methods bring together the advantages of both approaches and are extensively used.[5]

Recent years have witnessed rapid progress in the application of elements of artificial intelligence systems (machine learning methods, neural networks, knowledge-based systems, *etc*.) for the development of prediction systems in materials science and for the search for composition–structure–property relationships.[6] An important prerequisite for further progress in this line of research is the development of a system of descriptors, which characterize the chemical composition, specific features of the crystal structure and structural factors having an effect on the physical properties of crystals.[7] Local (at a level of the nearest environment of atoms and structural groups) and global (at a level of the periodic atomic net or lattice) geometric and topological parameters of the crystal structure comprise a significant part of these descriptors. It should be noted that the geometric descriptors, such as the length of the interatomic contact, the shape of the coordination polyhedron or the symmetry of the crystal lattice, have long been widely employed, while the topological descriptors (except for the coordination number) are still of limited application. The concept of the atomic net topology was introduced by Wells in a series of studies, dating from 1954[8] and culminated in the fundamental monograph,[9] in which the author suggested the first extensive topological classification of crystal structures. Meanwhile, other authors very rarely used topological approaches for about half a century (an example is the classification of atomic nets in intermetallic compounds[10]).

A rapid progress in the development of topological approaches was associated with the appearance of new objects, the structure and properties of which significantly depend on the overall connectivity of atomic nets of crystals. These objects were metal-organic coordination polymers (MOCPs). The systematic studies of MOCPs started in the mid-1990s.[11] Currently, these compounds are considered as one of the most promising classes of materials of the future.[12–16] Metal-organic coordination polymers are composed of inorganic (metal atoms or clusters) and organic (polydentate ligands) building units, which can be connected in numerous ways to form a virtually infinite set of topologically different architectures. In practical terms, the unique property of MOCPs is their record-high specific surface area of pores (up to 10 000 $m^2\ g^{-1}$) and outstanding adsorption properties of representatives of their important subclass — metal-organic frameworks. Besides, depending on the chemical composition, MOCPs can have unusual catalytic,[17,18] ion-exchange,[19–21] magnetic,[22–24] optical[25–27] and mechanical properties,[28,29] ionic[30–34] and electronic conductivity,[35,36] sensing activity.[37,38] The structures and properties of MOCPs can be varied as desired in a wide range by selecting appropriate inorganic and organic components, which are connected according to a certain topological motif, to form pores of a particular size. When applying this approach, it is important to have an idea of available building units and possible motifs of their assembly.

From a theoretical point of view, coordination polymers are also of interest due to the pronounced dependence of their properties on the structural features, primarily, on the mode of connection of building units (complexing atoms, ligands, clusters and polynuclear complex groups), *i.e*., on the topological properties of the polymer motif. Therefore, MOCPs served as the main testing ground for developing a topological approach in the crystal chemistry and materials science. Efforts of theorists and experimenters made in the past two decades resulted in the emergence of a new field of chemical science — reticular chemistry. This field of science focuses on the topological properties of polymeric periodic atomic motifs. In the past decade, methods of reticular chemistry have been greatly responsible for a rapid increase in the number of the synthesized MOCPs with specified structure and properties.

This review covers the topological methods of reticular chemistry, in particular in combination with mathematical modeling and machine analysis of data, which are used for the description and prediction of the structures and properties of MOCPs.

E.V.Alexandrov. Ph.D. in Chemistry, Assistant Professor at the Department of General and Inorganic Chemistry of the SamSTU.
E-mail: aleksandrov_ev1@mail.ru
Current research interests: crystal chemistry, coordination polymers, metal-organic frameworks, topological analysis.
A.P.Shevchenko. Ph.D. in Chemistry, Senior Researcher at the Samara Center for Theoretical Materials Science of the SamSTU.
E-mail: allex.shevchenko@gmail.com
Current research interests: coordination chemistry, theoretical crystal chemistry, storage of information in databases, intelligent data analysis, machine learning algorithms.
N.A.Nekrasova. Ph.D. in Chemistry, Junior Researcher at the same Research Center.
E-mail: nkrsvn@gmail.com
Current research interests: high-performance liquid chromatography, quantitative structure — activity, structure–property and structure–chromatographic retention relationship analysis, quantum chemical modeling of adsorption processes.
V.A. Blatov. Doctor of Chemical Sciences, Professor, Head of the Department of General and Inorganic Chemistry of the SamSTU.
E-mail: blatov@topospro.com
Current research interests: theoretical crystal chemistry, mathematical modeling in chemistry and materials science, information systems in materials science.

Translation: T.N.Safonova

2. Terminology, methods and tools of reticular chemistry

2.1. Terminology of periodic chemical graphs

In chemistry, the topology means the connectivity in atomic structures. However, this definition is too broad, and it is not always clear what exactly is meant by the 'topology of the structure', 'topological similarity', 'topological properties', *etc*. More strictly, the topology of an ensemble of N connected atoms is described by a graph, *i.e.*, a set of vertices (or nodes) $x_1, \ldots x_N$ and edges that connect pairs of vertices (x_i, x_j). Chemists widely employed graphs for the description of molecular structures; however, periodic systems of atoms in crystals are formally infinite, and special mathematical tools are required for their characterization. A brief summary of the terms, which are used in the review, is given below. A more detailed description of the nomenclature of periodic graphs is presented in the publication.[39]

In reticular chemistry, simple (chemical) graphs are considered. The edges of these graphs are not oriented, *i.e.* $(x_i, x_j) = (x_j, x_i)$, and the vertices do not have loops, *i.e.*, edges with $x_i = x_j$ are absent. A sequence of vertices is called a *chain*, and a closed chain is called a *cycle*. Cycles, which cannot be represented by the sum of any two smaller cycles, are called *rings*. Rings, which cannot be represented as the sum of any number of smaller rings (not only of two rings), are called *strong rings* (Fig. 1). A graph is said to be connected if every pair of vertices in the graph is connected at least by one chain. A periodic (infinite, having a periodic symmetry) connected simple graph is called a *net*. A *coordination number* (degree) of the vertex of the net is equal to the number of vertices incident to this vertex, *i.e.*, those sharing edges with the latter; these vertices form a geometric body — a *coordination figure* of the net. Two nets are *isomorphic* (have the same topology, belong to one *topological type*) if they can be superimposed without changes in the set of vertices and edges. All isomorphic permutations of vertices of the net, *i.e.*, permutations giving rise to isomorphic nets, form an *automorphism group* that characterizes the symmetry of the net. An *embedding of a net* is a realization in space, in which coordinates can be assigned to each vertex. The symmetry of the embedding is always lower or equal to the maximum symmetry of the net determined by its automorphism group. The symmetry of the embedding of the net in the Euclidean space is described by one of the space symmetry groups G; the embeddings with the maximum possible symmetry G_{max} are of particular interest because the symmetry groups of any lower-symmetry embeddings are subgroups of G_{max}. The net, the symmetry G_{max} of which is isomorphic to its automorphism group, is called *crystallographic*; otherwise, G_{max} is a subgroup in the automorphism group of the net and, consequently, the net cannot be realized in the Euclidean space with the maximum possible symmetry. These nets are referred to as noncrystallographic.[40] An n-dimensional net should be distinguished from an n-periodic net, although these concepts are often confused. An n-dimensional net allows the embedding without self-intersections in the n-dimensional space, but not in a lower-dimensional space. An *n-periodic net* has a translational symmetry exactly in n independent directions. In other words, the net dimensionality can be higher than the net periodicity. For example, a complex polynuclear cluster is a 3D net, but its periodicity is equal to zero.

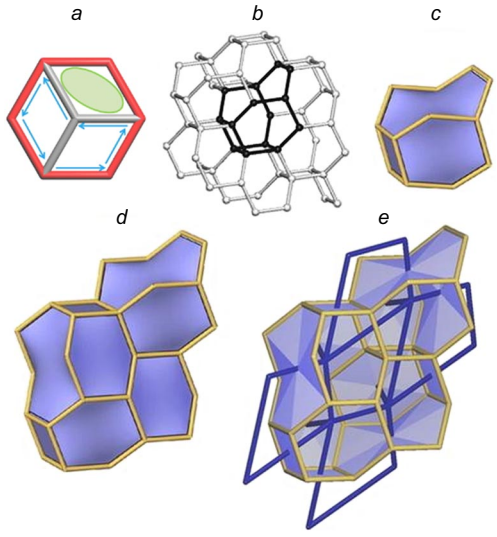


Figure 1. Tools of reticular chemistry: (*a*) examples of a strong ring (rhombus indicated by a green oval), a cycle, which is not a ring and is the sum of two strong rings (indicated by blue arrows), a ring, which is not strong and which is the sum of three strong rings (red hexagon); (*b*) a net with a highlighted natural tile; (*c*) the tile; (*d*) the natural tiling constructed for this net; *e*, the natural tiling and the correpsonding dual net (indicated by blue lines). The Figure was prepared by the authors using original data from the study.[39]

The above formal properties of the nets allow one to draw nontrivial conclusions about the structural features of crystalline compounds. Thus, the maximum-symmetry embedding of the net with a diamondoid topology has cubic symmetry (sp. gr. $Fd\bar{3}m$ corresponding to the symmetry of diamond). In particular, this fact is evidence that it is impossible to generate the diamondoid topology in hexagonal symmetry as well as with square coordination figures instead of tetrahedral ones because the symmetry groups corresponding to such embeddings are not subgroups of $Fd\bar{3}m$.[41] Strong rings are cross-sections of channels in the atomic net and are important for the analysis of the free space of the crystal. In particular, strong rings confine so-called *natural tiles*, which are polyhedral cages corresponding to the smallest cavities in the structure.[42] Natural tiles, adjoining each other through common faces (strong rings), fill the whole space of the crystal to form a *natural tiling*. If one connects the centres of tiles by edges passing through the adjoining faces, the resulting dual net will describe the topology of the free space in the crystal (see Fig. 1).

If the topology of the atomic net is identical to that of the dual net, the atomic net is referred to as *self-dual*. The atomic and dual nets do not intersect but become entangled, presenting an example of the entanglement of nets. In the general case, two (or more) nets are entangled if they do not have common nodes and edges but cannot be separated without breaking the edges in this embedding. If a system of entangled nets has the same periodicity as the nets themselves, the system is *interpenetrated*; if the periodicity of the system of entangled nets is higher than the periodicity of the individual net in the system, this system is *polycatenated*.

The polycatenation can be *parallel* or *inclined*, when entangled groups have the same or different spatial orientations, respectively.[43] The number of polycatenated nets is always infinite, which is responsible for an increase in the periodicity of the array of entangled nets. The number of

interpenetrating nets is, on the contrary, always finite and is referred to as the *degree of interpenetration*. Evidently, the polycatenation is possible only for 1- and 2-periodic nets, whereas the interpenetration is possible for nets of any periodicity. Self-dual nets play a great role in the interpenetration because the second atomic net can be located in the cavities of the first net, completely repeating it. For a long time, only the type of entanglement (interpenetration or polycatenation) and the number of entangled motifs were determined; only after the development of appropriate program packages, it became possible (see Section 2.4) to determine the geometric classes of entanglement depending on the symmetry of interpenetrated frameworks [44] and the topological types of entanglement.[45]

The special term *ring nets* was introduced to determine the topological types of entanglement. In the ring nets, the centroids of the rings of the initial (atomic or underlying) net serve as the nodes, and the edges connect the centroids of *incident* rings. In the *condensed ring net*, only rings of one and the same initial net, if they share an edge, are incident. In the *Hopf ring net*, the incidence is determined for catenated rings belonging to different initial entangled nets. An *extended ring net* combines both ring nets. The initial nets form the same topological type of entanglement if they are characterized by the same Hopf ring nets, while the initial nets can be topologically different. If it is important to take into account not only the topology of the entanglement but also the topology of entangled motifs, the extended ring nets are compared. The entanglement is particularly typical of atomic nets in MOCPs.[43] The corresponding examples are considered below.

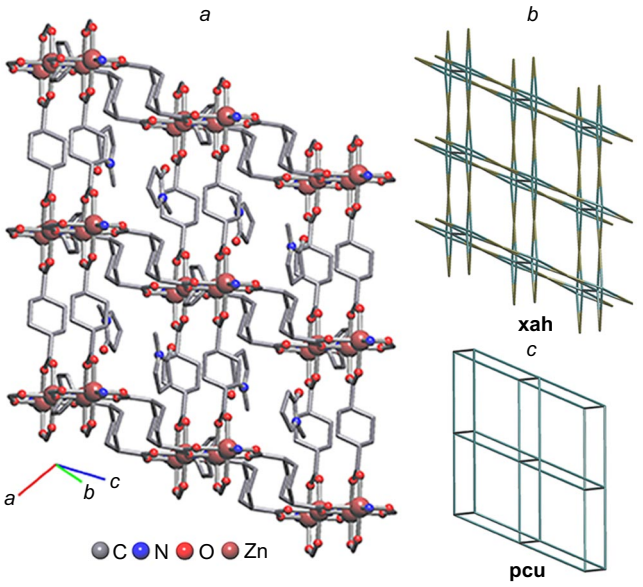


Figure 3. Initial (underlying) topology of the metal-organic framework (*a*) in the standard (*b*) and cluster (*c*) representations of the crystal structure of $[Zn_2(chdc)_2(dabco)]\cdot 2\,NMP$, where $chdc^{2-}$ is *trans*-cyclohexane-1,4-dicarboxylate, dabco is 1,4-diazabicyclo[2.2.2]octane and NMP is *N*-methylpyrrolidone (PACDAC [a]). Dimeric lantern zinc(II) complexes serve as clusters. The Figure was prepared by the authors using original data from the study.[47]

[a] Hereinafter, the refcodes of the compounds in the Cambridge Structural Database (CSD) are given in parentheses.

2.2. Topological structure simplification

Most of the crystal structures, in particular of MOCPs, have unique complex structures. Therefore, the topological classification or comparison of these structures requires their simplification by distinguishing the main topological motif and ignoring insignificant details. For example, the structure of the mineral cristobalite (polymorph of SiO_2) is topologically similar to the diamond structure, if oxygen atoms are considered as linkers and identified with the edges of the diamondoid net (Fig. 2). In MOCPs, complex polynuclear or cluster groups can be connected to form the diamondoid motif. To find this motif, these groups should be considered as an integral whole by replacing these groups with their centres of mass. The simplification gives an *underlying net* characterizing the connectivity of building units, *i.e.*, the general topological motif of the structure. The main simplification methods are described in the study.[46] For MOCPs, the following two simplifications are of particular importance:

— *standard simplification*, in which the underlying net is formed by metal atoms and the centres of mass of the ligands, and their connectivity is determined by the metal—ligand coordination bonds (Fig. 3); this method (standard) is generally used to consider the MOCP structures, which gives the name for this simplification;

— *cluster simplification*, in which the underlying net consists of the centres of mass of the valence-bonded polynuclear complex groups or clusters.

Two representation of ligands are possible in terms of the cluster simplification:[48] the single-node representation, in which each polydentate ligand is represented as one node of the underlying net, and the all-node representation, in which each ligand can be additionally separated into several parts represented in the underlying net by the connected centres of mass (Fig. 4). From the chemical standpoint, the single-node representation is more reasonable because it characterizes the assemblage of MOCPs from building units. However, the all-node representation can be useful for searching for the topological similarity between MOCPs containing ligands with different coordination modes.

The cluster simplification is important not only for compounds containing clusters in the chemical understanding of this term but also for MOCPs formed by any polynuclear building units, for example, for polyoxometa-

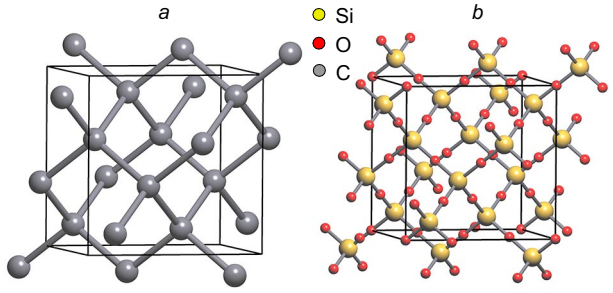


Figure 2. Structures of diamond (*a*) and cristobalite (*b*). The conversion of oxygen atoms (represented as red spheres) to the edges of the underlying net (secondary or 0-1-2 simplification) leads to the transformation of the topology of cristobalite into the standard representation coinciding with the topology of the diamondoid (**dia**) net.[a] The Figure was prepared by the authors using original data from the study.[46]

[a] Bold three-letter symbols of topological types are given according to the RCSR (Reticular Chemistry Structure Resource) nomenclature (see http://rcsr.net/).

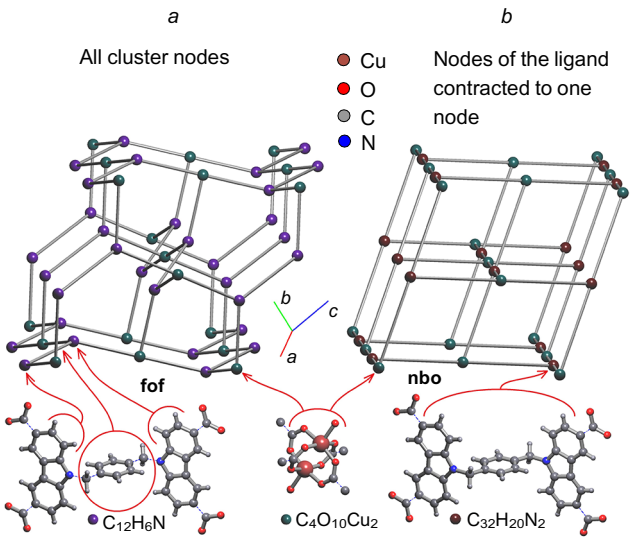


Figure 4. All-node (*a*) and single-node (*b*) cluster simplifications of the DUT-159 structure of the composition $Cu_2(pmcd)(H_2O)_2$ (pmcd is 1,4-bis [(3,6-dicarboxylato-9*H*- carbazol-9-yl)methyl]benzene) (QUSSAB). In the all-node representation, the ligand is separated into five groups (two carbazole, two methylene and one benzene moieties) with the methylene and benzene moieties forming an edge of the underlying net after the secondary simplification; in the single-node representation, all five groups are contracted to a single node of the underlying net. The Figure was prepared by the authors using original data from the study.[49]

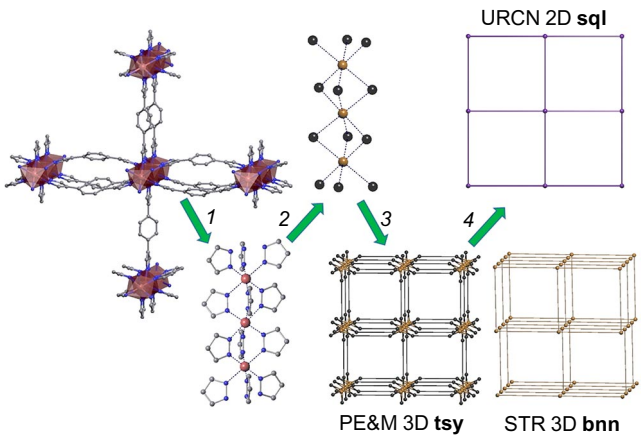


Figure 5. Illustration of four steps of the simplification of MOCPs with rod building units as exemplified by the metal-organic framework $[Cu_2(tapta)_3]Cl \cdot 12\,H_2O$ (AFOYOK; Htapta is 5-[4-(1,2,4-triazol-4-yl)phenyl]tetrazole). Hydrogen atoms are omitted for clarity. (*1*–*4*) See the text. Due to disorder, the uncoordinated nitrogen atoms are indistinguishable from the carbon atoms in the triazolate and tetrazolate groups; therefore, only two coordinated nitrogen atoms in the five-membered ring are shown. The Figure was prepared by the authors using original data from the study.[54]

lates and metallosiloxanolates. In contrast to clusters, polynuclear building units can be polymeric and form, for example, periodic chains (rods).[50] The crystal-chemical description of such MOCPs is based on several topological representations.[51–53] In addition to the standard representation, the points of extension and metals (PE&M) algorithm, the straight rod representation (STR) and underlying rod-containing nets (URCN, Fig. 5) are used. In these three approaches, the net is separated into 1-periodic clusters and linkers using the clustering method (step *1* in Fig. 5). In the PE&M algorithm, the metal–non-metal bonds are identified by marking to intercluster edges, the donor groups (functional groups of the ligand directly coordinated to metal atoms) being contracted to their centres of mass (step *2* in Fig. 5). In this representation, the metal atoms and the centres of anchoring groups form a 1-periodic underlying net of the rod, which, in turn, can be assigned to a particular topological type. The underlying nets of rods formed by small rings, which generally include 3–6 atoms, are separated in the 3-periodic PE&M-underlying net of the framework (step *3* in Fig. 5). This approach can be used to decorate PE&M nets by different donor groups and linkers according to their crystal-chemical role (metal, donor group, the centre of the ligand, linker) of each node and edge of the underlying net.

In the STR representation, dummy nodes are inserted into the centres of dimeric units of the rods, which are connected to the neighboring centres of anchoring groups and metal atoms, while the bonds between these groups and metal atoms are removed. This approach allows the representation of the rod group as a simple chain of 2-coordinated nodes and the determination of the most general template for the framework formation. For example, several different simple chains can be chosen in the **dia** net and they can be decorated to form rods.

To construct the underlying URCN net, the rods running along a certain [*hkl*] direction and the linkers between the rods are projected onto the (*hkl*) plane (step *4* in Fig. 5). The resulting plane net describes the topological motif of the rod arrangement.

Each simplification can give rise to a net containing terminal or bridging vertices with the coordination numbers of 1 or 2, respectively. In this case, an additional (*secondary*) simplification should be accomplished to remove terminal vertices and transform the bridging vertices into edges of the net (see Fig. 4). If the cavities in the net additionally contain isolated (uncoordinated) vertices (which correspond to intraframework atoms or molecules of the initial structure), these vertices are also removed. Therefore, the secondary simplification can also be referred to as the 0-1-2 simplification, where the numbers indicate the coordination numbers of the removed vertices. The 0-1-2 simplification has no effect on the connectivity of the net but makes it possible to represent the net in a standardized way (see Fig. 3).[55]

However, different simplifications can be applied to one and the same crystal structure, resulting in different *topological representation* characterized by different underlying nets. It should be emphasized that there is no the best representation; each representation can be useful in searching for the topological similarity or in addressing other problems of the topological analysis. All the above simplification methods, including those applied to other classes of compounds, are accomplished by rigorous algorithms described in the study,[46] which allows one to perform topological analysis of large sets of crystal structures and avoid human subjectivity.

2.3. Isoreticular series, topological isomerism, polymorphism, reconstruction and relationship

The notion of underlying nets provides a definition for an important taxon used for the topological classification in

reticular chemistry, such as an *isoreticular series*. This taxon is a set of crystal structures with the same topology of the underlying net. The geometry and the chemical composition and, consequently, many properties of such structures can be significantly different, but they can be assembled using the same method. This is especially important for the design of the synthesis. In particular, MOCPs of the same isoreticular series can be synthesized using different complexing metals and ligands having the same coordination properties. This may give rise to series of isoreticular adsorbents with different pore sizes by using ligands with different lengths or having different catalytic properties, through the insertions of different coordination sites. For example, the CSD contains 1485 structures with the coordination formula $A_2G^{62}M_2^1$ and 198 structures with the coordination formula A_2G^{62} and the 4.8T1 topology of the underlying net (see Section 2.6). These frameworks belong to the isoreticular IRMOF-74 series [56] and are topologically similar to honeycombs with a free space from 37% in the framework with the short 2,5-dioxidobenzene-1,4-dicarboxylate ligand (TODZAQ) [57] to 72.5% (GINYIO) [58] in the framework with the 1^3,3^3-dioxido-2^2,2^5-dimethyl[1^1,2^1:2^4,3^1-terphenyl]-1^4,3^4-dicarboxylate ligand. The pore sizes in the IRMOF-74-V framework are so large (the radius is 4.2 nm) that the pores can accommodate DNA strands. The presence of free metal coordination sites on the surface of pores of IRMOF-74 enables the catalytic activation of hydrogen and hydrogenolysis of C–O bonds.[59]

The consideration of the global topology of the atomic net makes it possible to introduce new types of topological isomerism of coordination compounds [60–78] If two MOFs are composed of the same building units and, consequently, have the same chemical composition but differ in the topology of the underlying net, these compounds are referred to as *network isomers*. The *entanglement isomerism* is another type of topological isomerism, when two crystal structures contain entangled coordination polymer networks that have the same chemical composition and topology but differ in their entanglement patterns. For example, triply interpenetrated 2-periodic MOCPs of the composition [Zn(bpdc)(dpipa)]·DMF (XILSAO) and [Zn(bpdc)(dpipa)]·DMF·2H_2O (XILSAO01) (dpipa is *N*,*N*′-di(4-pyridyl)isophthalamide, H_2bpdc is biphenyl-4,4′-dicarboxylic acid) with underlying nets of the same **sql** topological type have the same number of entangled rings but a different long-range order of the entanglement, which is distinguished by the construction of the extended ring net (Fig. 6).[61,64]

The topological isomerism of coordination polymer networks does not mean that the corresponding compounds are polymorphs, because the coordination frameworks can contain different guest molecules, as in the above case. Examples of *topological polymorphism* are very rare. For instances, the isomeric compounds GINTAA and GINTAA01 have the completely identical composition [Zn(glut)(bix)]·2H_2O (H_2glut is glutaric acid, bix is 1,4-bis(imidazol-1-ylmethyl)benzene) and the **sql** topology of the underlying net; however, the structure of the former compound shows an interpenetrated framework, whereas the structure of the latter one exhibits a parallel polycatenation of the nets (Fig. 7). Other examples of the topological isomerism are zeolite-like zinc complexes with imidazole. For these complexes, at least 13 topologies of single nets are known, such as 4,4,4,4,4,4,4,4,4,4T12 (GOQSIQ),[65] **afi** (IMIDZB13),[66] **cag** (IMIDZB11, VEJYUF01),[67,68] **can** (PAJRUQ),[66] **coi** (IMIDZB07, EQOCOC),[69,70] **crb** (VEJYEP),[71] **dft** (VEJYOZ),[71] **gis** (HIFVUO),[68] **neb** (KEVLEE),[72,73] **nog** (HIFWAV),[68] **zni** (IMIDZB),[74] **sod** (IMIDZB10),[75] and one doubly interpenetrated **dia** network (IMIDZB14).[76]

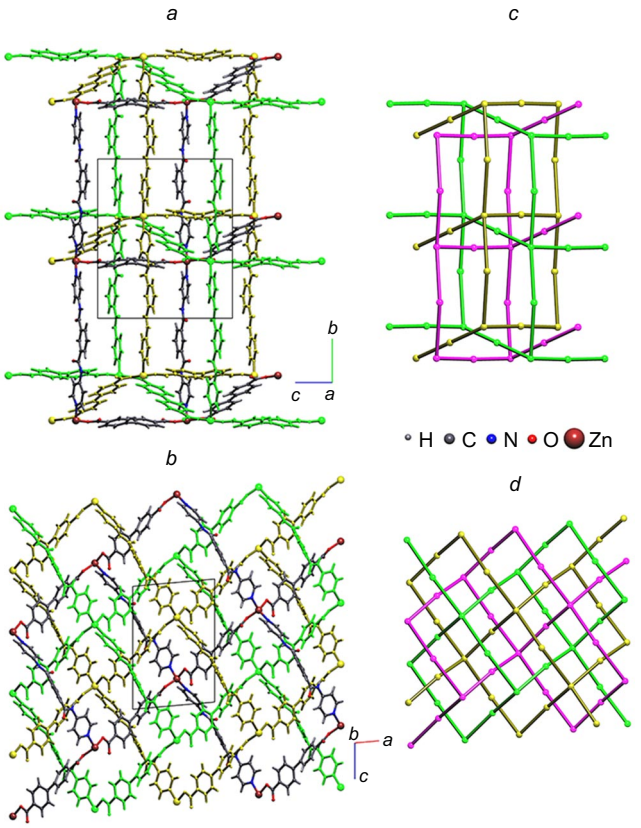


Figure 6. Fragments of the structures of the entanglement isomers XILSAO (*a*) and XILSAO01 (*b*) and the corresponding underlying nets (*c*, *d*). The Figure was prepared by the authors using original data from the study.[64]

Taking into account the topological isomerism, questions naturally arise whether it is possible to transform one isomer into another one and, if it is possible, what is the mechanism of this transformation. Since this transformation should be accompanied by a change in the connection of building units, *i.e.*, the breaking and(or) formation of bonds between these units, it can be considered as an analogue of reconstructive phase transitions in crystals. In terms of nets, this topological reconstruction means the sequence of elementary transitions, resulting in the removal of some edges of the initial net to form a subset and new edges, with the transition to a supernet.[79] These transitions can be accompanied by a change in the symmetry of the initial net. The scanning of all possible subnets and supernets for each topology can be performed in an automated mode. This allows one to determine all reconstructive transitions between the specified nets and also to generate new topologies related to the initial one.[80] An analysis of possible topological reconstructions is important, in particular, in studies of single crystal–single crystal transitions in MOCPs [81] and covalent organic frameworks.[82] For example, the heating of MOF of the composition [Cu_4I_4(dabco)$_2$] (Fig. 8) followed by its storage in acetonitrile or methanol vapours led to the transformation between two isomeric framework structures with

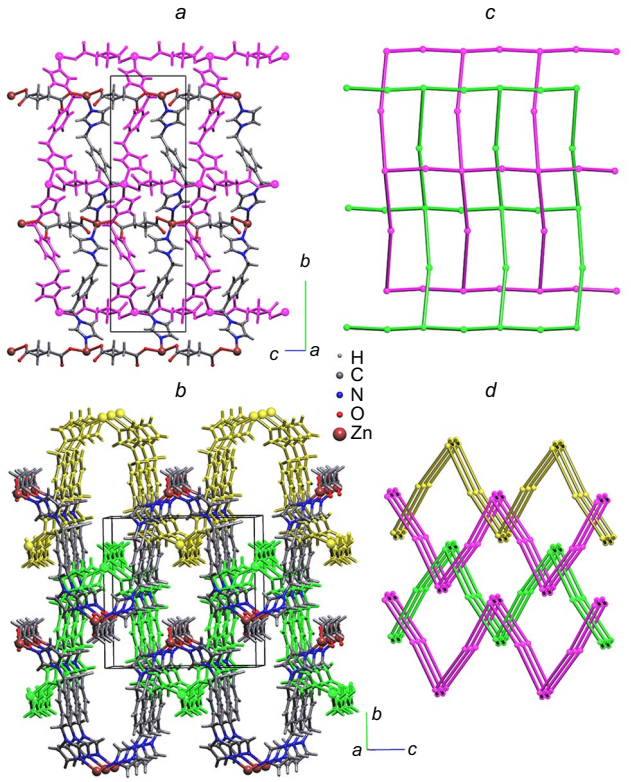


Figure 7. Structures of the isomeric coordination polymers GINTAA (*a*, *c*) with interpenetrating (the view perpendicular to the layers) and GINTAA01 (*b*, *d*) with parallel polycatenated (the projection along the planes of the layers) coordination networks. (*a*, *b*), fragments of the structures; (*c*), (*d*), corresponding fragments of the underlying nets. The Figure was prepared by the authors using original data from the studies.[77, 78]

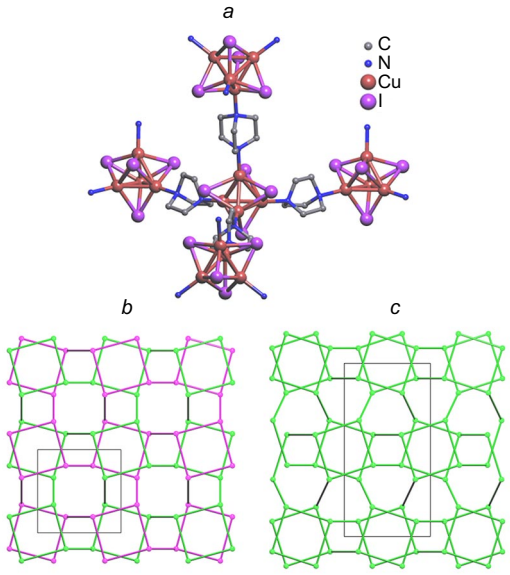


Figure 8. Structures of the isomeric coordination polymers RIPKEH and GUPBEZ of the composition $[Cu_4I_4(dabco)_2]$ (*a*) and the corresponding underlying nets **crb** (*b*) and 4,4T42 (*c*) projected onto the (001) plane. Hydrogen atoms are omitted for clarity. The Figure was prepared by the authors using original data from the studies.[83, 84]

the doubly interpenetrated motif of the 4-coordinated **crb** net (GUPBEZ, sp. gr. *P*4/*mcc*) and the self-catenated motif of the 4-coordinated 4,4T42 net (RIPKEH, sp.gr. *Ibca*). The use of the topological reconstruction method can help in determining a set of breaking and forming bonds, which is a challenge for structures with different symmetry space groups and unit cell parameters.

Apart from subnet – supernet relationships, which define the topological similarity of MOCPs, the topological relationship between different nets can be determined by another method. Since one and the same MOCP structure can have several topological representations, which differ in the topology of the underlying net, it can be suggested that the corresponding nets should also have the topological similarity, *i.e.*, should be transformed into each other with a certain choice of the building units. Generally, the corresponding topological reconstruction implies the contraction or, on the contrary, splitting of the nodes of one of the nets. Examples of the supramolecular structure approach to the design of metal-organic frameworks are given in the review.[85] One of the most well-known examples is the structure of **rth**-MOF-7 of the composition $[Cu_3L(H_2O)_3]$ [XALXUF; L is 5,5′,5″-(1,3,5-triazine-2,4,6-triyltriimino)-triisophthalate], which can be separated into building units in two ways. In one case of the topological assembly, 3-coordinated triazine and benzene rings and 4-coordinated dimers $\{Cu_2(CO_2)_4\}$ are linked by bridging NH groups and C – C bonds to form the 3,4-coordinated **ntt** net. In another case, the assembly includes 3-coordinated triazine rings and 24-coordinated nets $\{Cu_{24}(H_2O)_{24}(Isophthalate)_{24}\}$ linked by bridging NH groups to form the 3,24-coordinated **rht** net. The latter assembly seems to be chemically unreasonable; however, it is important for the reticular design (see Section 4) because the 3-coordinated cluster $\{Cu_3O(N_4CR)_3\}$ and the phenylene group can be used instead of the triazine ring and the NH bridge to construct the isoreticular framework **rht**-MOF-1.

2.4. Computer programs for topological analysis

Since the first studies by Wells[8] and up to the beginning of the 21st century, the topological analysis of crystal structures was performed visually using atomic nets, which significantly limited its application. The direct visual comparison even of rather simple nets can be a difficult problem in the case of geometric distortions. Therefore, it was proposed to use topological invariants,[86] which characterize the topology of nets with high accuracy. However, these invariants can be manually calculated only for rather simple nets.

The synthesis of new MOCPs with a complex architecture has generated a need to develop computer programs for topological analysis. The first program, Systre [Symmetry, Structure Refinement (Recognition)],† was published in 2003.[87] The Systre program determines the automorphism group, nets, the space group isomorphic to the automorphism group and the embedding geometry of the net corresponding to this space group. The topological invariant used in the Systre (Systre key) unequivocally defines the topology of the net. Therefore, this program makes it possible to automatically determine the topology of periodic structures. The Systre was the first to utilize a unified system of notations of topological types based on three-letter symbols (for example, the symbol **dia** indicates the

† http://www.gavrog.org/

diamondoid topology). The Systre collection of topological types has laid the basis for the first database of topologies of nets (RCSR database) and, consequently, the three-letter symbols of topologies are also referred to as RCSR symbols.[88] In the present review, we mainly use RCSR symbols. The limitation of Systre is that it allows one to analyze only crystallographic nets.

The capabilities of topological analysis capabilities are most completely realized in the ToposPro program package ‡ (see Ref. 89). Apart from the determination of the topological type of the net based on a set of topological invariants, the ToposPro implements the following procedures, particularly important for the modeling of MOCPs:

— the determination of the connectivity (identification of chemical bonds of different types) according to the rigorous algorithm [53] and the representation of an infinite periodic net of bonds as a final quotient graph;[90]

— the determination of the shape of the coordination polyhedron and the coordination figure using three independent algorithms;[91]

— the simplification of the structure, including the standard and cluster simplifications, the secondary simplification, and the construction of the underlying net;

— the determination of the periodicity of the net;

— the search for topological isomers;

— the determination of the geometric class of the entanglement [92] and the topological type of the entanglement using extended ring nets and Hopf ring nets;[61]

— the automatic search for subnets and supernets with a specified topological complexity and the determination of reconstruction pathways of this net;[79]

— the construction of the natural tiling by the algorithm.[42]

‡ https://topospro.com/

To identify the topology of the net, ToposPro uses the most complete database of reference topological types (TTD collection, see Sections 2.5 and 2.6).[93] The TTD database is accessible through the TopCryst web service,[94] which automatically generates possible topological representations of the structure and determines the topological types of the corresponding underlying nets. The standard CIF file serves as the input structure data in the TopCryst; the topological analysis is accomplished by ToposPro algorithms. The service automatically determines the chemical class of the compound and chooses appropriate topological simplifications of the structure (Fig. 9).

For all known topologies, TopCryst provides information on their occurrence in known crystal structures by addressing to the TTO collection of ToposPro (see Section 2.6).

In the recent study,[96] Snurr's research team presented two programs, MOFid and MOFkey, for the deconstruction of metal-organic frameworks into building units and underlying networks and calculations of the descriptors used in cheminformatics.

2.5. Topological databases

Crystallographic data from the CSD, which is the largest repository of the crystal structures of organic and metal–organic compounds,[97,98] serve as the initial data for topological databases. Although the CSD is available for ~45 years, the development of electronic databases containing data on the topology of periodic nets has become possible only in the beginning of the 21st century due to the design of suitable software. For the RCSR database, which was the first one, the selection of nets and the simplification of the initial structures for the construction of these nets were performed manually, and the topological analysis of each net was accomplished using the Systre program. As at June

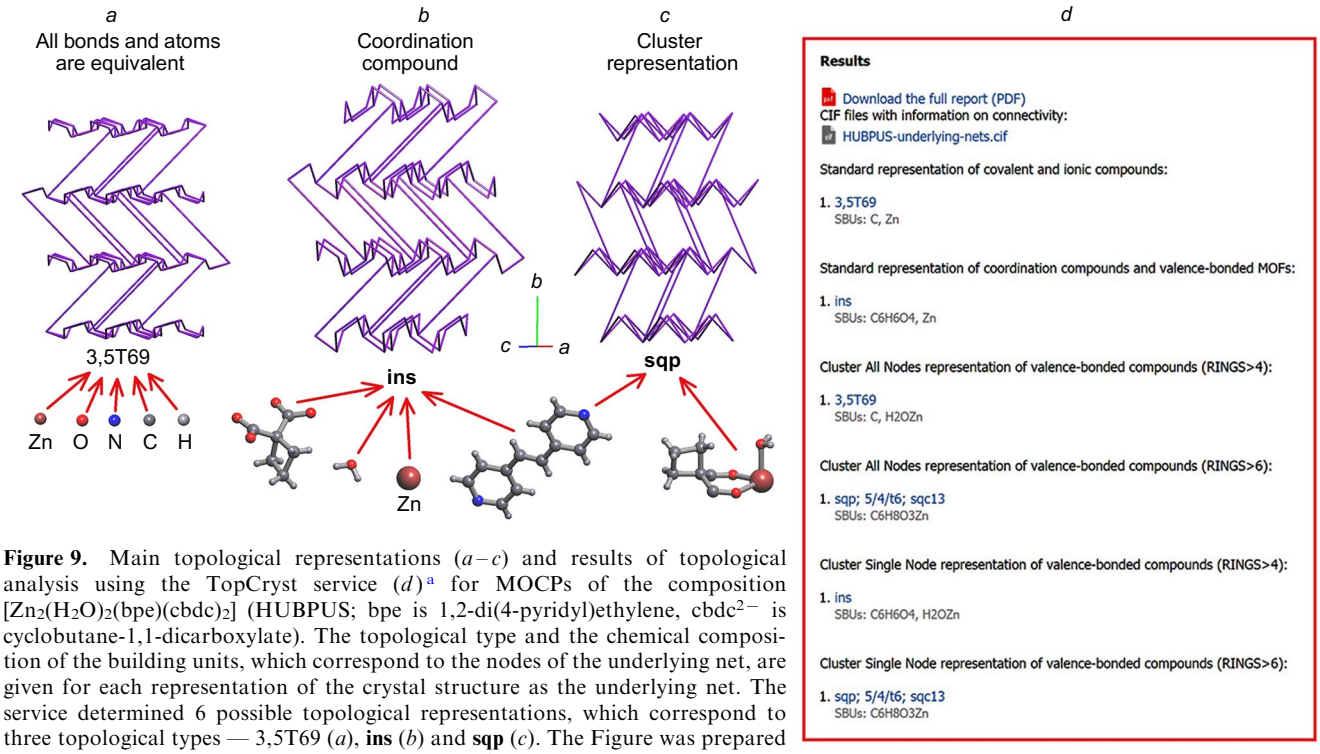
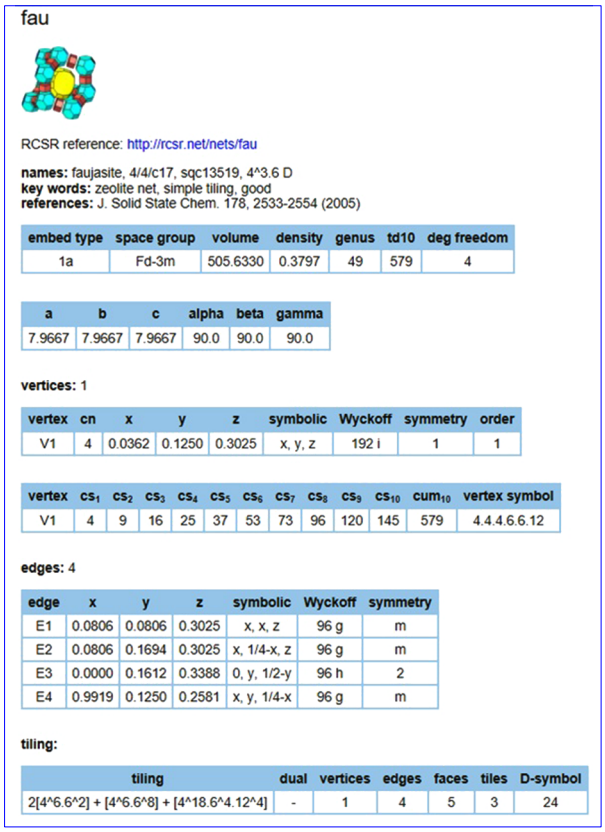


Figure 9. Main topological representations (*a*–*c*) and results of topological analysis using the TopCryst service (*d*) [a] for MOCPs of the composition $[Zn_2(H_2O)_2(bpe)(cbdc)_2]$ (HUBPUS; bpe is 1,2-di(4-pyridyl)ethylene, $cbdc^{2-}$ is cyclobutane-1,1-dicarboxylate). The topological type and the chemical composition of the building units, which correspond to the nodes of the underlying net, are given for each representation of the crystal structure as the underlying net. The service determined 6 possible topological representations, which correspond to three topological types — 3,5T69 (*a*), **ins** (*b*) and **sqp** (*c*). The Figure was prepared by the authors using original data from the study.[95]

[a] http://topcryst.com



fau

RCSR reference: http://rcsr.net/nets/fau

names: faujasite, 4/4/c17, sqc13519, 4^3.6 D
key words: zeolite net, simple tiling, good
references: J. Solid State Chem. 178, 2533-2554 (2005)

embed type	space group	volume	density	genus	td10	deg freedom
1a	Fd-3m	505.6330	0.3797	49	579	4

a	b	c	alpha	beta	gamma
7.9667	7.9667	7.9667	90.0	90.0	90.0

vertices: 1

vertex	cn	x	y	z	symbolic	Wyckoff	symmetry	order
V1	4	0.0362	0.1250	0.3025	x, y, z	192 i	1	1

vertex	cs_1	cs_2	cs_3	cs_4	cs_5	cs_6	cs_7	cs_8	cs_9	cs_{10}	cum_{10}	vertex symbol
V1	4	9	16	25	37	53	73	96	120	145	579	4.4.4.6.6.12

edges: 4

edge	x	y	z	symbolic	Wyckoff	symmetry
E1	0.0806	0.0806	0.3025	x, x, z	96 g	m
E2	0.0806	0.1694	0.3025	x, 1/4-x, z	96 g	m
E3	0.0000	0.1612	0.3388	0, y, 1/2-y	96 h	2
E4	0.9919	0.1250	0.2581	x, y, 1/4-x	96 g	m

tiling:

tiling	dual	vertices	edges	faces	tiles	D-symbol
2[4^6.6^2] + [4^6.6^8] + [4^18.6^4.12^4]	-	1	4	5	3	24

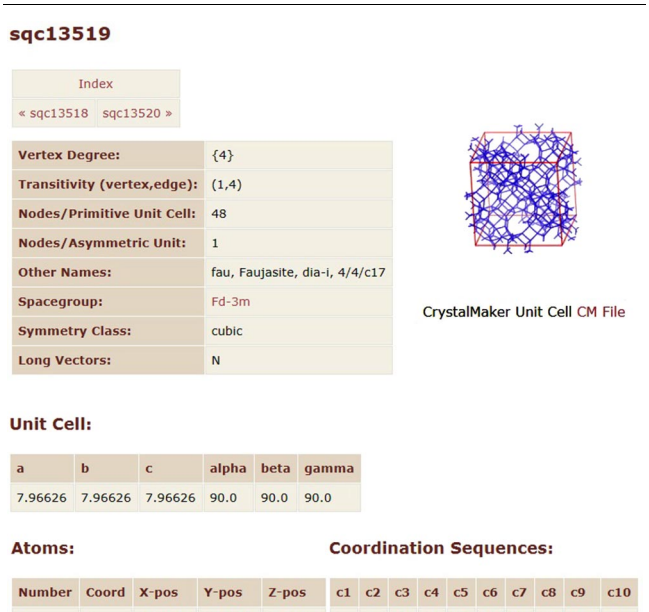
Figure 10. Data on the framework type **fau** taken from the RCSR database (http://rcsr.anu.ed.au).

2021, the RCSR database contains data for 134 0-periodic (polyhedral), 11 1-periodic (chain), 200 2-periodic (layered) and 2930 3-periodic (framework) topologies. The topologies are designated by three-letter RCSR symbols (Fig. 10).

The second database of topologies of nets, the so-called EPINET (Euclidean Patterns in Non-Euclidean Tilings) project, was announced in 2005. The EPINET database contains data for 14532 3-periodic nets, generated by the projection of two-dimensional hyperbolic tilings onto the three-dimensional Euclidean space (Fig. 11). The EPINET nets are denoted as *sqc*X, where X is the serial number of the net. Unlike RCSR nets, EPINET nets were generated by the abstract mathematical procedure without using any data on the crystal structures. Therefore, these nets can be considered as random in terms of the occurrence in real crystals. Taking into account this fact, EPINET nets are important in theoretical studies related to the elucidation of the factors responsible for the frequency of the occurrence of a particular topology in crystals. It was demonstrated [99] that only ~13% of EPINET nets are present in real structures, which indicates that frequently occurring topologies are not random but are determined by specific features of chemical interactions between building units.

When discussing the topology of coordination polymers, a note should be made of the Database of Zeolite Structures, which contains data on 253 zeolite structure types approved by the Structure Commission of the International Zeolite Association (IZA-SC). In the Database of Zeolite Structures, like in RCSR, three-letter notations of topologies, but given in capital letters, are used (Fig. 12). Despite the fact that zeolite frameworks are formed only by inorganic building units, their topology is typical of many metal-organic frameworks. For example, 57 topologies are observed in MOFs from the Database of Zeolite Structures.[100]

Currently, the TTD (ToposPro Topological Database) collection [93] is the most comprehensive database of topological types. It contains values for topological invariants of >800 000 topological types of 0-, 1-, 2- and 3-periodic graphs and nets, which occur in real and hypothetical crystal structures (Fig. 13). The TTD collection fully includes topological types, which are available in the above topological databases. Since new topological types are automatically added to the TTD collection, *N*D*k* symbols are also automatically assigned to these types, where *N* is the sequence of coordination numbers of all independent vertices of the net, D indicates its periodicity (M, C, L or T for 0-, 1-, 2- or 3-periodic nets, respectively), *k* is the serial number of the net with this set of *N*D, for



sqc13519

Index
« sqc13518 sqc13520 »

Vertex Degree:	{4}
Transitivity (vertex,edge):	(1,4)
Nodes/Primitive Unit Cell:	48
Nodes/Asymmetric Unit:	1
Other Names:	fau, Faujasite, dia-i, 4/4/c17
Spacegroup:	Fd-3m
Symmetry Class:	cubic
Long Vectors:	N

CrystalMaker Unit Cell CM File

Unit Cell:

a	b	c	alpha	beta	gamma
7.96626	7.96626	7.96626	90.0	90.0	90.0

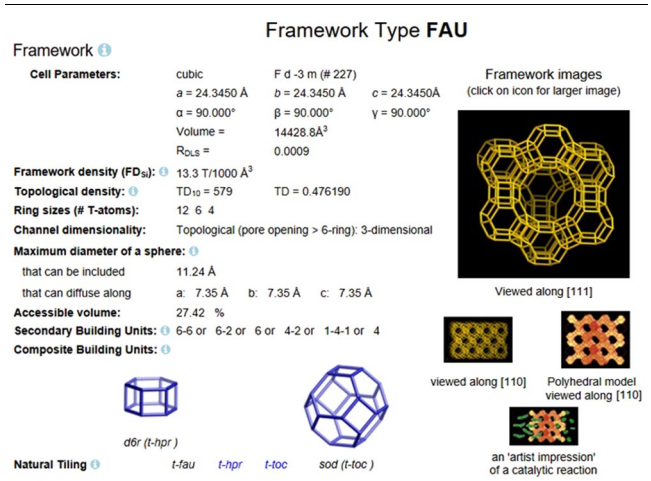
Atoms:

Number	Coord	X-pos	Y-pos	Z-pos
1	4	0.03624	0.62500	0.30253

Coordination Sequences:

c1	c2	c3	c4	c5	c6	c7	c8	c9	c10
4	9	16	25	37	53	73	96	120	145

Figure 11. Data on the framework type **fau** taken from the EPINET database (http://epinet.anu.edu.au).



Framework Type **FAU**

Framework

Cell Parameters:	cubic	F d -3 m (# 227)	
	a = 24.3450 Å	b = 24.3450 Å	c = 24.3450Å
	α = 90.000°	β = 90.000°	γ = 90.000°
	Volume =	14428.8Å^3	
	R_{OLS} =	0.0009	
Framework density (FD_{Si}):	13.3 T/1000 Å^3		
Topological density:	TD_{10} = 579	TD = 0.476190	
Ring sizes (# T-atoms):	12 6 4		
Channel dimensionality:	Topological (pore opening > 6-ring): 3-dimensional		
Maximum diameter of a sphere:			
that can be included	11.24 Å		
that can diffuse along	a: 7.35 Å	b: 7.35 Å	c: 7.35 Å
Accessible volume:	27.42 %		
Secondary Building Units:	6-6 or 6-2 or 6 or 4-2 or 1-4-1 or 4		
Composite Building Units:			

Framework images
(click on icon for larger image)

Viewed along [111]

viewed along [110]

Polyhedral model viewed along [110]

an 'artist impression' of a catalytic reaction

d6r (t-hpr) t-fau t-hpr t-toc sod (t-toc)

Natural Tiling

Figure 12. Data on the framework type FAU taken from the Database of Zeolite Structures (http://www.iza-structure.org/databases/).

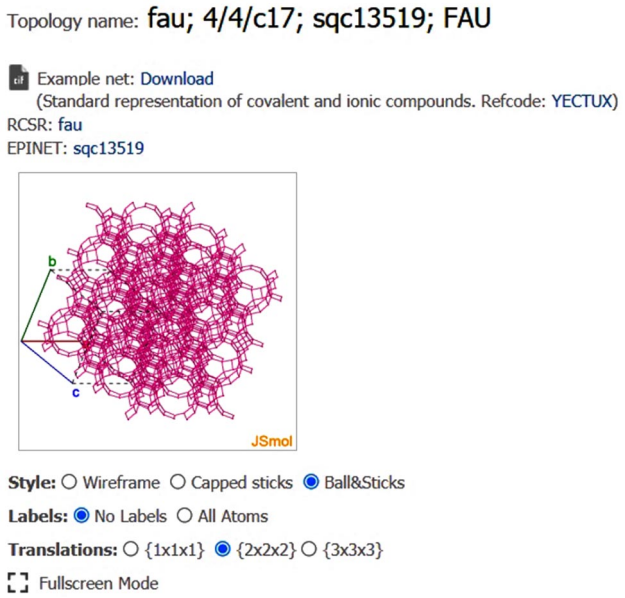


Figure 13. Data on the framework type **fau** from the TTD collection provided by the TopCryst service (https://topcryst.com).

example, 4,4,6T58. The ToposPro and TopCryst programs use the TTD collection for the identification of topological types.

Topological methods have rapidly evolved due to the progress in the crystal chemistry of MOCPs. Hence, unsurprisingly, specialized databases of certain groups of compounds are most well developed for coordination polymers. These databases made it possible to perform the fast search for desired materials. The known databases including the data on the structures of both real and hypothetical MOCPs are listed below:

— the first database includes 137 953 hypothetical MOCPs,[101] generated from 102 different building units based on the screening of their connection modes; however, the screening was limited to one type of nodes and two types of connections between the nodes;

— the database of zeolite-like zinc imidazolate MOFs,[102] generated from 300 000 structures of hypothetical zeolites by replacing silicon and oxygen atoms, respectively, by Zn^{II} ions and imidazolate linkers;

— the Goldsmit database[103] of real MOCPs, which were generated based on the analysis of real structures from the CSD; this database includes the structural data, porosity values and pore surface areas for 22 700 disordered MOCPs; these data may be useful and demanded for mathematical modeling of MOCPs (solvent molecules are removed from the frameworks); in particular, Goldsmit *et al.*[103] employed this database to search for materials optimal for hydrogen storage;

— the database of real MOCPs suitable for calculations,[104, 105] which contains structures of ~14 000 MOCPs, was generated in a similar way as described above based on the analysis of the CSD but using more rigorous criteria of selection;[‡] the database includes data on the maximum pore size and the minimum channel size, which were used to estimate the methane adsorption capacity of MOCPs;

— First *et al.*[107, 108] created the publicly available MOFOMICS database of nanoporous materials;[§] the authors divided the porous structures into channels and pores, which were approximated by the simplest geometric figures (spheres and cylinders); the database includes data on the sizes of these spheres and cylinders for the structures of 251 real and 1424 hypothetical MOCPs;

— the staff of the Cambridge Crystallographic Data Centre created a database of >80 000 MOCPs,[109–111] which includes, apart from structural data, the data on the porosity and sizes of the narrowest channels and the largest pores.

Most investigations of microporous MOCPs were related to the search for new materials for adsorption, separation and storage of practically important gases, such as methane,[101, 112] carbon dioxide[102] and noble gases.[113, 114] However, none of the above databases contains comprehensive information on the building units in the format necessary for the analysis of the mode of binding and the formation of new structures and on the topological motifs of real and hypothetical MOCPs.

2.6. Topological descriptors, knowledge bases and elements of artificial intelligence

As mentioned above, the development of structural descriptors is an important prerequisite for the transition from the accumulation of experimental data (and the data obtained by *in silico* mathematical modeling) on crystal structures to the data processing, the elucidation of the general features and the prediction of the structures and properties of new compounds and materials. The descriptors, *i.e.*, the structural parameters calculated from the initial crystallographic data, serve as the basis for prediction systems, which are at their infancy in the crystal chemistry and materials science.[115] The descriptors and correlations between them are used as the information basis of knowledge-based systems, machine learning methods, neural networks and other elements of artificial intelligence systems.[116–119] The most well-known topological descriptors, employed for the description and prediction of the MOCP structures in computer systems (see also Sections 2.1 and 2.4) are listed below:

— the coordination number of the atom or the node of the underlying net; since the node of the underlying net corresponds to the building unit, its coordination number means the number of other building units connected to this unit;

— the coordination figure of the atom or the node of the underlying net;

— the coordination mode of the building unit. The symbol $L^{mbtk\ldots}$, which characterizes the local connectivity of the building unit, was initially proposed for ligands in coordination compounds[120, 121] and was then extended to molecular structures as the symbol characterizing the binding mode of the molecule;[122] in this symbol, different letters L designate the number of active sites of the building unit (M, 1; B, 2; T, 3; K, 4; *etc.*), and the sequence of superscripts *mbtk*... at L indicates the number of other groups coordinated by one (*m*), two (*b*), three (*t*), four (*k*), *etc.* active (coordination) sites of this group (Fig. 14);

‡ This and three previous databases were combined within the framework of the project 'The Materials Project' (https://www.materialsproject.ogr/) and are available online through a special program interface.[106]

§ See https:///ares.tamu.edu/mofomics/

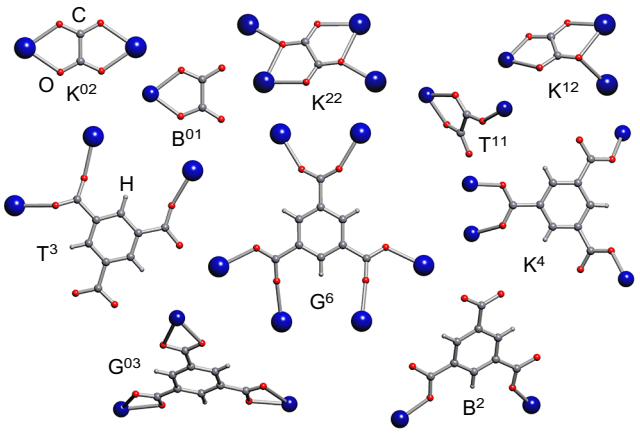


Figure 14. Frequently observed coordination modes of oxalate and trimesate anions. Metal atoms are in blue.[93] Reproduced with the permission of American Chemical Society.

— the coordination formula,[120,121] which characterizes the local topology of MOCPs and includes the coordination modes of all ligands in the corresponding stoichiometric ratios; the complexing atoms are denoted by the letter A, *e.g.*, $A_2G^{62}M^1_2$;

— the topological type of the underlying net; if the structure allows multiple representations, several topological types can be given, specifying a set of building units corresponding to each representation;

— parameters of entanglement, including the type of interpenetration (interpenetration or polycatenation), the type of polycatenation (parallel or inclined) and the topological type of entanglement (type of the Hopf ring net).

Collections of the ToposPro program package[123] are examples of knowledge bases, which accumulate the properties of MOCPs at different levels of the structural organization. In this system, four hierarchical levels of structural organization are considered. For each level, the knowledge base contains descriptors corresponding to this level (Table 1). For all structural elements described in the knowledge bases, the frequencies of their occurrence in the crystal structures of MOFs are given.

The correlations between the descriptors are stored in the knowledge base as a set of rules with the probabilities of their occurrence in MOCP structures.[115] The total number of possible combinations of descriptors and related correlations is very large; however, only the most significant combinations, which have a clear chemical meaning, are considered. For example, for copper-organic frameworks, it is important to consider the group of the following three descriptors: the coordination mode of the ligand (CML), the coordination formula (CF) and the underlying net in standard representation (UNSR).[94] Each sequence of descriptors belongs to a particular chemical problem. Thus, when using bridging ligands with CML = 'B^2' for the synthesis of copper-containing compounds, an underlying net with the square net topology **sql** will be obtained with the probability (p) > 50%. Other topologies (**hcb**, **dia**, **qzd**, **cds**, **pcu**) can also occur but with a much lower probability (from 2.8 to 10.7%). For the basic **sql** topology, the coordination formulae AB^2_2, $AB^2_2M^1$, $AB^2_2M^1_2$ are possible, *i.e.*, the ligands should be polyatomic bridging (B^2) or terminal (M^1). However, if only ligands with the bridging coordination modes B^2 and M^2 are employed, the hexagonal plane net (**hcb**) topology will be the most probable (with a probability of 62%).

Table 1. Content of the knowledge bases of the ToposPro program package. The numbers of entries are for July 2021 and are updated once a year.

Structural element	Knowledge base	Number of entries	Descriptors
	Atomic-level structural organization		
Atom	TTA (Topological Types of Atoms)	1 281 254	Coordination number and figure, volume, radius, occurrence
	Structural organization at the building unit level		
Ligand	TTL (Topological Types of Ligands)	204 828	Coordination number and figure, coordination mode, volume, radius, occurrence
Molecule	TTM (Topological Types of Molecules)	211 374	Coordination number and figure, binding mode, volume, radius, occurrence
Cluster	TTN (Topological Types of Nanoclusters)	1 372	Topological type of cluster, occurrence
Cavity (tile)	TTT (Topological Types of Tiles)	405	Topological type of tile, occurrence
	Structural organization at the network level		
Polymeric complex group	TTD (ToposPro Topological Database)	805 538	Topological type of the underlying net and the type of topological representation
	TTO (Topological Types Observed)	2 647 653	Frequency of occurrence of topological types
	TTR (Topological Types Relations)	9915	Topological types relations specified by different selections of topological representations
	Structural organization at the entanglement level		
See [a]	TTD	–	Degree of interpenetration

[a] The structural element consists of several entangled polymeric complex groups.

Hence, the following rules can be saved in the knowledge base (Me is metal):

Rule I: IF (Me = 'Cu') AND (Number_of_sorts(Me) = 1) AND (CML = 'B^2') THEN UNSR IN (**sql** WITH p = 51.6%, **hcb** WITH p = 10.7%, **dia** WITH p = 9.9%, **qzd** WITH p = 4.0%, **cds** WITH p = 4.0%, **pcu** WITH p = 2.8%).

Rule II: IF (Me = 'Cu') AND (Number_of_sorts(Me) = 1) AND (CML = 'B^2&M^2') THEN UNSR = **hcb** WITH p = 62.0%.

Artificial intelligence systems, which are becoming integrated into modern technologies and fields of science

addressing big data,[124–127] can utilize these rules to assist chemists in the design of new coordination compounds (see Section 4). The major component of these systems is a knowledge base, which contains data on the correlations, rules and patterns used for addressing the tasks of this subject area. In the chemistry and materials science, knowledge bases and artificial intelligence systems have been applied relatively recently,[128–130] while such systems are still lacking in the crystallography and crystal chemistry. As for crystallographic databases, only the CSD is positioned as a knowledge base and is equipped with tools of geometric-topological analysis of the local environment of molecular moieties and quantum chemical methods.[98, 131] Nevertheless, the CSD has no tools for the analysis and prediction of the topology of polymer groups and the related properties (for example, adsorption).

There is increasing popularity of artificial intelligence systems based not on the rules but on particular models derived from training sets using sophisticated machine-learning techniques.[132] Taking into account the diversity of such systems, there are published guidelines with recommendations on the development and implementation of such models and the representation of the results of these studies.[6, 133] Most of the models were created based on data sets obtained by quantum chemical modeling, and these models predict the properties, which can be obtained from these calculations (the formation energy of compounds, the bandgap width, effective charges on atoms, *etc.*).[134, 135] Machine learning techniques are often used to study MOCP structures and predict their adsorption parameters;[132, 136–138] however, the topological properties of MOCPs are, as a rule, ignored in these investigations.

3. Topological structural patterns of coordination polymers

3.1. Classification of topological motifs

3.1.1. Framework coordination polymers

The summary analysis of topologies of framework (3-periodic) MOCPs was published for the first time in 2004.[44] In this study, interpenetrated frameworks were considered, a comprehensive analysis of the CSD was given and 301 structures with interpenetrations were selected. The authors used for the first time automated methods of topological analysis and the ToposPro program package. One year later, 1127 single networks in MOCPs were topologically classified,[139] the analysis being performed manually. Later, the topological classifications of MOCPs were reported several times.[55, 140] The most comprehensive analysis was performed for 33 790 structures of both single and entangled frameworks.

The topological analysis of 33 790 MOFs demonstrated that the most abundant types (found in more than 100 structures) out of 8 555 topological types of underlying nets are the primitive cubic (**pcu**) net, the diamond (**dia**) topology, the strontium silicide (**srs**) topology, the thorium silicide (**ths**) topology and the underlying net of cadmium sulfate (**cds**). These topologies were also most abundant in the arrays analyzed in previous studies (Fig. 15). In the MOCPs, synthesized in the past decade, the **pts**, **sra**, **xah** and **bpq** topological types became more frequent due to the development of new methods of design of metal-organic frameworks for adsorption applications. The **pts** topological type is often observed in a combination of tetrahedral and square coordination figures, which are produced by the selection of the ligand and the d metal having appropriate coordination properties.[141, 142] The **sra** topology is often observed in different combinations of trimesate anions and d- or f-metal cations.[143, 144] The **xah** topological type is characteristic of metal-organic frameworks based on $\{M_2(CO_2)_4\}$ dimeric nodes, and the corresponding cluster representation has the **pcu** topology.[145, 146] The **bpq** topology is typical of MOCPs with rod building units.[147, 148] All these types correspond to topologically rather simple frameworks and serve as templates for the design of coordination polymers using compositionally different building units.

Among 5035 interpenetrated structures, $[Ag_3(OH)(H_2O)_2(tipa)_{2.5}][Mo_2O_7]\cdot 4.5\,H_2O$ (tipa is tris[4-(imidazol-1-yl)phenyl]amine) with the **srs** topology of

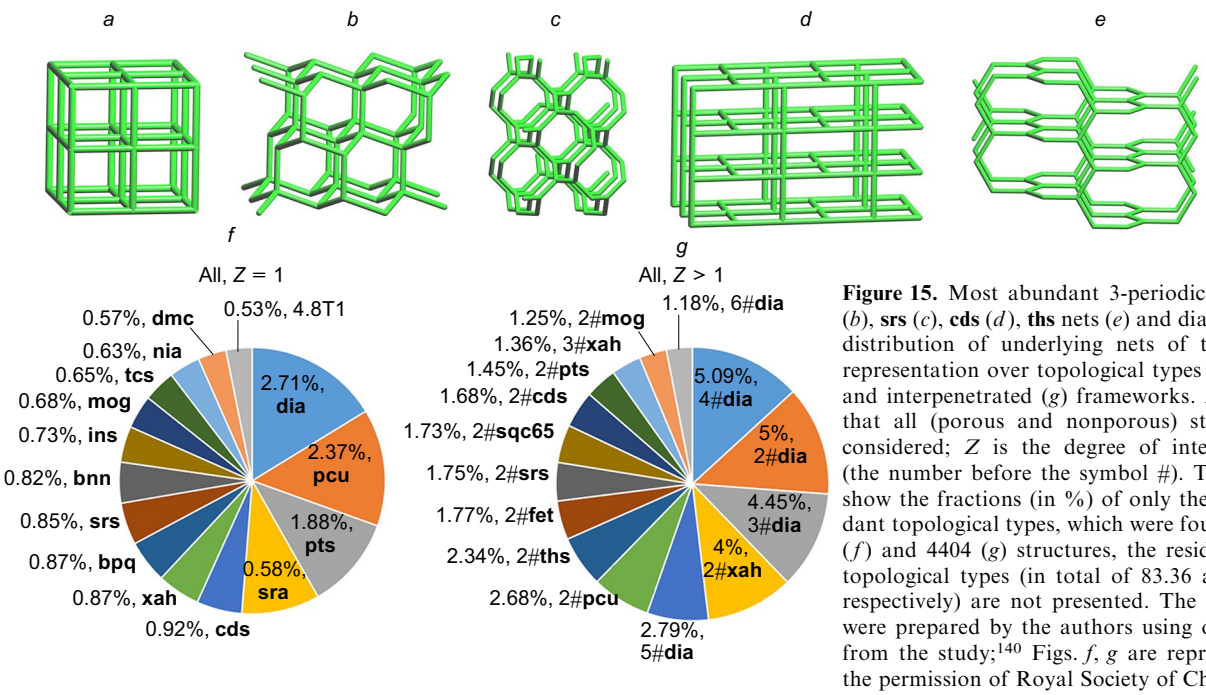


Figure 15. Most abundant 3-periodic **pcu** (*a*), **dia** (*b*), **srs** (*c*), **cds** (*d*), **ths** nets (*e*) and diagrams of the distribution of underlying nets of the standard representation over topological types in single (*f*) and interpenetrated (*g*) frameworks. All indicates that all (porous and nonporous) structures are considered; *Z* is the degree of interpenetration (the number before the symbol #). The diagrams show the fractions (in %) of only the most abundant topological types, which were found in 23 647 (*f*) and 4404 (*g*) structures, the residuals of rare topological types (in total of 83.36 and 61.49%, respectively) are not presented. The Figures *a*–*e* were prepared by the authors using original data from the study;[140] Figs. *f*, *g* are reproduced with the permission of Royal Society of Chemistry.

the underlying net has the maximum degree of interpenetration (54).[149] Only 20 structures exhibit heterointerpenetration (topologically different frameworks), and the other structures are unevenly distributed over 1032 topological types. The frequency of occurrence exponentially decreases with increasing number of frameworks in one structure (the degree of interpenetration). The interpenetration is not characteristic of frameworks composed of rod (chain) building units. The interpenetration is most often found in structures with simple topologies and with the coordination numbers limited to 6. An analysis of tilings demonstrated that the cavities in the most abundant networks are arranged in the same topological manner as the nets by themselves. Therefore, the significance of self-dual nets for the interpenetration was statistically confirmed.

Heterointerpenetrated frameworks are often (10 examples out of 20) formed in the case of different chemical compositions of interpenetrated polymeric networks. These differences are observed when comparing underlying nets in the standard representation, whereas the cluster representation gives underlying nets with the same topology. For example, MOCP of the composition $[WS_4Cu_4(dpbp)_4]^{2+} \cdot [WS_4Cu_3(dpbp)_2I_2]^{-} \cdot I^{-}$ (AMUWIP; dpbp is 4,4′-di(4-pyridyl)biphenyl) contains four anionic and four cationic interpenetrated frameworks with the 3,5,8T8 and 3,3,5,5T11 topologies, respectively.[150] In the cluster representation, both types of the framework belong to the **dia** topological type.

Eleven examples of the interpenetration of 2-periodic nets into cavities of the 3-periodic framework were found.[21] An increase in the density of the structure can also be achieved through self-catenation — the entanglement of cyclic chains of bonds in one polymer net. The self-catenation can be considered as resulting from the connection of entangled structural groups through additional edges (Fig. 16).

3.1.2. Layered coordination polymers

The first topological classification of 2-periodic (layered) MOCPs was reported only in 2013 despite the fact that these compounds are topologically much more simple compared to three-dimensional MOCPs.[152] The data for 10 371 compounds were considered in a systematic way. One year later, the comprehensive analysis of all types of entanglements of layered MOCPs in 783 structures was performed.[153] In the present review, we report the results of topological analysis of 25 042 layered MOCPs from the CSD release (October 2020).

All these layered MOCPs are distributed over 1388 topological types, with the square **sql** (51.9%), hexagonal **hcb** (15.8%) and kagome dual **kgd** topologies (3.9%,

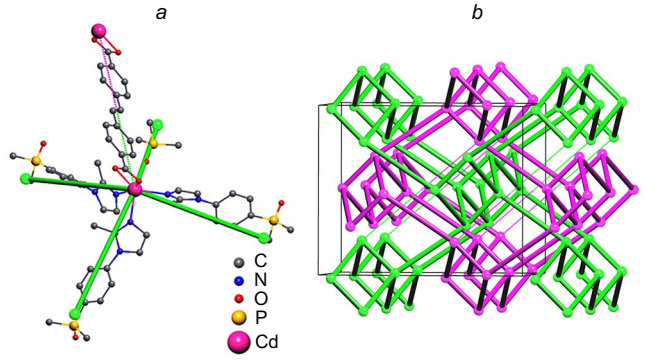


Figure 16. Structure of the coordination polymer $[Cd_2(bpedc)(tmpo)_2] \cdot 2\,NO_3 \cdot 4\,H_2O \cdot 2DMF$ (ZORFEU; H_2bpedc is stilbene-4,4′-dicarboxylic acid, tmpo is tris[4-(2-methylimidazol-1-yl)phenyl]phosphine oxide) (*a*) and the related self-catenated 4,5-coordinated underlying net *cnk*4 (*b*), which can be represented as two interpenetrating 4-coordinated networks with the **sra** topology if the $bpedc^{2-}$ linker is ignored. Additional edges, which connect the **sra** networks to form a single framework, are indicated by dashed lines. Hydrogen atoms are omitted for clarity. The Figure was prepared by the authors using original data from the study.[151]

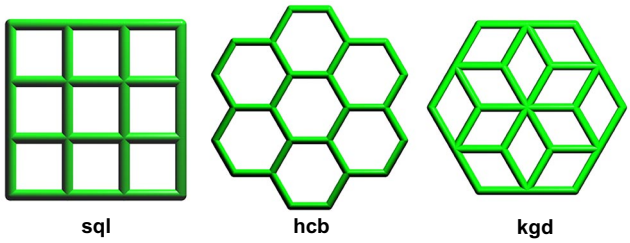


Figure 17. 2-Periodic underlying nets most frequently observed in layered MOCPs. The Figure was prepared by the authors using original data from the study.[152]

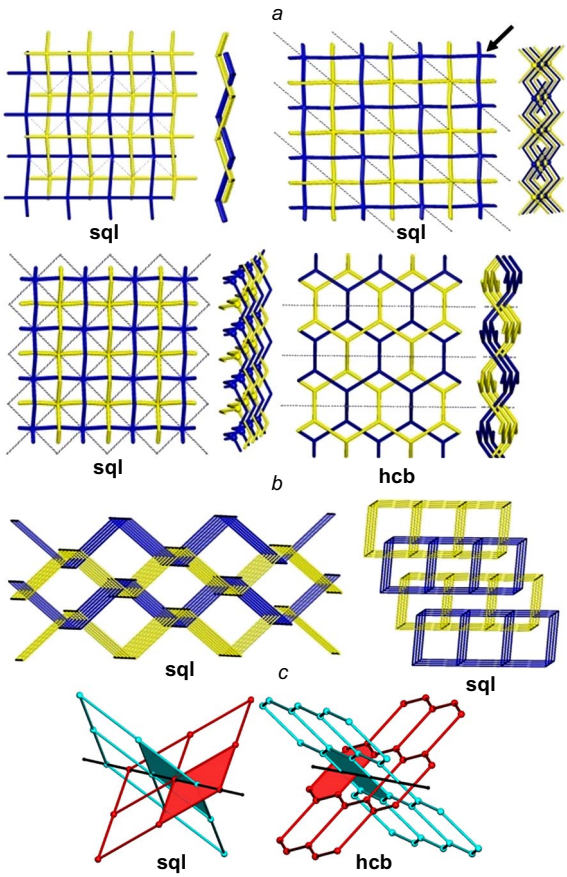


Figure 18. Main types of interpenetration (*a*), parallel (*b*) and inclined (*c*) polycatenation of underlying nets with the **sql** and **hcb** topologies in layered entangled MOCPs. Figure *a* presents the entanglement of nets in two views: perpendicular to the layer and along the layer (the arrow indicates the direction of the lateral view); in Fig. *b*, the first view (on the left) is in the plane of the layer; the second view (on the right) is perpendicular to the first one in the plane of the layer. The Figure was prepared by the authors using original data from the study.[61]

Fig. 17) being most abundant. These nets are characterized by the lowest topological complexity because their formation requires no more than two independent nodes (building units) and only one edge (linker).

The entanglement phenomenon was disclosed in 1319 layered MOCPs, in which 216 topological types of entanglement characterized by different Hopf ring nets were found. Assemblies of nets with the minimum complexity of entanglement are observed most frequently (Fig. 18); 10 simplest types of entanglements account for 75% of the total set.

3.1.3. Chain coordination polymers

The comprehensive topological classification of chain (1-periodic) MOCPs is still lacking, although there are reviews on the main characteristic features of their structures.[154–157] The general classification of 37 046 chain MOCPs, the structures of which are available in the CSD releases (October 2020), is given below.

As in the case of layered and framework polymers, the simplest nets 2C1 (47.5%), 2,4C4 (21.1%), 2,2,3C6 (5.1%), 2,2,3C3 (4.7%), 2,6C1 (2.7%), 2,2,3C4 (2.5%) and (4,4)(0,2) (2.3%) (Fig. 19 *a*) are the most abundant among 1396 topological types of chain MOCPs. In the structures, the polymer chains can run along one (35 601 examples), two (1520 examples), three (136 examples), four (7 examples) or five (one example) directions. Five directions of the extension of the coordination chains, [10$\bar{1}$], [101], [110], [$\bar{1}$10], [100], are observed in the unique coordination polymer [Au{Sn(CH_3)$_3$}(CN)$_2$] (Fig. 19 *b*).

One-periodic coordination polymers can form architectures of higher complexity and dimensionality through entanglement.[158–167] For example, the entanglement types include braids, fabric, weavings, polyrotaxanes, interpenetration and polycatenation (Fig. 20).

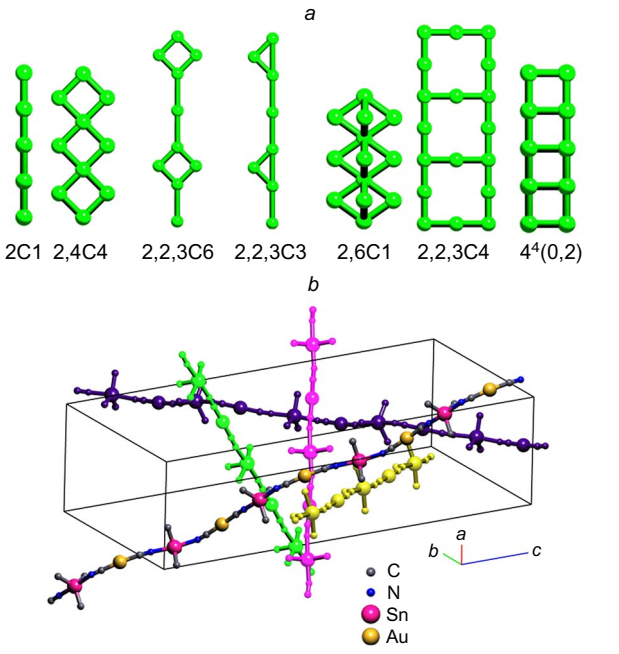


Figure 19. Most abundant 1-periodic underlying nets of MOCPs (*a*) and a fragment of the structure of [Au{Sn(CH_3)$_3$}(CN)$_2$] (POZKOF) illustrating five directions of the extension of coordination chains (*b*). Hydrogen atoms are omitted for clarity. The Figure was prepared by the authors using original data from the study.[158]

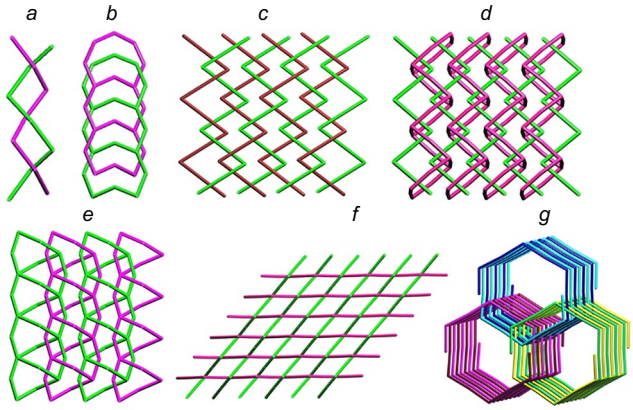


Figure 20. Types of entanglement of chain coordination polymers: (*a*) 1-periodic braid (IXIQIP01); (*b*) 1-periodic interpenetration (CUWXEY); (*c*) 2-periodic weaving (QAGSUO); (*d*) 2-periodic polyrotaxane (INOHEZ); (*e*) 2-periodic polycatenation (ESADEJ); (*f*) 2-periodic fabric (EXAJOE); (*g*) 3-periodic braiding (KEQDOB). The Figure was prepared by the authors using original data from the studies.[160–166]

The entanglements of periodic polymer networks were discussed in a number of publications in recent years.[43, 167, 168] However, the development of straightforward strategies for the synthesis of materials with desired parameters of entanglement have attracted little attention. A significant breakthrough in this field was the design and synthesis of new materials with structures based on 3-periodic woven patterns.[169] In woven fabric structures, the chains interlock.[170] The weaving of one-dimensional structural groups implies their close arrangement and interactions through weak van der Waals or electrostatic forces. This results in the mechanical linking of polymer chains through the mutual superimposition but, as opposed to the interpenetration and polycatenation, woven structures can be, in principle, separated without breaking covalent bonds.

Carlucci *et al.*[43] described 1-periodic helices and 2-periodic fabric and woven (chicken wire) entanglements of 1-periodic coordination polymers.

After the publication of this review, numerous new entangled coordination polymers were reported. For example, in the crystal structure of the complex of a rather simple composition [Cu(ox)(dpa)(H_2O)] (USUMEC; H_2ox is oxalic acid, dpa is di(4-pyridyl)amine), there are two sets of perpendicularly oriented chains connected to form a fabric layer (1D + 1D → 2D).[170] The entanglement can stabilize an original porous crystal structure.[171–173] Besides, such materials serve as dye adsorbents and catalysts[160] and exhibit luminescence mechanochromism,[174] photoluminescence,[175, 176] enantioselective adsorption recognition[177] and selective anion exchange.[178] The topological classification of entanglements of MOCPs can help in developing new procedures for the design of such materials.

3.2. Relationships between local and overall topology

Main general features of the topological structures of MOCPs were investigated in terms of relationships between the local topology of the net, *i.e.*, the specific features of the coordination of its nodes and also various finite fragments

(rings, tiles, clusters), and the overall topology.[115, 139, 179] In particular, the following correlations were found.

1. Nets with the highest possible topological symmetry, which contain the minimum number of topologically different nodes and edges, are the most frequently observed.[139] It should be emphasized that this refers to the topological symmetry (automorphism group of the net) because particular embeddings of these nets can have low spatial symmetry. The high topological symmetry in fact indicates that the minimum number of building units and linkers is required for the assembly of this net, and the assembly is realized in the simplest and rapid way. For example, only one type of building units and one type of linkers are required for the construction of the most abundant topological types of 1-periodic (2C1), 2-periodic (**sql**, **hcb**) and 3-periodic (**dia**, **pcu**) underlying nets although these nets can certainly be composed of a larger number of such components. Therefore, the physical meaning of a particular topological motif is primarily that it encodes the assembly pattern of the MOCP structure, *i.e.*, it reflects the kinetic features of the structure formation process, whereas the geometric properties of the structure (its embedding) reflect the thermodynamic properties (in particular, the energy on interatomic interaction).

2. The coordination figure of the net node in the most symmetric embedding should correspond to the typical coordination of the building unit assigned to this node. For example, in the case of coordination sites in the square environment, the formation of the **dia**, **lon**, **lcs** and **neb** topological types with a tetrahedral environment of the nodes is unlikely. On the contrary, the **nbo** or **cds** nets with square coordination figures are predominantly formed in the case of square building units [*e.g.*, in copper(II) complexes or octahedral complexes with two terminal ligands in *trans* positions]. This correlation between the symmetry of the node and the net generally corresponds to the above relationship between the automorphism group of the net (topological symmetry) and the space group of its embedding (geometric symmetry).

3. In the case of several topological types of net nodes, the formation of this net requires building units, which are prone to generate the corresponding coordination figures in a desired stoichiometric ratio. For example, the **pts** net in the most symmetric embedding contains two types of nodes with tetrahedral and square coordination in a ratio of 1 : 1, and the formation of this net requires building units, which have an appropriate coordination and which can be connected in an equimolar ratio. The ratio of the building units with different compositions and structures in solution can differ from that observed in the crystalline phase. This fact should be taken into account in the design of the experiment.

4. Additional limitations on the possible topology of the underlying net can be introduced when using polynodal building units (polynuclear clusters or low-dimensional periodic polymeric groups). For example, the structures of heteroleptic cyanometallates with the **pcu** and **rob** topologies can be considered in terms of connection of 2-periodic cyanide networks with the **sql** topology though non-cyanide ligands (Fig. 21).

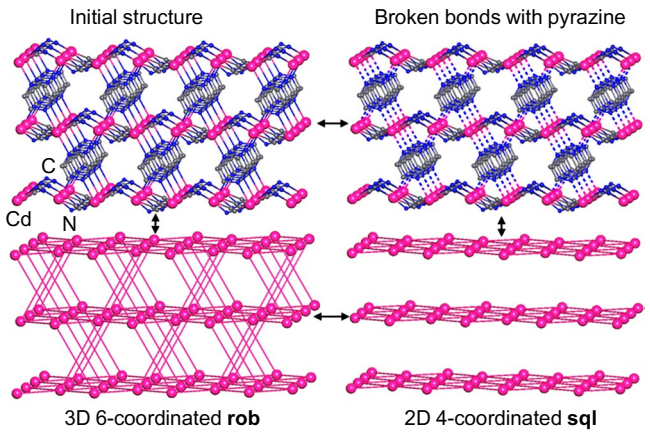


Figure 21. Relationship between the **rob** topology of the [$Cd(CN)_2$(Pyrazine)] framework and the **sql** topology of the {$Cd(CN)_2$} layers.[179] The figure was reproduced with the permission of American Chemical Society.

3.3. Composition – topology – property relationships

The topology is an important property of the crystal structure, which is responsible for its architecture and describes the overall system of interatomic interactions. Therefore, it would be expected that many physical and chemical properties of the crystalline compound depend to some extent on its topology. However, until recently, the main tasks of reticular chemistry were the design of MOCPs with the aim of achieving a desired topology and the examination of methods for the selection of appropriate building units without focus on the particular physical or chemical properties (except for porosity) of the predicted structural motif.[180] Recent studies addressing the relationship between the topology and properties of MOCPs include investigations of diffusion of molecules in pores,[181] controlled solid-state transformations,[182] the development of methods for increasing the adsorption selectivity of light hydrocarbons,[183] the tuning of catalytic[184] and photocatalytic[185] activity and enhancing hydrolytic stability.[186] The correlations between the chemical composition and the topological and physical properties of MOCP structures have been extensively studied in the past decade. However, such investigations were performed only for a limited number of useful physical properties of metal-organic polymers. Besides, the relationships between the structure of the polymer motif and the chemical properties of MOCPs are poorly understood. The physical properties characterized by significant correlations with the MOCP architectures are considered below.

3.3.1. Porosity

High porosity is a very important property of the subclass of MOCPs, metal-organic frameworks. Investigations of these compounds resulted in the emergence of reticular chemistry. Although the topological properties are extensively used in the design of the synthesis of these polymers, the dependence of the porosity on the global topology of the framework has remained unknown for a long time. Actually, the porosity (the free-volume fraction of the framework) seems to be exclusively the geometric parameter and, consequently, the topological properties should have no effect on this property. The comprehensive analysis of the porosity of 33 790 MOFs was performed in the study.[140] For these compounds, the main topological descriptors were also calculated. The following correlations were found:

— there are topologies, which are typical only of low-porosity or high-porosity frameworks, whereas many other topologies can describe frameworks of any porosity;

— most of topologies have an average porosity of about 0.40 – 0.45, with a large spread of values (the rms deviation is > 0.30), which cover almost the whole range of porosity; these topologies can be considered as deformable because they can be robust against strong geometric distortions of the net, thereby providing the diversity of the free volumes and high frequency of the occurrence because all topologies typical of MOFs belong to this groups;

— all groups of structures with a small spread of porosity values are isostructural compounds with one and the same ligand (generally, single-ligand complexes) or with structurally similar building units (ligands and complexing atoms); therefore, rare topologies occur in the case of a special combination of building units, which have an appropriate shape and coordination;

— if the underlying net in the most symmetric embedding is taken as the standard, all other embeddings can be considered as distortions of this net; the same is true for natural tiles for nets. It was found that some tiles can be strongly distorted, while other tiles generally remain close to the standard; it was proposed to use the degree of distortion of tiles for the recognition of deformable topologies and for the design of breathing frameworks. Besides, the recognition is performed using an algorithm of identification of frameworks with the same topology of atomic nets and descriptors of their porosity.[60, 187, 188]

3.3.2. Mechanical properties

The mechanical properties are of great importance for the evaluation of practical applications of MOFs. For the use in industry, adsorbents and catalysts are often subjected to extrusion and granulation (pelletization). By no means all MOFs retain the structure and properties after the compression. For example, HKUST-1 undergoes irreversible collapse under a pressure of > 200 MPa, whereas ZIF-8 loses up to 14% of crystallinity and 10% of the active surface area but retains the adsorption and catalytic (in the esterification of vegetable oils) properties at a high level.[189] It is worth noting than both materials have a very low density (< 2 g mL^{-1}). The Young's modulus of HKUST-1 varies in the range of 3.5 – 10 GPa, whereas it is lower for ZIF-8 (3 – 4 GPa).[190 – 193] These facts indicate that the deformation of the nanoporous MOCP structure leads to structural changes under very low loads, which can be used in experiments. This unique property of MOCPs distinguishes these compounds from traditional nanoporous metals, ceramics and polymers.[194] The collapse and amorphization (vitrification) of the porous structure lead to an increase in its density and, as a consequence, an increase in the elastic modulus and hardness.[195]

The elastic modulus and hardness are proportional to the density and strength (rigidity) of the bonds of microporous materials.[191] For materials with a low density (0.9 – 1.5 g mL^{-1}) and a large porous volume, the elastic modulus is < 9 GPa; for such materials, the elastic modulus weakly depends on the density. The elastic modulus of denser MOCPs (> 2 g mL^{-1}) varies in the range of 20 – 100 GPa, which is also typical of zeolites.[196 – 198] The experimental study of five isostructural UiO-66-type MOFs containing central $Zr^{III,IV}$ and $Hf^{III,IV}$ ions demonstrated that the frameworks with stronger coordination bonds and highly coordinated caboxyoxometallate clusters have higher elastic moduli (34 – 104 GPa).[198]

The density of the material can be increased by introducing guest molecules into pores, which generally prevent the framework from collapse under pressure, for example, in the adsorbent formation process. The elastic modulus and the hardness of the material increase with increasing size of the guest molecules and with increasing strength and number of interactions with the framework.[199, 200] The presence of defects leads to a decrease in the bulk elastic modulus and can cause phase transitions, making it possible to create stimuli-responsive MOFs.[201]

It is worth noting that for different series of structures (*e.g.*, MOFs and zeolites) with the same topology and with different densities and strength of bonds, the general trends in changes in the mechanical properties are retained in going from one topology to another.[192] The Young's modulus strongly depends on the directionality of chemical bonds and the density of node rows in the structure. The highest Young's moduli and the largest linear compressibility are observed along the directions, where the maximum number of rigid bonds and atoms is accumulated. Thus, the mechanical properties of the zeolite-like imidazolate framework ZIF-68 are significantly anisotropic, which is attributed to the anisotropy of pores dictated by the **gme** topology of the framework: the largest channels run along the [001] direction.[191] The structures, which are characterized by a highly nonuniform density distribution of bonds and atoms along different directions, exhibit significant anisotropy of the mechanical properties, which facilitates the appearance of large structural deformations and even negative values of the linear compressibility coefficient along the directions of the lowest density of bonds and atoms. This behaviour is typical of the structures with the so-called wine-rack topology, *e.g.*, MIL-53, MCF-34 and MIL-122(In).[202, 203] Routine porosimetry measurements demonstrated that MOCPs can be used for mechanical energy storage. For example, MIL-53(Cr) absorbs the energy of ~12 J g^{-1}, which is higher than the storage capacity of mesoporous hydrophobic solid materials.[204] The level of absorption of mechanical energy by bumpers or molecular springs can be controlled by selecting appropriate MOCPs. The study of 22 frameworks[205] demonstrated that the anisotropy of the elastic properties of MOFs is largely determined by the geometric-topological type of the frameworks. Thus, the reversible swelling of frameworks during the adsorption of some molecules depends on the presence of inelastic deformation directions and is manifested in metal-organic frameworks with the same geometric-topological motif, *e.g.*, in the isoreticular frameworks MIL-53.

For 2-periodic MOCPs, high anisotropy of the Young's modulus in the directions parallel and perpendicular to the layers is indicative of facile exfoliation, which is of importance for the development of 2D materials.[206]

3.3.3. Proton conductivity

Compounds exhibiting ionic conductivity have attracted attention due to the promising applications of materials based on these compounds in different fields, from energy conversion devices to biological systems.[207] Great attention is given to the development of environmentally friendly and efficient energy sources, in particular in fuel cells.[208] Proton-conducting materials are used as membranes separating the anode and cathode compartments of fuel cells. In such

materials, protons, which are produced by the oxidation of hydrogen at the anode, can be transported to the cathode, at which oxygen is reduced to form water molecules.[209]

Two large classes of compounds, such as amorphous polymers and porous crystalline compounds, hold promise as ion-conducting materials.[210] Metal-organic coordination polymers, which are characterized by the structural order due to the presence of regular and predictable ion migration channels and significantly variable properties,[210] are advanced representatives of the latter class.

The proton transport can occur through the following two mechanisms:[209]

— the relay or Grotthuss mechanism, according to which protons hop from one molecule to another accompanied by the formation and breaking of hydrogen bonds; this mechanism requires the presence of a periodic system of hydrogen bonds and the reorganization of the proton environment, providing a continuous migration pathway of protons;

— the diffusion or vehicle-type mechanism, according to which protons migrate through diffusion of proton-containing groups; the proton conductivity is strongly dependent on the concentration and the diffusion rate of charge carriers; for this mechanism, strong hydrogen bonds act as a retardation factor because these bonds hinder free migration of proton carriers.

Therefore, the presence of a periodic hydrogen bond network formed by functional groups of ligands and(or) adsorbed molecules, serving as proton carriers, is a key factor responsible for the proton transport. From the practical point of view, there are two main lines of the development of proton-conducting membranes:[209]

— the search for new materials providing proton transport in an aqueous medium above 100 °C;

— the development of efficient conductors operating under water-free conditions above 100 °C.

Under anhydrous conditions, the functional groups of the framework or guest molecules with a boiling point of >100°C serve as proton carriers. In this case, rigid frameworks cannot be deformed to be adapted to changes in humidity. Therefore, a hydrogen bond network formed at high humidity can be destroyed with decreasing water content, and the migration pathway of protons will be disrupted. In this respect, flexible MOCPs have an advantage because they are robust against changes in the humidity, retaining the integrity of the framework and the hydrogen bond network.[211, 212]

In particular, the degree of interpenetration of nets was discussed in the literature as the topological property of proton-conducting MOCPs. For example, MOCP with two interpenetrated frameworks shown in Fig. 22 exhibits higher proton conductivity compared to the compositionally similar polymer with four-fold interpenetration, because its structure contains a larger void volume accessible to guest molecules as proton carriers.

However, rigorous structural, geometric or topological criteria for the appearance of proton conductivity are lacking. We analyzed the known crystal structures derived from the CSD,[97, 98] which exhibit proton conductivity, and revealed 119 3-periodic, 68 2-periodic and 40 1-periodic structures, with the **pcu**, **acs**, **rtl**, **sql**, **hcb** and 2C topologies, characteristic of MOCPs, being predominant.

The distribution of the structures according to the nature of the complexing metal is shown in Fig. 23. Zinc, copper, cobalt, calcium and manganese are the most abundant metal centres in proton-conducting MOFs. Iron and nickel atoms characteristic of other classes of MOCPs are rarely observed in proton-conducting frameworks.

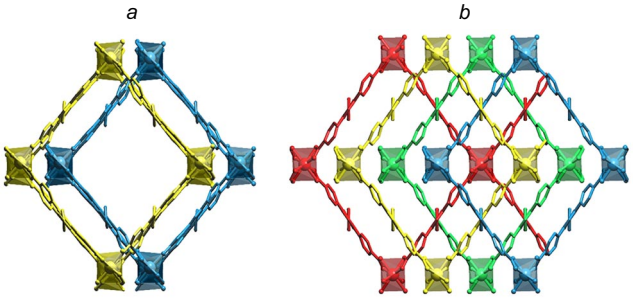


Figure 22. Framework FJU-17 with doubly interpenetrated networks (*a*) exhibiting an order of magnitude higher proton conductivity compared to that of FJU-16 with four-fold interpenetrated networks (*b*). The Figure was prepared by the authors using original data from the study.[213]

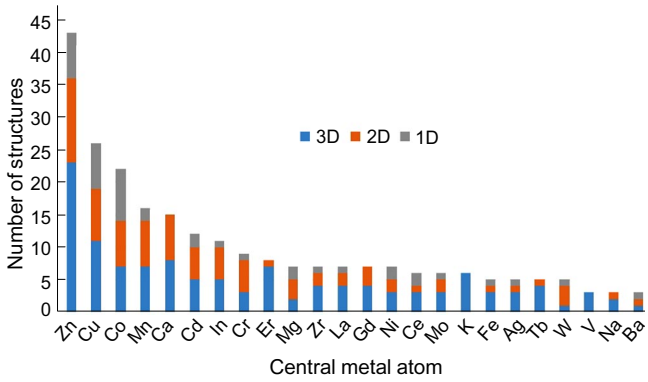


Figure 23. Distribution of proton-conducting MOCPs according to the nature of the central atom and the dimensionality. The Figure was prepared by the authors using data from the CSD.

The diagram presented in Fig. 23 shows that proton-conducting MOCPs containing Zn and Cu as the central atoms predominantly have framework structures; framework, layer and chain structures are approximately equally frequent in Co-containing MOCPs; in MOCPs containing Ca, K, Eu, Tb, Na or V, the chain structures are absent.

The distribution of the structures according to the coordination modes of the ligands involved in proton-conducting MOFs (Fig. 24) shows that monodentate ligands M^1 are the most abundant ligands in the frameworks with any periodicity. Water molecules coordinated to metal atoms and promoting conductivity most often serve as such ligands.

The metal-organic framework of the composition $[Co(bpy)(H_2O)_4](Hbtc)(H_2O)_{1.5}$ (bpy is 4,4′-bipyridine, H_3btc is benzene-1,3,5-tricarboxylic acid) has the highest proton conductivity (0.149 $Ohm^{-1}\,cm^{-1}$ at a relative humidity of 98% at 80 °C) compared to all characterized compounds. As can be seen from the structure (the fragment of this structure is presented in Fig. 25 *a*), benzenetricarboxylic acid molecules interact with water molecules coordinated to cobalt atoms to form hydrogen bond chains providing migration pathway of protons. The structurally similar compound (Fig. 25 *b*), which was synthesized using the dianion of furan-2,5-dicarboxylic acid (H_2fdc) as the

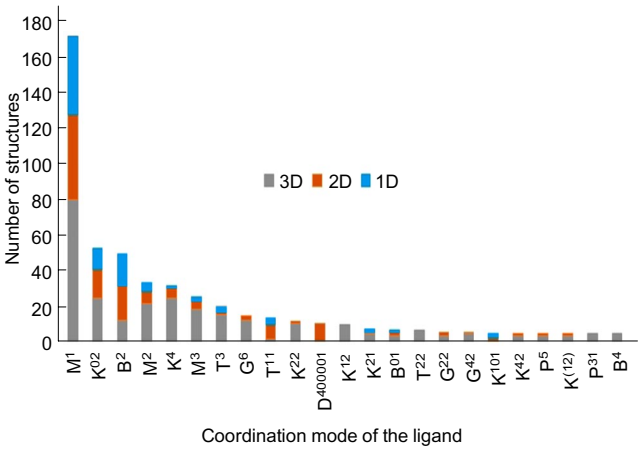


Figure 24. Distribution of proton-conducting structures according to the coordination modes of the ligand. The Figure was prepared by the authors using data from the CSD.

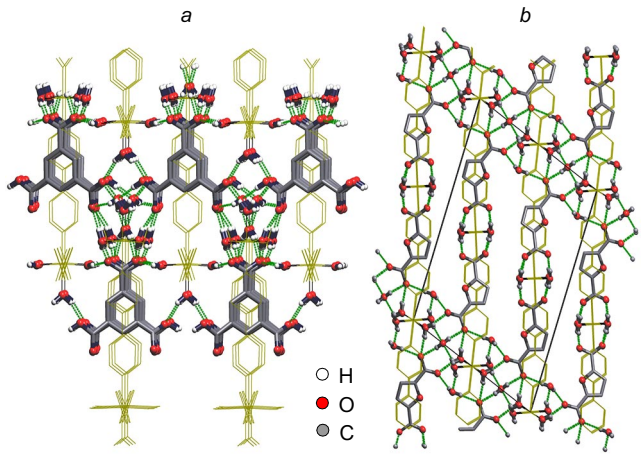


Figure 25. Fragments of the structures of $\{[Co(bpy)(H_2O)_4](Hbtc)(H_2O)_{1.5}\}_n$ (PIHSIL) (*a*) and $[Co(bpy)(H_2O)_4](fdc)\cdot(H_2O)_{1.5}\}_n$ (PIHSEN) (*b*). Green dashed lines indicate hydrogen bond chains responsible for proton transport. The Figure was prepared by the authors using original data from the study. [214]

template, also contains infinite hydrogen bond chains but has 30 times lower proton conductivity due to the lower concentration of carboxyl groups serving as proton carriers.

Since the presence of infinite hydrogen bond chains is one of the key conditions for the frameworks to exhibit proton transport, we screened the CSD for MOCPs containing networks of O···O contacts with distances < 5 Å. At such distances between the oxygen atoms, water molecules can be inserted into the frameworks to form stable hydrogen bonds. Significantly different ratios of 1-, 2- and 3-periodic networks of such contacts in proton-conducting MOCPs (227 structures) and MOCPs, the conductivity of which is unknown (17 857 structures), are evidenced by the data given in Table 2 and presented in Fig. 26.

A significant difference in the fractions of networks of O···O contacts in sets of proton conductors and MOCPs indicates that these networks can serve as the criterion for the screening of potential proton conductors. In proton-conducting structures, in which there are no periodic O···O

Table 2. Distribution of 1-, 2- and 3-periodic networks of O···O contacts with distances < 5 Å in MOCPs.

Type of network	*n* (%)	*m* (%)
1-Periodic	11.6	17
2-Periodic	12	16
3-Periodic	68.2	36.4
Periodic network is absent	8	30.6

Note. *n* is the fraction of the total number (227) of structures of proton-conducting MOCPs; *m* is the fraction of the total number (17 857) of MOCP structures, the conductivity of which is unknown.

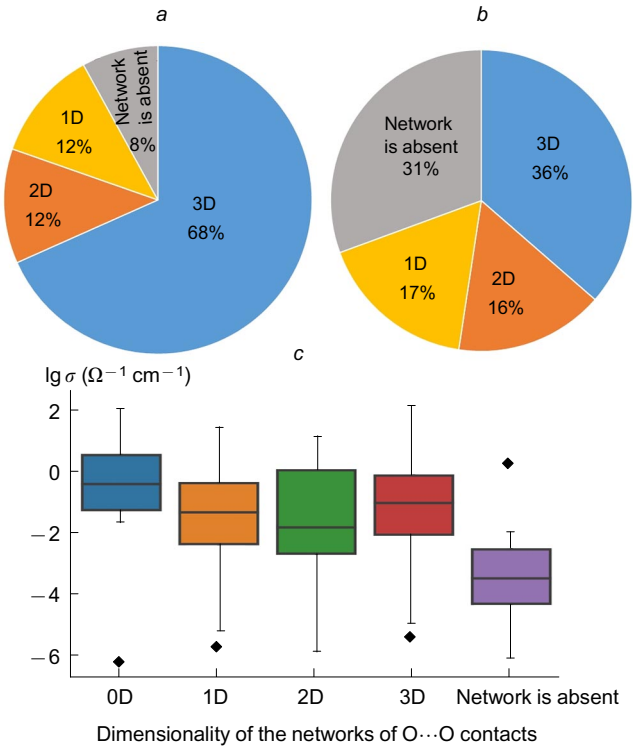


Figure 26. Distribution of the structures according to the periodicity of the network of O···O contacts with distances < 5 Å for the known proton-conducting MOCPs (227 structures) (*a*) and for MOCPs, the conductivity of which is unknown (17 857 structures) (*b*), and the relationship between the proton conductivity and the periodicity of these nets (*c*). The Figure was prepared by the authors using data from the CSD.

networks, hydrogen bonds can be formed by other atoms (nitrogen, halogens, *etc*.) or their pores can be occupied by molecules (water, imidazole, *etc*.) transferring protons through the vehicle-type mechanism. However, the conductivity of such structures is significantly lower compared to that of MOCPs containing periodic networks of O···O contacts, the conductivity being almost independent of the periodicity (see Fig. 26).

4. Reticular design

The progress in the reticular chemistry has triggered the emergence of new ideas regarding approaches to the design of crystalline compounds and materials. Like organic chemistry, where the topological factors (modes of binding of atoms and the formation of particular topological motifs,

such as chains, rings or cages) play a great role in the design of the synthesis of new molecules, the reticular chemistry utilizes topological motifs, which serve as templates for the synthesis of polymer structures with different compositions and different properties. The design of the structures, based on such templates and the principles of their formation and modification, is referred to as the reticular design.[88, 139, 215–218] It should be emphasized that not all principles of reticular design directly employ the topological properties of the structure. For example, the introduction of particular functional groups into the framework or the encapsulation of molecules into the cavities of the framework can be considered as tools of chemical design. However, this modification occurs on an appropriate topological template, the topology of which should be controlled during the modification (either remained unchanged or be varied in a desired manner); therefore, the role of the topological parameters of the structure is retained.

This Section considers only the main topological principles of reticular design, without discussing approaches, in which the topological properties of the structure are indirectly taken into account. The basics of the reticular design are comprehensively summarized in reviews and monographs (see, *e.g.*, Refs. 219–228). It was demonstrated in detail how various tools of reticular design can be used to achieve desired properties of materials in relation to proton-conducting MOCPs (see Section 4.2.2). It is worth noting that the reticular design has moved beyond the borders of the MOCP class and are increasingly being used for the straightforward synthesis of other classes of compounds, such as zeolites,[229] covalent organic frameworks,[230, 231] hydrogen-bonded organic frameworks,[232–235] covalently linked hydrogen-bonded organic frameworks,[82, 236] coordination cages.[237] The possibility of controlling the assembly of polymeric groups in the structure is important for this extension of applications.

4.1. Topological design principles

Main principles of the topological design are presented in the reviews[88, 139, 215–218] on the basic principles of reticular chemistry. These principles demonstrate how the structural motif (underlying net) with the desired topology can be obtained, how this motif can be changed in a desired way or, on the contrary, how to retain this motif upon the modification of the chemical composition.

4.1.1. Decoration and expansion of the underlying net

As mentioned above, the underlying net encodes the mode of assembly of the structure from atoms or polyatomic groups (building units), and the methods of simplification allows the separation of these units. The decoration is inverse to the simplification procedure. The decoration involves the replacement of nodes of the underlying net by building units and of the edges of the underlying net by linkers between these units; interatomic distances, bridging atoms or polyatomic groups (ligands or complex groups) can served as linkers.[238] For example, the known structure of prussian blue has the **pcu** topology of the underlying net due to the ideal octahedral coordination of cyano groups in the framework. However, the clusters $[Nb_6Cl_{12}(CN)_6]^{x-}$ and $[Me_6Q_8(CN)_6]^{x-}$ (Me = Re^{II}, Mo^{II}, W^{II}; Q = S, Se, Te) also can provide the octahedral arrangement of terminal cyano groups due to which the frameworks decorated by cyano groups have the **pcu** topology.[239–241] A combination of the octahedral and trigonal-prismatic coordination figures typical of the **nia** net is observed also in the series of d–f cyanometallates $[LnMe(CN)_6](H_2O)_n$ (Ln = Bi^{III}, Y^{III}; Me = Fe^{III}, Co^{III}, Cr^{III}, Ru^{III}; n = 0, 0.5, 1.5) and in the framework $[La\{Re_6Te_8\}(H_2O)_3(CN)_6]$ decorated by the octahedral cluster.[242, 243] In both structures, the lanthanide has a trigonal-prismatic coordination environment involving cyanide groups (the other 1–3 sites are occupied by water molecules).

The expansion of the underlying net is a special case of the decoration. In this procedure, the edges are replaced by linkers of different lengths, which are often long bridging ligands or linear complex groups; this procedure can formally be considered as the replacement of the edge of the underlying net by chains of nodes with the coordination 2. The potential applications of the isoreticular expansion were investigated in most detail for frameworks with the **pcu** topology. The expansion was used for nets with mononuclear and polynuclear nodes. Thus, bidentate bridging ligands in a ratio of 3 : 1 with the coordination sites form frameworks with the **pcu** topology in 594 structures (without disorder) derived from the CSD, which allows the variation of the percentage of the extraframework space from 20.7% in $[Ni(N_3)_2(btae)]$ (LUGTUD; btae is 1,2-bis(tetrazol-1-yl)ethane)[244] to 40–50% in metal formate frameworks containing cations in the cavities (*e.g.*, $C(NH_2)_3[Mn(HCOO)_3]$)[245] to 72.7% in the cuboid frameworks $[Zn(bpb)(SiF_6)]\cdot CHCl_3\cdot H_2O$ (WONZUV; bpb is 1,4-di(4-pyridyl)benzene).[246] The isoreticular series of 103 structures was found for MOF-5 structures to within the coordination mode of the ligand and the presence of tetranuclear building units $\{M_4O(CO_2)\}$ with a percentage of the extraframework space varying from 60.7% in the framework with the ((4-chlorobenzoyl)amino)terephthalate ligand (HOLQIK)[247] to 86.1% in the framework with 4,7-bis(4-carboxylatophenyl)-1,3-dimethyl-1*H*-benzimidazol-3-ium (RUTNOK).[248]

4.1.2. Principles for the selection of building units for decoration

For the correct selection of building units, it is necessary to know their coordination capacities, such as the typical coordination numbers and figures for complexing atoms and polynuclear complex groups, coordination modes of ligands and the compatibility of the building units. These data are available in topological knowledge bases under the development, which should become important tools of reticular design in the near future. The principle of isoreticular chemistry was applied to vary the ligands in the beginning of the 21st century.[249, 250] The approach is based on the replacement of ligands having similar coordination capacities in the structures of known frameworks. This may give rise to similar structures with the same topological motif but with different properties (*e.g.*, with different densities and porosity).

This strategy was used to construct framework structures with the MIL-88 topology,[251] analogues of MOF-5,[252] to predict the highly porous metal-organic framework NU-100.[253] By employing *ab initio* modeling tools and empirical methods, this approach was applied to generate 204 hypothetical frameworks using the $\{Zr_6O_4\}$ building units with 12 dicarboxylate and 36 tetracarboxylate ligands for nets with the **fcu**, **ftw**, **scu** and **csq** topologies.[254] As a result, the new metal-organic framework NU-800 with the **fcu** topology, exhibiting high methane adsorption capacity, was predicted and then synthesized; besides, it was demonstrated how the arrangement of functional groups in the

ligand affect the efficiency of the packing of methane molecules about the clusters under high pressure. The predicted methane adsorption was confirmed by adsorption isotherm measurements; the H_2 and CO_2 adsorption was also high under high pressure. The CSD contains 93 structures of isoreticular UIO-66-type polymers with the **fcu** topology of the underlying net and with the extraframework space varying from 55.2% in [{$Zr_6O_4(OD)_4$}$(bedo)_6$] (BOHXIH; H_2bedo is but-2-en-1,4-dioic acid)[255] to 82.4% of the unit cell volume in [{$Zr_6O_4(OH)_4$}$(hdmdb)_6$] (KOPJUX; H_2hdmdb is *N*,*N*′-bis(4-carboxyphenylmethylidene)hydrazinyldibenzoic acid).[256]

4.1.3. Reconstruction

There are the following two modes of reconstruction:[257–264]

— the solid-state reaction resulting in the change in the connectivity of the structure, in particular in a decrease or an increase in the periodicity or the appearance (disappearance) of entanglement;

— the replacement of one type of building units by another one; this replacement can be formally represented as subnet — supernet transitions, but is chemically accomplished using different methods of synthesis.

The former mode of reconstruction can occur under appropriate thermodynamic conditions even without destruction of crystallinity (single crystal – single crystal transition). The second mode of reconstruction is considered as the way of selecting building units in the step of experimental design. The applicability of the topological approach to the prediction of the solid-state reaction products was demonstrated in relation to the dehydration of [$M(tcnopr3OH)_2(H_2O)_2$] (M = Ni^{II} and Co^{II}; tcnopr3OH is 1,1,3,3-tetracyano-2-(3-hydroxypropoxy)prop-2-en-1-ide accompanied by the transformation of the 1-periodic coordination polymer into the 3-periodic polymer (1D → 3D). The method is based on the generation of subnets and(or) supernets, which can display potential bonds in intermediate structures or stable phases produced in solid-state transformations. All possible contacts about the coordination site in a radius of 7 Å were taken into account. As a result, the total number of the bond cleavage and formation combinations was 760 254, and the number of underlying nets was 93. The larger number of symmetrically independent atoms and potential coordination bonds in [$Co(tcnopr3OH)_2(H_2O)_2$] compared to [$Ni(tcnopr3OH)_2(H_2O)_2$] leads to 2 184 182 combinations but only to 45 different topological types. Nevertheless, the transformations of parallel chains with the 2,4C4 topology into the framework with the **flu**-3,6-*C*2/*c* topology are limited by chemical and geometric requirements. As a result, only 72 different transitions of the compound [$Ni(tcnopr3OH)_2(H_2O)_2$] and 86 transitions of the compound [$Co(tcnopr3OH)_2(H_2O)_2$] were found that are consistent with the exact topology of the compounds [$Ni(tcnopr3OH)_2$] and [$Co(tcnopr3OH)_2$] but with different sets of bonds.

The second mode of reconstruction can be illustrated by a series of coordination polymers with different degrees of linking of the parallel [Zn(ndc)] layers (H_2ndc is naphthalene-2,6-dicarboxylic acid) with the **sql** topology (Fig. 27). The {$Zn(CO_2)_2$} dimers act as 4-coordinated nodes. They are connected by phenylene bridges to form a 2-periodic network. In the directions perpendicular to the layers, there are vacant coordination sites at Zn^{II} ions. In the clathrate structure [Zn(ndc)(DMF)]·0.5C_6H_6 (EWEVAD) containing layers of the composition, these coordination sites are occupied by terminal dimethylformamide ligands. The replacement of 3/4 of the terminal ligands by the bridging ligands in [$Zn(ndc)(bpdpca)_{3/8}(H_2O)_{1/4}$] (NILFAS; bpdpca is 4,4′-bis(4-pyridylcarbonylaminobiphenyl) leads to the connection of four thin layers to form one thick layer with the 5,6L48 topology. Due to the penetration of bpdpca through four-membered rings of two thin layers, thick layers form a polycatenated assembly. The complete replacement of the terminal ligand with the bridging one results in the formation of the 3-periodic coordination polymer [Zn(ndc)(bpe)] with the **pcu** topology, which can be, depending on the conditions of the synthesis, doubly (RELLAW)[145] or triply (PITREQ)[146] interpenetrated with a free volume fraction of 62.5 and 42.5%, respectively.

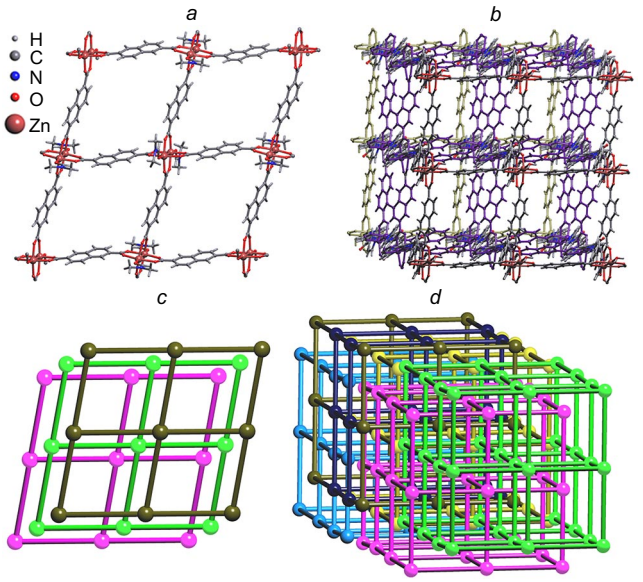


Figure 27. Fragments of the [Zn(ndc)(DMF)] (*a*) and [$Zn(ndc)(bpdpca)_{3/8}(H_2O)_{1/4}$] (*b*) structures and the **sql** (*c*) and 5,6L48 (*d*) underlying net topologies, respectively. The Figure was prepared by the authors using original data from the studies.[263,264]

The combinatorial analysis of closely related zinc(II) malonates with a rod structure, which are connected by diaza-containing linkers in different fashion, was considered in the publication.[257] Other types of topological reconstruction were described in the reviews.[258–262]

4.2. Examples of the design of coordination polymers and metal-organic frameworks

4.2.1. Design of coordination polymers and metal-organic frameworks with a given network topology

Due to the progress over the past two decades, reticular chemistry became an important tool in the design of new MOCPs with specified structure and properties. There are many examples of the theoretical design and the subsequent successful synthesis of MOCPs,[265] in which the above principles and general patterns were used in complex.[265]

The relationships between the geometry of the building units and the framework topology were determined for Zr-MOFs with octahedral clusters{Zr_6O_8}.[266] The detailed topological analysis of 211 structures based on the hexanuclear clusters {Zr_6O_8} and di- or polycarboxylate ligands, including 44 Zr-MOFs with tetracarboxylate ligands, was performed.[266] In particular, 39 structures contain the planar

tetracarboxylate ligand and have the topology of 4,12-coordinated **ftw** and **shp** nets, 4,8-coordinated **csq**, **sqc**, **scu** nets and the 4,6-coordinated **she** net according to the cluster coordination of 12, 8 and 6, respectively.

Frameworks with the **ftw** topology combine the highest thermodynamic stability with the most extensive system of channels and the lowest probability of interpenetration. Four frameworks of this type are less symmetric than the other frameworks due to the deviation of the ligand geometry from square towards rectangular (the ratio of the edge lengths $a:b$ = 1.03 and 1.15). However, the synthesis demonstrated that the **ftw** topology is stable only up to a particular $a:b$ ratio. Thus, the most significant deviation of the ligand configuration from square ($a:b$ = 1.78) leads to a decrease in the coordination of the cluster from 12 to 8 and the appearance of the 4,8-coordinated **scu** net. The ligand with a higher ratio $a:b$ = 2.28 stabilizes the 4-coordinated cluster environment and the **lvt** topology. It is worth noting that each underlying net with this connectivity is characterized by the minimum possible diversity of vertices and edges. For example, the **ftw**, **shp**, **csq**, **sqc**, **scu**, **she** nets contain two types of nodes (corresponding to the cluster and the ligand) and only one type of edges.

The revealed relationships were used in the design of three new porous frameworks of the compositions $[Zr_6O_4(OH)_4(bptc)_3]$ (Zr-bptc; H_4bptc is biphenyl-3,3′,5,5′-tetracarboxylic acid), $[Zr_6O_4(OH)_4(abtc)_2(OH)_4(H_2O)_4]$ (Zr-abtc; H_4abtc is 3,3′,5,5′-tetracarboxyazodibenzene) and $[Zr_6O_4(\mu_3\text{-}OH)_4(tptcMe_2)(HCOO)_4(OH)_4(H_2O)_4]$ (Zr-tptcMe$_2$; H_4tptcMe$_2$ is 2′,5′-dimethyl-[1,1′:4′,1″-terphenyl]-3,3″,5,5″-tetracarboxylic acid) with an optimized pore size for the efficient separation of C_6 alkane isomers (Fig. 28). This separation is of great practical importance because it is a key step in the production of premium unleaded petrol. The optimized pore size of the Zr-bptc framework allows the adsorption of a considerable amount of n-hexane (70% higher compared to the industrial zeolite 5A) but not of branched isomers. The Zr-abtc framework is able to separate three C_6 isomers with the highest selectivity for 3-methylpentane over 2,3-dimethylbutane.

To search for new MOCPs of this family, the topological reconstruction was performed using the net–subnet approach. It was found that 4,8-, 4,6- and 4-coordinated MOCPs can be derived from the 4,12- coordinated **ftw** net by the exclusion of a part of 4-coordinated nodes, which is equivalent to the modeling of ordered lattice defects associated with a decrease in the amount of the ligand in the framework. The analysis of all possible topologically simple (with the smallest number of nonequivalent nodes and edges) **ftw** subnets revealed all possible underlying nets of MOCPs with such topologies as 4,6-coordinated **soc**, 4,6-coordinated **stp** and 4,8-coordinated **sql** (Fig. 29).

Other limitations on the symmetry and the coordination numbers of the nodes of the underlying nets are considered in the studies [51, 267–269] related to the design of new frameworks. For example, it was demonstrated that the assembly of ring hexagonal building units based on the hexanuclear Zr^{IV} cluster can be controlled in order to create a hypothetical structure from polybenzene (**pbz**) or cubic graphite, which was described ~70 years ago.[270] The cationic and mixed-valence trigonal-prismatic clusters $\{Fe_3O(CO_2)_6\}$

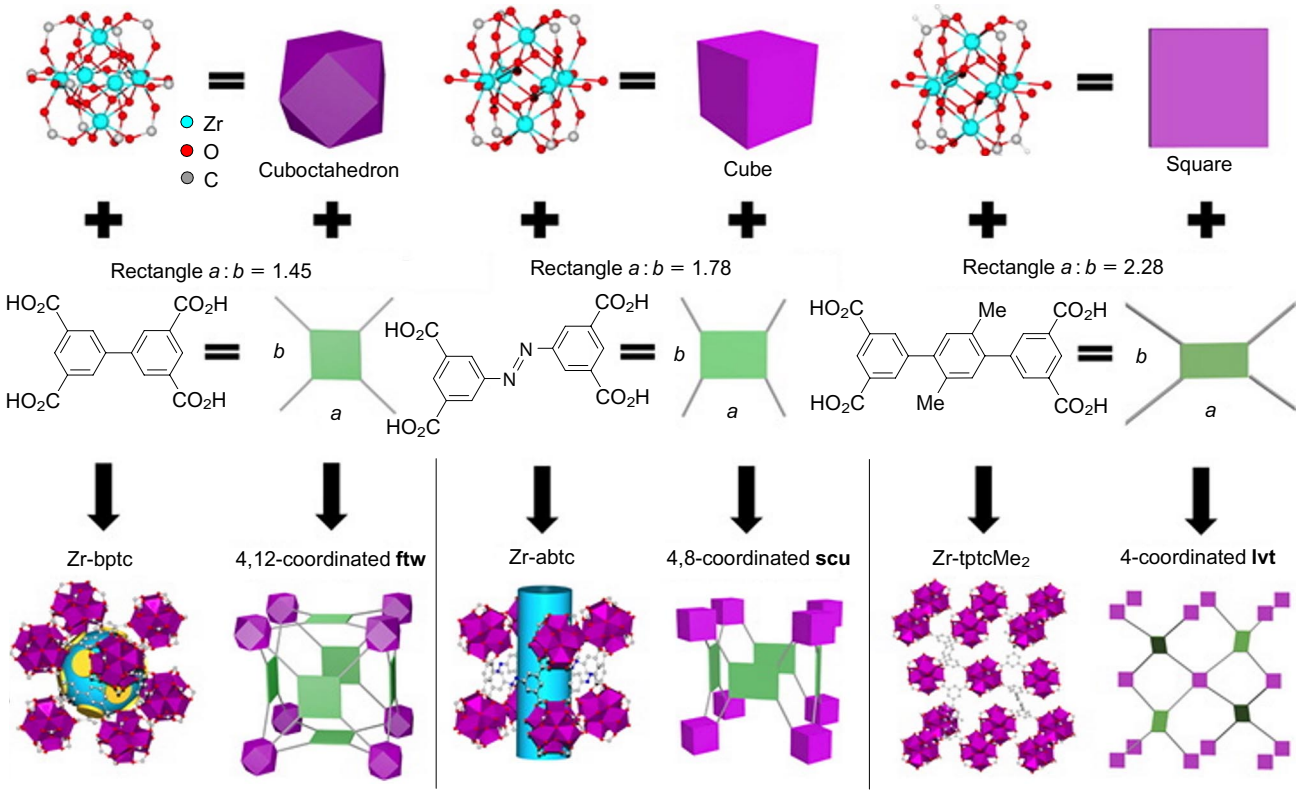


Figure 28. Schematics of the design of three porous frameworks (lower row) $[\{Zr_6(O)_4(OH)_4\}(bptc)_3]$ (left column), $[\{Zr_6(O)_4(OH)_4\}(abtc)_2(OH)_4(H_2O)_4]$ (central column) and $[\{Zr_6(O)_4(OH)_4\}(tptcMe_2)(HCOO)_4(OH)_4(H_2O)_4]$ (right column) from organic linkages with a rectangular coordination figure (middle row) and octahedral clusters with the cuboctahedral, cubic and square coordination figures (upper row).[266] Reproduced with the permission of Nature Research.

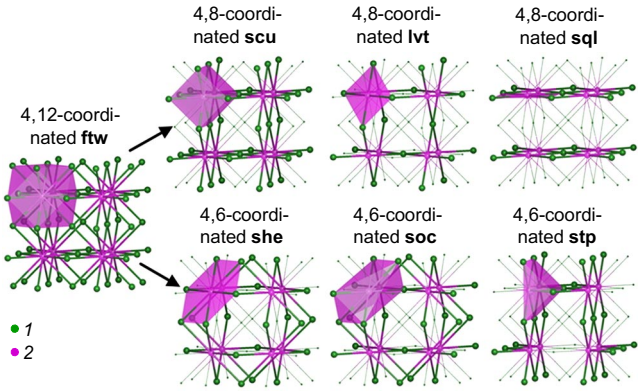


Figure 29. Schematics of the reconstruction of the underlying nets of Zr-MOFs based on hexanuclear clusters $\{Zr_6O_8\}$ and tetracarboxylate ligands.[266] *1*, the center of the $\{Zr_6O_4(OH)_4\}$ cluster; *2*, the center of the tetratopic ligand. Reproduced with the permission of Nature Research.

combined with benzene-1,4- and benzene-1,3-dicarboxylic acid linkers were used in the design and synthesis of two metal-organic frameworks with the highly symmetric underlying net with the **acs** topology characteristic of the connection of nodes with trigonal-prismatic coordination figures.[179] The photoinduced solid-state [2 + 2]-cycloaddition reactions are also applied in the design and synthesis of frameworks with a new topology.[271]

4.2.2. Design of proton-conducting metal-organic frameworks

Let us consider proton-conducting MOCPs as an example of a class of compounds possessing the specified physical property, which were synthesized using different approaches to the design.[265] As demonstrated above (see Section 3.3.3), the proton conductivity correlates with the topology (dimensionality) of a hydrogen bond network. Apparently, the proton conductivity is not directly related to the framework topology, thereby making it possible to produce proton conductors based on frameworks of any topological type by choosing appropriate building units according to the design principles I–VI listed below. In this case, the goal of design is not to form a particular topological type but to chemically modify the framework with a specified topology in order to impart proton conductivity to the framework and preserve other useful properties (*e.g.*, flexibility) determined by its topology.

I. The use of ligands containing functional groups capable of participating in hydrogen bonding. One of the main conditions for the appearance of proton conductivity is the presence of an extensive hydrogen bond network, providing the proton migration. Frameworks, the structures of which have such continuous hydrogen bond networks, are capable of proton transfer even in the absence of incorporated molecules. Thus, in the $[La(H_5L)(H_2O)_4]$ structure (L is 1,2,4,5-tetrakis(phosphonomethyl)benzene), trivalent metal atoms form a water-stable network with phosphonic acid moieties. Water molecules enter the channels of the structure and form hydrogen bonds with the phosphonate groups, thereby providing proton migration paths.[272] Some MOCPs were found to have anisotropy of conductivity, and the direction along which the highest conductivity was observed coincides with the arrangement of hydrogen-bonded chains.[273–275]

II. The use of ligands containing nonpolar moieties. The presence of nonpolar moieties along with functional groups in the ligands is favourable for proton hopping through the vehicle mechanism due to weaker interactions between the framework and the extraframework proton carriers. In particular, MOF with naphthalenedicarboxylate ligands has a higher proton conductivity compared to that of the structurally similar MOF with benzenedicarboxylate ligands.[276]

III. An enhancement of stability of the framework under high humidity conditions. The proton transfer through the vehicle mechanism can occur in the frameworks, which are capable of adsorbing a large amount of water molecules retaining the mobility in the pores.[207] Correspondingly, it is necessary that the MOCP structure is water-stable. The most commonly used approach to enhancing stability in an aqueous environment is based on an increase in the strength of coordination bonds, for example, due to the use of hard acids (Cr^{III}, Al^{III}, Zr^{IV} ions) for the more selective binding to hard base anions, or the use of a negatively charged N-donor ligand, *e.g.*, the imidazolate anion, as the linker.[210]

IV. The surface modification of the pores with hydrophilic functional groups. Using coordination polymers of the MIL-53 series modified by amino, hydroxy or carboxyl groups, it was demonstrated that, at the same humidity, the conductivity increases with decreasing pK_a (with increasing acidity constant). An increase in the acidity also leads to a decrease in the activation energy for proton transport.[277]

Metal-organic coordination polymers, which contain sulfonic groups, form a hydrogen bond network and act as proton donors, can form structurally mobile frameworks,[78] resulting in an increase in their proton transport capability.[279,280] Kitagawa and co-workers[282] demonstrated that the presence of uncoordinated sulfonic groups in MOCP pores (Fig. 30) provides their proton conductivity even at low relative humidity (60%). However, the insertion of uncoordinated sulfonic groups into the polymer structure is hindered due to their tendency to interact with metal ions. Therefore, Phang *et al.*[281] proposed a method of postsynthetic modification of MOCPs, which was considered in

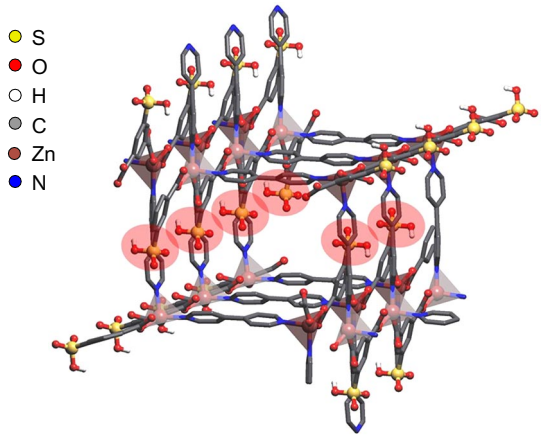


Figure 30. Fragments of the $Zn[(bpy)(C_6H_3(COO)_2SO_3H)]\cdot\cdot DMF\cdot 2H_2O$ structure (PULMAM). Uncoordinated sulfonic groups (enclosed in pink ovals) are responsible for high proton conductivity of this MOF. The Figure was prepared by the authors using original data from the study.[282]

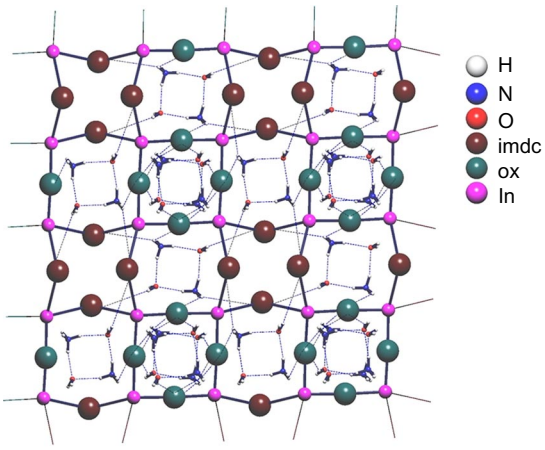


Figure 31. Structure of $[In(Himdc)(ox)]\cdot(NH_4)(H_2O)_{1.5}$. The Figure was prepared by the authors using original data from the study.[283]

relation to the oxidation of thiol groups in UiO-66$(SH)_2$ with hydrogen peroxide.

V. The use of a charged network with incorporated countercations. The compound $[In(Himdc)(ox)]\cdot(NH_4)(H_2O)_{1.5}$ ($imdc^{2-}$ is imidazole-4,5-dicarboxylate) has a high proton conductivity. This compound is characterized by the presence of negatively charged layers of the framework hydrogen-bonded to ammonium cations (Fig. 31).[283] The structure of this MOCP contains two types of channels, along which protons can migrate. In one type of channels, ammonium cations are involved in the proton transport; in the pores of another type, the proton migration occurs through carboxyl groups of the channels and water molecules. The high proton conductivity of this compound is due, in particular, to the dual role of the imidazoledicarboxylate anion. The latter is involved in an extended hydrogen bond network and serves as the proton carrier.

The high anhydrous proton conductivity of $[((CH_3)_2NH_2)_3(SO_4)]_2[Zn_2(ox)_3]$ with the anionic zinc oxalate framework and the 1-periodic cationic dimethylammonium sulfate assembly (Fig. 32) is attributed to the presence of a hydrogen bond network at the interface between the cationic assembly and the anionic framework. In the presence of water, the conductivity of this compound is significantly enhanced because its structure contains groups exhibiting acidic and basic properties,

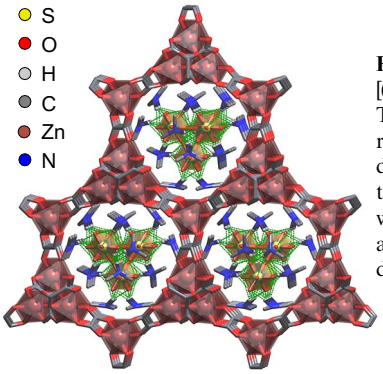


Figure 32. Structure of $[((CH_3)_2NH_2)_3(SO_4)]_2[Zn_2(ox)_3]$. The hydrogen bond chains responsible for proton conductivity are indicated by thin green lines. The Figure was prepared by the authors using original data from the study.[275]

and water molecules can easily be transferred through the framework.

The design approaches, which do not involve the selection and modification of the building units of MOCPs, can be considered separately.

1. The modification of the nature of counterions. High proton conductivity can be achieved by modifying the nature of counterions because they can be significantly different in the size and ability to form hydrogen bonds (Fig. 33).[284, 285] The use of small polycarboxylic acid molecules, which form a hydrogen bond network, holds promise for compensating the framework charge.[214]

2. The incorporation of proton carriers into MOF pores. Molecules incorporated into MOF pores can significantly change the properties of the material.[286] The proton conductivity in aqueous media significantly increases with increasing number of water molecules coordinated to or adsorbed on the framework.[287] This is most clearly shown for a series of five Ca-MOFs synthesized from different solvents (water, dimethylformamide, dimethylamine, dimethyl sulfoxide) and containing different amounts of water molecules.[288] Sadakiyo *et al.*[289] studied the polymer $(NH_4)_2(adp)[Zn_2(ox)_3]\cdot n\,H_2O$ (n = 0, 2, 3; H_2adp is adipic acid) and demonstrated that a change in the proton conductivity is associated with a change in the periodicity of a hydrogen bond network in the MOF structure. Anhydrous MOF does not exhibit proton conductivity, the dihydrate is characterized by moderate proton conductivity, while the conductivity of the trihydrate is two orders of magnitude higher than that of the dihydrate. In the dihydrate, the number of hydrogen bonds between ammonium anions, oxalate anions, water and adipic acid molecules is significantly smaller and these bonds are weaker. The anhydrous

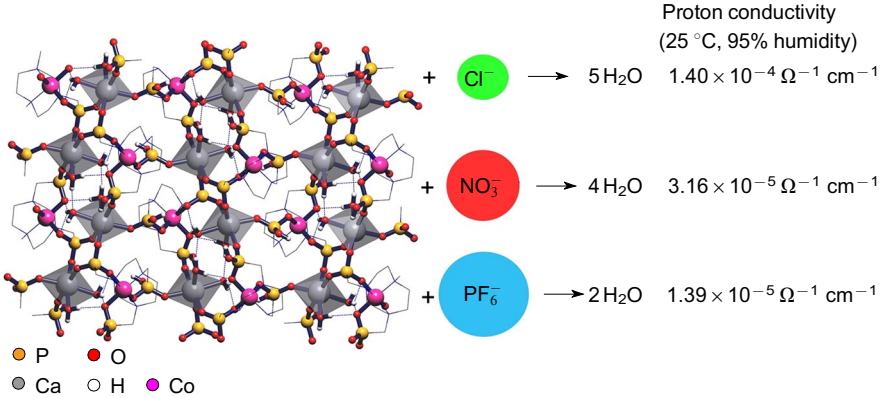


Figure 33. Effect of the nature of the anion on the number of water molecules of crystallization in the structures with chloride (EFEDAX), nitrate (BECXUF) and hexafluorophosphate ions (BECYAM) consisting of compositionally identical $\{Ca(H_2O)_2[Co(C_9H_{20}N_3P_3O_9)]\}_n^+$ polymer layers. The number of water molecules of crystallization decreases with increasing size of the ions, resulting in a decrease in the conductivity. Hydrogen bond chains responsible for proton conductivity are indicated by thin blue lines. The Figure was prepared by the authors using original data from the study.[284]

structure contains hydrogen bonds between the oxalate ion, the ammonium cation and adipic acid, while a hydrogen bond network between the layers of the structure is absent. The authors attributed the significant difference in the conductivity of the dihydrate and the trihydrate to the presence of chains of water molecules and additional hydrogen bonds between water and adipic acid molecules in the trihydrate.

The incorporation of imidazole molecules into the pores of a material is often used to increase the proton conductivity under anhydrous conditions. The treatment of MOFs, stable in an acidic medium, with strong acids [290–293] is quite often employed. In this case, acidic drops consisting of hydrogen-bonded water and acid molecule are formed within the pores of the framework. These drops are involved in the proton transport through the Grotthuss mechanism, as in the MIL-101 structure in toluenesulfonic acid and trifluoromethanesulfonic acid.[291] A decrease in the pH value of the medium leads to an increase in the conductivity and a decrease in the activation energy for proton transfer.[290] Polyoxometalate clusters, which form strong hydrogen bonds with water molecules, also can occupy MOF pores, providing proton conductivity.[294]

3. The control of the mobility of proton carriers. A comparison of the conductivity of In-MOFs, in which dimethylammonium cations (either encapsulated or freely moving in the cavities) serve as proton carriers, demonstrated that the mobility of the carriers is among the key factors responsible for the enhancement of proton conductivity.[295–297]

4. The use of open metal coordination sites for the immobilization of water molecules or other protonic (ionic) molecules. Metal cations having open coordination sites can coordinate water molecules, thereby also facilitating an increase in the proton conductivity. Figure 34 presents an example of sulfonate MOF, in which some metal—ligand bonds are absent, resulting in the presence of coordinatively unsaturated Cu^{2+} ions and the free sulfonate group. The proton conductivity of the resulting material is more than twice higher than the conductivity of other sulfonate MOFs.

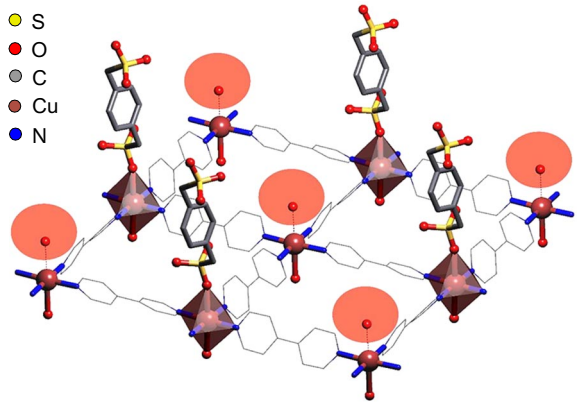


Figure 34. Fragment of one of the interpenetrated frameworks in the $[Cu_2(bpy)_4(C_6H_4(CH_2SO_3)_2)\text{-}1,4\cdot H_2O]$ structure (TARCUN), in which half of Cu^{II} ions remain coordinatively unsaturated after the coordination of sulfonate ligands, thereby allowing these ions to additionally coordinate water molecules (shown as pink spheres). The Figure was prepared by the authors using original data from the study.[298]

5. Phase transformations. Some MOFs undergo temperature- or humidity-induced phase transformations (reconstructions). The proton conductivity of different phases can be significantly different. Therefore, phase transformations are applied to prepare highly conducting polymers. In particular, the compound $[CoLa(Hnotp)(H_2O)_6]ClO_4\cdot 5H_2O$ [H_6notp is 1,4,7-triazacyclononane-1,4,7-triyl-tris(methylenephosphonic acid)] with hydrophilic layers and water molecules in the interlayer space is transformed to a new phase of the composition $H_3O[CoLa(notp)(H_2O)_4]ClO_4\cdot 3H_2O$ upon heating to >45 °C at a humidity of >93%. This process is accompanied by a release of hydrated protons to the interlayer space and the corresponding enhancement of proton conductivity.[299]

The prolonged heating of MOF of the composition $H_2Im[Cu(H_2PO_4)_2Cl]\cdot H_2O$ (H_2Im^+ is the protonated imidazole molecule) leads to its dehydration and the transformation accompanied by a structural disorder.[300] In the initial hydrated structure, there are numerous hydrogen bonds between the anionic framework, the encapsulated water molecules and protonated imidazole molecules, due to which water and imidazole molecules are kept fixed, resulting in low proton conductivity. However, upon prolonged heating, the structure loses water, which leads to the breaking of some hydrogen bonds, and the H_2Im^+ ions that become mobile can ensure proton transfer.

6. A combination of different approaches. Combinations of different approaches are applied to improve the proton-transport properties of materials. For example, Lo *et al.*[301] inserted imidazole molecules, serving as the proton transfer agent, into the pores of MOF, which contains sulfonic groups in close proximity to each other. This resulted in the additional increase in the conductivity of the new material. Similar results were obtained in the study,[302] where carboxylate ligands were employed as the building units and dimethylammonium cations were inserted into the MOF pores.

In the study,[31] the proton conductivity was enhanced by replacing the metal coordination site by a metal in lower oxidation state, reducing the length of the organic ligand and introducing additional acidic protons to the MOF surface. A decrease in the oxidation state of the central metal atom is accompanied by the release of protons to compensate the charge. The use of short ligands that connect the metal phosphate chains, like in the treatment of the framework with acids, leads to an increase in the framework proton density. The increased framework proton density in the material can lead to an increase in the proton conductivity of up to four orders of magnitude.

Umeyama *et al.*[303] developed an approach to the synthesis of proton-conducting MOCP, having both its own proton conductivity and capable adsorbing proton carrier molecules due to a high porosity. Ligands functionalized by phosphate groups and benzimidazole molecules were employed. A significant conductivity of the framework, reaching 1.3 $m\Omega^{-1}$ cm^{-1} at 120 °C under anhydrous conditions, is attributed to high mobility of benzimidazole molecules. The adsorption of molecules capable of acting as a proton donor or acceptor, *e.g.*, methanol, leads to the enhancement of the proton conductivity of MOF by a factor of 24.

Summarizing all the above, it is worth noting that the possibilities of combining different approaches to control the proton conductivity of MOFs are rapidly evolving due

to the introduction of new methods of reticular design, accompanied by an exponential growth of the number of synthesized MOFs. The total number of proton conductors among the synthesized MOFs is as yet unknown. As our analysis demonstrated, the number of known structures with hydrogen bond chains is two orders of magnitude larger than the number of characterized conductors. This provides a basis for the application of MOF-based proton conductors in industry in the near future.

5. Conclusion

The topological approaches to the analysis, classification and prediction of the crystal structures considered in this review are versatile and can be applied to compounds of any nature. Metal-organic coordination polymers serve as a convenient testing ground for the development of these approaches, because their structures can be clearly represented as an assembly of building units, the existence of which in the isolated state in solution is generally easily substantiated and experimentally verified. Therefore, it would be expected that the topological methods will be most widely applied in the reticular design of MOCPs in the near future. Besides, synthetic chemists and materials scientists will increasingly use approaches of reticular chemistry for other classes of chemical compounds, the efficiency of these approaches for which was demonstrated in recent years, *e.g.*, for zeolites, intermetallides, ionic and covalent inorganic compounds, molecular crystals.

Topological methods will also play a role in the development of artificial intelligence systems in the crystal chemistry and materials science, because the topological descriptors significantly expand the possibilities of searching composition–structure–property relationships and also for the application of machine learning methods and other methods of analysis of large sets of data on the structures and properties of crystalline compounds. These trends will inevitably lead to the extension of reticular chemistry to all fields of synthetic chemistry and materials science and will make it a practical tool in modern laboratories, as was the case with quantum chemical methods in recent years.

This review was written with the financial support of the Russian Foundation for Basic Research (Project No. 20-13-50007).

6. List of abbreviations and designations

bix — 1,4-bis(imidazol-1-ylmethyl)benzene,
bpb — 1,4-di(4-pyridyl)benzene,
bpdpca — 4,4′-bis(4-pyridylcarbonylamino)biphenyl or *N*,*N*′-([1,1′-biphenyl]-4,4′-diyl)di(pyridine-4-carboxamide),
bpe — 1,2-di(4-pyridyl)ethylene,
bpy — 4,4′-bipyridine,
btae — 1,2-bis(tetrazol-1-yl)ethane,
$cbdc^{2-}$ — cyclobutane-1,1-dicarboxylate,
CF — coordination formula,
$chdc^{2-}$ — *trans*-cyclohexane-1,4-dicarboxylate,
CML — coordination mode of the ligand,
CSD — Cambridge Structural Database,
dabco — 1,4-diazabicyclo[2.2.2]octane,
DMF — dimethylformamide,
dpa — di(4-pyridyl)amine,
dpbp — 4,4-di(4-pyridyl)biphenyl,
dpipa — *N*,*N*′-di(4-pyridyl)isophthalamide,
G — space symmetry group,
G_{max} — maximum possible symmetry,
H_2adp — adipic acid,
H_2bedo — but-2-ene-1,4-dioic acid,
H_2bpdc — biphenyl-4,4′-dicarboxylic acid,
H_2bpedc — stilbene-4,4′-dicarboxylic acid,
H_2fdc — furan-2,5-dicarboxylic acid,
H_2glut — glutaric acid,
H_2hdmdb — *N*,*N*′′-bis(4-carboxyphenylmethylidene)-hydrazinodibenzoic acid or 4,4′-(hydrazinediylidenedimethylidene)dibenzoic acid,
H_2Im^+ — protonated imidazole molecule,
H_2ndc — naphthalene-2,6-dicarboxylic acid,
H_2ox — oxalic acid,
H_3btc — benzene-1,3,5-tricarboxylic acid,
H_4abtc — 3,3′-5,5′-tetracarboxyazobenzene or 5,5′-(diazene-1,2-diyl)diisophthalic acid,
H_4bptc — biphenyl-3,3′,5,5′tetracarboxylic acid,
H_4tptcMe$_2$ — 2′,5′-dimethyl[1,1′:4′,1′′-terphenyl]-3,3′′,5,5′′-tetracarboxylic acid,
H_6notp — 1,4,7-triazacyclononane-1,4,7-triyltris(methylenephosphonic acid),
Htapta — 5-[4-(1,2,4-triazol-4-yl)phenyl)]tetrazole,
$imdc^{2-}$ — imidazole-4,5-dicarboxylate,
IZA — International Zeolite Association,
$\log\sigma$ — logarithm of proton conductivity,
MOCP — metal-organic coordination polymer,
MOF — metal-organic framework
NMP — *N*-methylpyrrolidone,
PE&M — points of extension and metals representation,
pmcd — 1,4-bis[(3,6-dicarboxylato-9- carbazol-9-yl)methyl]benzene or 9,9*displaystyle*′-[1,4-phenylenebis(methylene)]di(9H-carbazole-3,6-dicarboxylato,
RCSR — Reticular Chemistry Structure Resource,
STR — straight rod representation,
$tcnopr3OH^-$ — 1,1,3,3-tetracyano-2-(3-hydroxypropoxy)prop-2-en-1-ide,
tipa — tris[4-(imidazol-1-yl)phenyl]amine,
tmpo — tris[4-(2-methylimidazol-1-yl)phenyl]phosphine oxide,
UNSR — underlying net in standard representation,
URCN — underlying rod-containing net representation.

7. References

1. A.R.Oganov, C.J.Pickard, Q.Zhu, R.J.Needs. *Nat. Rev. Mater.*, **4**, 331 (2019)
2. R.Ferro, A.Saccone. *Intermetallic Chemistry*. (Oxford: Pergamon Press, 2008)
3. M.O'Keeffe, B.G.Hyde. In *Cation Ordering Electron Transfer. Structure and Bonding*. Vol 61. (Berlin, Heidelberg: Springer, 2007). P. 77
4. A.I.Kitaigorodskii. *Molecular Crystals and Molecules*. (New York, London: Academic Press, 1973)
5. K.Griffiths, V.A.Blatov, G.E.Kostakis. In *Single-Molecule Magnets: Molecular Architectires and Building Blocks for Spintronics*. (Ed. M.Holynska). (Weinheim: Wiley-VCH Verlag, 2019). P. 353
6. A.Y.-T.Wang, R.J.Murdock, S.K.Kauwe, A.O.Oliynyk, A.Gurlo, J.Brgoch, K.A.Persson, T.D.Sparks. *Chem. Mater.*, **32**, 4954 (2020)
7. A.P.Shevchenko, E.V.Alexandrov, O.A.Blatova, D.E.Yablokov, V.A.Blatov. In *Materials Informatics: Methods, Tools, and Applications*. (Weinheim: Wiley, 2019). P. 107
8. A.F.Wells. *Acta Crystallogr.*, **7**, 535 (1954)

9. A.F.Wells. *Three-Dimensional Nets and Polyhedra*. (New York: Interscience, 1979)
10. W.B.Pearson. *The Crystal Chemistry and Physics of Metals and Alloys*. (New York: Wiley-Interscience, 1972)
11. B.F.Abrahams, B.F.Hoskins, D.M.Michail, R.Robson. *Nature (London)*, **369**, 727 (1994)
12. R.F.Mendes, F.Figueira, J.P.Leite, L.Gales, F.A.Almeida Paz. *Chem. Soc. Rev.*, **49**, 9121 (2020)
13. M.Usman, K.-L.Lu. *NPG Asia Mater.*, **8**, e333 (2016)
14. C.H.Hendon, A.J.Rieth, M.D.Korzyński, M.Dincă. *ACS Cent. Sci.*, **3**, 554 (2017)
15. A.Bavykina, N.Kolobov, I.S.Khan, J.A.Bau, A.Ramirez, J.Gascon. *Chem. Rev.*, **120**, 8468 (2020)
16. A.L.Semrau, Z.Zhou, S.Mukherjee, M.Tu, W.Li, R.A.Fischer. *Langmuir*, **37**, 6847 (2021)
17. H.Huang, K.Shen, F.Chen, Y.Li. *ACS Catal.*, **10**, 6579 (2020)
18. W.Gong, Y.Liu, H.Li, Y.Cui. *Coord. Chem. Rev.*, **420**, 213400 (2020)
19. P.Kumar, A.Pournara, K.-H.Kim, V.Bansal, S.Rapti, M.J.Manos. *Prog. Mater. Sci.*, **86**, 25 (2017)
20. Y.Sun, R.Ma, F.Wang, X.Guo, S.Sun, H.Guo, E.V.Alexandrov. *Cryst. Growth Des.*, **19**, 5267 (2019)
21. Y.Sun, X.Chen, F.Wang, R.Ma, X.Guo, S.Sun, H.Guo, E.V.Alexandrov. *Dalton Trans.*, **48**, 5450 (2019)
22. W.Li, L.Sun, J.Qi, P.Jarillo-Herrero, M.Dincă, J.Li. *Chem. Sci.*, **8**, 2859 (2017)
23. P.Perlepe, I.Oyarzabal, A.Mailman, M.Yquel, M.Platunov, I.Dovgaliuk, M.Rouzières, P.Négrier, D.Mondieig, E.A.Suturina, M.-A.Dourges, S.Bonhommeau, R.A.Musgrave, K.S.Pedersen, D.Chernyshov, F.Wilhelm, A.Rogalev, C.Mathonière, R.Clérac. *Science*, **370**, 587 (2020)
24. N.V.Gogoleva, E.N.Zorina-Tikhonova, A.S.Bogomyakov, N.N.Efimov, E.V.Alexandrov, E.A.Ugolkova, M.A.Kiskin, V.V.Minin, A.A.Sidorov, I.L.Eremenko. *Eur. J. Inorg. Chem.*, 547 (2017)
25. L.R.Mingabudinova, V.V.Vinogradov, V.A.Milichko, E.Hey-Hawkins, A.V.Vinogradov. *Chem. Soc. Rev.*, **45**, 5408 (2016)
26. R.Medishetty, J.K.Zaręba, D.Mayer, M.Samoć, R.A.Fischer. *Chem. Soc. Rev.*, **46**, 4976 (2017)
27. A.V.Sokolov, A.V.Vologzhanina, E.D.Barabanova, S.Y.Stefanovich, P.V.Dorovatovskii, I.V.Taydakov, E.V.Alexandrov. *Chem. – Eur. J.*, **27**, 9180 (2021)
28. F.X.Coudert, A.Boutin, A.H.Fuchs, A.V.Neimark, Z.Chang, D.H.Yang, J.Xu, T.L.Hu, X.H.Bu, N.C.Burtch, J.Heinen, T.D.Bennett, D.Dubbeldam, M.D.Allendorf, S.S.Nagarkar, A.V.Desai, S.K.Ghosh, J.C.Tan, A.K Cheetham, A.Schneemann, V.Bon, I.Schwedler, I.Senkovska, S.Kaskel, R.A.Fischer, L.R.Redfern, O.K.Farha, A.J.Howarth, Y.Liu, P.Li, Z.Li, T.C.Wang, J.T.Hupp, O.K.Farha, T.D.Bennett, A.K.Cheetham, A.H.Fuchs, F.X.Coudert, J.P.Zhang, H.L.Zhou, D.D.Zhou, P.Q.Liao, X.M.Chen, W.Li, S.Henke, A.K.Cheetham, I.E.Collings, A.L.Goodwin, M.Mani-biswas, T.Cagin, J.Hwa, S Jeoung, Y.G.Chung, H.Ri, X.H.Bu, M.J.Zaworotko. *Adv. Mater.*, **9**, 11 (2019)
29. L.R.Redfern, O.K.Farha. *Chem. Sci.*, **10**, 10666 (2019)
30. J.Escorihuela, R.Narducci, V.Compañ, F.Costantino. *Adv. Mater. Interfaces*, 1801146 (2018)
31. S.Pili, P.Rought, D.I.Kolokolov, L.Lin, I.da Silva, Y.Cheng, C.Marsh, I.P.Silverwood, V.García Sakai, M.Li, J.J.Titman, L.Knight, L.L.Daemen, A.J.Ramirez-Cuesta, C.C.Tang, A.G.Stepanov, S.Yang, M. Schröder. *Chem. Mater.*, **30**, 7593 (2018)
32. Y.Yu.Enakieva, A.A.Sinelshchikova, M.S.Grigoriev, V.V.Chernyshev, K.A.Kovalenko, I.A.Stenina, A.B.Yaroslavtsev, Yu.G.Gorbunova, A.Yu.Tsivadze. *Chem. – Eur. J.*, **27**, 1598 (2021)
33. J.Cepeda, S.Pérez-Yáñez, G.Beobide, O.Castillo, E.Goikolea, F.Aguesse, L.Garrido, A.Luque, P.A.Wright. *Chem. Mater.*, **28**, 2519 (2016)
34. M.Sadakiyo, H.Kasai, K.Kato, M.Takata, M.Yamauchi. *J. Am. Chem. Soc.*, **136**, 1702 (2014)
35. L.S.Xie, G.Skorupskii, M.Dincă. *Chem. Rev.*, **120**, 8536 (2020)
36. J.Liu, X.Song, T.Zhang, S.Liu, H.Wen, L.Chen. *Angew. Chem., Int. Ed.*, **60**, 5612 (2021)
37. H.-Y.Li, S.-N.Zhao, S.-Q.Zang, J.Li. *Chem. Soc. Rev.*, **49**, 6364 (2020)
38. C.Chuang, C.Kung. *Electroanalysis*, **32**, 1885 (2020)
39. O.Delgado-Friedrichs, M.O Keeffe. *J. Solid State Chem.*, **178**, 2480 (2005)
40. W.E.Klee. *Cryst. Res. Technol.*, **39**, 959 (2004)
41. I.A.Baburin, V.A.Blatov. *Acta Crystallogr., Sect. B*, **63**, 791 (2007)
42. V.A.Blatov, O.Delgado-Friedrichs, M.O'Keeffe, D.M.Proserpio. *Acta Crystallogr., Sect. A*, **63**, 418 (2007)
43. L.Carlucci, G.Ciani, D.M.Proserpio. *Coord. Chem. Rev.*, **246**, 247 (2003)
44. V.A.Blatov, L.Carlucci, G.Ciani, D.M.Proserpio. *CrystEngComm*, **6**, 377 (2004)
45. E.V.Alexandrov, V.A.Blatov, D.M.Proserpio. *Acta Crystallogr. Sect. A*, **68**, 484 (2012)
46. A.P.Shevchenko, V.A.Blatov. *Struct. Chem.*, **32**, 507 (2021)
47. P.A.Demakov, A.S.Poryvaev, K.A.Kovalenko, D.G.Samsonenko, M.V.Fedin, V.P.Fedin, D.N.Dybtsev. *Inorg. Chem.*, **59**, 15724 (2020)
48. C.Bonneau, M.O Keeffe, D.M.Proserpio, V.A.Blatov, S.R.Batten, S.A.Bourne, M.S.Lah, J.G.Eon, S.T.Hyde, S.B.Wiggin, L.Öhrström. *Cryst. Growth Des.*, **18**, 3411 (2018)
49. S.Krause, J.D.Evans, V.Bon, I.Senkovska, S.Ehrling, P.Iacomi, D.M.Többens, D.Wallacher, M.S.Weiss, B.Zheng, P.G.Yot, G.Maurin, P.L.Llewellyn, F.-X.Coudert, S.Kaskel. *Chem. Sci.*, **11**, 9468 (2020)
50. N.L.Rosi, J.Kim, M.Eddaoudi, B.Chen, M.O'Keeffe, O.M.Yaghi. *J. Am. Chem. Soc.*, **127**, 1504 (2005)
51. A.Schoedel, M.Li, D.Li, M.O'Keeffe, O.M.Yaghi. *Chem. Rev.*, **116**, 12466 (2016)
52. L.S.Xie, E.V.Alexandrov, G.Skorupskii, D.M.Proserpio, M.Dincă. *Chem. Sci.*, **10**, 8558 (2019)
53. V.A.Blatov. *Struct. Chem.*, **27**, 1605 (2016)
54. O.A.Bondar, L.V.Lukashuk, A.B.Lysenko, H.Krautscheid, E.B.Rusanov, A.N.Chernega, K.V.Domasevitch. *CrystEngComm*, **10**, 1216 (2008)
55. E.V.Alexandrov, V.A.Blatov, A.V.Kochetkov, D.M.Proserpio. *CrystEngComm*, **13**, 3947 (2011)
56. H.Deng, S.Grunder, K.E.Cordova, C.Valente, H.Furukawa, M.Hmadeh, F.Gandara, A.C.Whalley, Z.Liu, S.Asahina, H.Kazumori, M.O'Keeffe, O.Terasaki, J.F.Stoddart, O.M.Yaghi. *Science*, **336**, 1018 (2012)
57. S.E.Henkelis, S.M.Vornholt, D.B.Cordes, A.M.Z.Slawin, P.S.Wheatley, R.E.Morris. *CrystEngComm*, **21**, 1857 (2019)
58. S.Peng, B.Bie, Y.Sun, M.Liu, H.Cong, W.Zhou, Y.Xia, H.Tang, H.Deng, X.Zhou. *Nat. Commun.*, **9**, 1 (2018)
59. V.Stavila, M.E.Foster, J.W.Brown, R.W.Davis, J.Edgington, A.I.Benin, R.A.Zarkesh, R.Parthasarathi, D.W.Hoyt, E.D.Walter, A.Andersen, N.M.Washton, A.S.Lipton, M.D.Allendorf. *Chem. Sci.*, **10**, 9880 (2019)
60. S.Barthel, E.V.Alexandrov, D.M.Proserpio, B.Smit. *Cryst. Growth Des.*, **18**, 1738 (2018)
61. E.V.Alexandrov, V.A.Blatov, D.M.Proserpio. *CrystEngComm*, **19**, 1993 (2017)
62. B.Moulton, M.J.Zaworotko. *Chem. Rev.*, **101**, 1629 (2001)
63. T.A.Makal, A.A.Yakovenko, H.C.Zhou. *J. Phys. Chem. Lett.*, **2**, 1682 (2011)
64. X.L.Wu, F.Luo, G.M.Sun, A.M.Zheng, J.Zhang, M.B.Luo, W.Y.Xu, Y.Zhu, X.M.Zhang, S.Y.Huang. *ChemPhysChem*, **14**, 3594 (2013)
65. Q.Shi, X.Kang, F.-N.Shi, J.Dong. *Chem. Commun.*, **51**, 1131 (2015)

66. Q.Shi, W.-J.Xu, R.-K.Huang, W.-X.Zhang, Y.Li, P.Wang, F.-N.Shi, L.Li, J.Li, J.Dong. *J. Am. Chem. Soc*., **138**, 16232 (2016)
67. M.T.Wharmby, S.Henke, T.D.Bennett, S.R.Bajpe, I.Schwedler, S.P.Thompson, F.Gozzo, P.Simoncic, C.Mellot-Draznieks, H.Tao, Y.Yue, A.K.Cheetham. *Angew. Chem., Int. Ed.*, **54**, 6447 (2015)
68. Y.-Q.Tian, Y.-M.Zhao, Z.-X.Chen, G.-N.Zhang, L.-H.Weng, D.-Y.Zhao. *Chem. – Eur. J*., **13**, 4146 (2007)
69. E.C.Spencer, R.J.Angel, N.L.Ross, B.E.Hanson, J.A.K.Howard. *J. Am. Chem. Soc*., **131**, 4022 (2009)
70. Y.Q.Tian, C.X.Cai, X.M.Ren, C.Y.Duan, Y.Xu, S.Gao, X.Z.You. *Chem. – Eur. J*., **9**, 5673 (2003)
71. K.S.Park, Z.Ni, A.P.Cote, J.Y.Choi, R.Huang, F.J.Uribe-Romo, H.K.Chae, M.O Keeffe, O.M.Yaghi. *Proc. Natl. Acad. Sci. USA*, **103**, 10186 (2006)
72. C.A.Schröder, I.A.Baburin, L.van Wüllen, M.Wiebcke, S.Leoni. *CrystEngComm*, **15**, 4036 (2013)
73. C.A.Schröder, S.Saha, K.Huber, S.Leoni, M.Wiebcke. *Z. Kristallogr. – Cryst. Mater*., **229**, 807 (2014)
74. R.Lehnert, F.Seel. *Z. Anorg. Allg. Chem*., **464**, 187 (1980)
75. O.Karagiaridi, M.B.Lalonde, W.Bury, A.A.Sarjeant, O.K.Farha, J.T.Hupp. *J. Am. Chem. Soc*., **134**, 18790 (2012)
76. R.N.Widmer, G.I.Lampronti, S.Chibani, C.W.Wilson, S.Anzellini, S.Farsang, A.K.Kleppe, N.P.M.Casati, S.G.MacLeod, S.A.T.Redfern, F.-X.Coudert, T.D.Bennett. *J. Am. Chem. Soc*., **141**, 9330 (2019)
77. L.Wu, M.Xue, G.Chaplais, G.S.Zhu, S.L.Qiu, A.Simon-Masseron, J.Patarin. *Adv. Mater. Res*., **543** (2013)
78. J.X.Yang, Y.Y.Qin, J.K.Cheng, X.Zhang, Y.G.Yao. *Cryst. Growth Des*., **15**, 2223 (2015)
79. V.A.Blatov, A.A.Golov, C.Yang, Q.Zeng, A.A.Kabanov. *Sci. Rep*., **9**, 6007 (2019)
80. V.A.Blatov, C.Yang, D.Tang, Q.Zeng, A.A.Golov, A.A.Kabanov. *npj Comput. Mater*., **7**, 15 (2021)
81. A.O.Dmitrienko, M.I.Buzin, Z.Setifi, F.Setifi, E.V.Alexandrov, E.D.Voronova, A. V.Vologzhanina. *Dalton Trans*., **49**, 7084 (2020)
82. X.Jiang, X.Cui, A.J.E.Duncan, L.Li, R.P.Hughes, R.J.Staples, E.V.Alexandrov, D.M.Proserpio, Y.Wu, C.Ke. *J. Am. Chem. Soc*., **141**, 10915 (2019)
83. D.Braga, L.Maini, P.P.Mazzeo, B.Ventura. *Chem. – Eur. J*., **16**, 1553 (2010)
84. M.Bi, G.Li, J.Hua, X.Liu, Y.Hu, Z.Shi, S.Feng. *CrystEngComm*, **9**, 984 (2007)
85. V.Guillerm, D.Kim, J.F.Eubank, R.Luebke, X.Liu, K.Adil, M.S.Lah, M.Eddaoudi. *Chem. Soc. Rev*., **43**, 6141 (2014)
86. M.O'Keeffe, S.T.Hyde. *Zeolites*, **19**, 370 (1997)
87. O.Delgado-Friedrichs, M.O'Keeffe. *Acta Crystallogr., Sect. A*, **59**, 351 (2003)
88. M.O'Keeffe, M.A.Peskov, S.J.Ramsden, O.M.Yaghi. *Acc. Chem. Res*., **41**, 1782 (2008)
89. V.A.Blatov, A.P.Shevchenko, D.M.Proserpio. *Cryst. Growth Des*., **14**, 3576 (2014)
90. S.J.Chung, T.Hahn, W.E.Klee. *Acta Crystallogr., Sect. A*, **40**, 42 (1984)
91. A.P.Shevchenko, I.A.Blatov, E.V.Kitaeva, V.A.Blatov. *Cryst. Growth Des*., **17**, 774 (2017)
92. I.A.Baburin, V.A.Blatov, L.Carlucci, G.Ciani, D.M.Proserpio. *J. Solid State Chem*., **178**, 2452 (2005)
93. E.V.Alexandrov, A.P.Shevchenko, V.A.Blatov. *Cryst. Growth Des*., **19**, 2604 (2019)
94. A.P.Shevchenko, R.A.Eremin, V.A.Blatov. *CrystEngComm*, **22**, 7298 (2020)
95. I.E.Ushakov, A.S.Goloveshkin, E.N.Zorina-Tikhonova, A.S.Chistyakov, A.A.Sidorov, I.L.Eremenko, A.D.Volodin, A.V.Vologzhanina. *Mendeleev Commun*., **29**, 643 (2019)
96. B.J.Bucior, A.S.Rosen, M.Haranczyk, Z.Yao, M.E.Ziebel, O.K.Farha, J.T.Hupp, J.I.Siepmann, A.Aspuru-Guzik, R.Q.Snurr. *Cryst. Growth Des*., **19**, 6682 (2019)
97. C.R.Groom, I.J.Bruno, M.P.Lightfoot, S.C.Ward. *Acta Crystallogr., Sect. B*, **72**, 171 (2016)
98. R.Taylor, P.A.Wood. *Chem. Rev*., **119**, 9427 (2019)
99. V.A.Blatov, D.M.Proserpio. In *Modern Methods of Crystal Structure Prediction*. (Weinheim: Wiley-VCH Verlag, 2010). P. 1
100. V.A.Blatov, O.A.Blatova, F.Daeyaert, M.W.Deem. *RSC Adv*., **10**, 17760 (2020)
101. C.E.Wilmer, M.Leaf, C.Y.Lee, O.K.Farha, B.G.Hauser, J.T.Hupp, R.Q.Snurr. *Nat. Chem*., **4**, 83 (2012)
102. L.C.Lin, A.H.Berger, R.L.Martin, J.Kim, J.A.Swisher, K.Jariwala, C.H.Rycroft, A.S.Bhown, M.W.Deem, M.Haranczyk, B.Smit. *Nat. Mater*., **11**, 633 (2012)
103. J.Goldsmith, A.G.Wong-Foy, M.J.Cafarella, D.J.Siegel. *Chem. Mater*., **25**, 3373 (2013)
104. Y.G.Chung, J.Camp, M.Haranczyk, B.J.Sikora, W.Bury, V.Krungleviciute, T.Yildirim, O.K.Farha, D.S.Sholl, R.Q.Snurr. *Chem. Mater*., **26**, 6185 (2014)
105. Y.G.Chung, E.Haldoupis, B.J.Bucior, M.Haranczyk, S.Lee, H.Zhang, K.D.Vogiatzis, M.Milisavljevic, S.Ling, J.S.Camp, B.Slater, J.I.Siepmann, D.S.Sholl, R.Q.Snurr. *J. Chem. Eng. Data*, **64**, 5985 (2019)
106. A.Jain, S.P.Ong, G.Hautier, W.Chen, W.D.Richards, S.Dacek, S.Cholia, D.Gunter, D.Skinner, G.Ceder, K.A.Persson. *APL Mater*., **1**, 011002 (2013)
107. E.L.First, C.E.Gounaris, J.Wei, C.A.Floudas. *Phys. Chem. Chem. Phys*., **13**, 17339 (2011)
108. E.L.First, C.A.Floudas. *Microporous Mesoporous Mater*., **165**, 32 (2013)
109. P.Z.Moghadam, A.Li, S.B.Wiggin, A.Tao, A.G.P.Maloney, P.A.Wood, S.C.Ward, D.Fairen-Jimenez. *Chem. Mater*., **29**, 2618 (2017)
110. P.Z.Moghadam, A.Li, X.-W.Liu, R.Bueno-Perez, S.-D.Wang, S.B.Wiggin, P.A.Wood, D.Fairen-Jimenez. *Chem. Sci*., **11**, 8373 (2020)
111. A.Li, R.B.Perez, S.Wiggin, S.C.Ward, P.A.Wood, D.Fairen-Jimenez. *Matter*, **4**, 1105 (2021)
112. C.M.Simon, J.Kim, D.A.Gomez-Gualdron, J.S.Camp, Y.G.Chung, R.L.Martin, R.Mercado, M.W.Deem, D.Gunter, M.Haranczyk, D.S.Sholl, R.Q.Snurr, B.Smit. *Energy Environ. Sci*., **8**, 1190 (2015)
113. C.M.Simon, R.Mercado, S.K.Schnell, B.Smit, M.Haranczyk. *Chem. Mater*., **27**, 4459 (2015)
114. B.J.Sikora, C.E.Wilmer, M.L.Greenfield, R.Q.Snurr. *Chem. Sci*., **3**, 2217 (2012)
115. E.V.Alexandrov, A.P.Shevchenko, A.A.Asiri, V.A.Blatov. *CrystEngComm*, **17**, 2913 (2015)
116. K.Mukherjee, Y.J.Colón. *Mol. Simul*., **47**, 857 (2021)
117. C.Altintas, O.F.Altundal, S.Keskin, R.Yildirim. *J. Chem. Inf. Mod*., **61**, 2131 (2021)
118. T.C.Nicholas, A.L.Goodwin, V.L.Deringer. *Chem. Sci*., **11**, 12580 (2020)
119. V.V.Korolev, A.Mitrofanov, E.I.Marchenko, N.N.Eremin, V.Tkachenko, S.N.Kalmykov. *Chem. Mater*., **32**, 7822 (2020)
120. V.N.Serezhkin, A.V.Vologzhanina, L.B.Serezhkina, E.S.Smirnova, E.V.Grachova, P.V.Ostrova, M.Yu.Antipin. *Acta Crystallogr. Sect. B*, **65**, 45 (2009)
121. A.V.Savchenkov, A.S.Uhanov, M.S.Grigoriev, A.M.Fedoseev, D.V.Pushkin, L.B.Serezhkina, V.N.Serezhkin. *Dalton Trans*., **50**, 4210 (2021)
122. F.Aman, A.M.Asiri, W.A.Siddiqui, M.N.Arshad, A.Ashraf, N.S.Zakharov, V.A.Blatov. *CrystEngComm*, **16**, 1963 (2014)
123. V.A.Blatov, E.V.Alexandrov, A.P.Shevchenko. In *Comprehensive Coordination Chemistry III*. Vol. 2. (Eds E.C.Constable, G.Parkin, L.Que Jr.). (Amsterdam, Oxford, Cambridge: Elsevier, 2021). P. 389
124. S.-H.Liao. *Expert Syst. Appl*., **28**, 93 (2005)
125. P.Jackson. *Introduction to Expert Systems*. (3rd Edn). (Boston: Addison-Wesley, 1999)
126. M.C.Hemmer. *Expert Systems in Chemistry Research*. (Boca Raton, FL: CRC Press, 2008)

127. P.Judson. *Knowledge-Based Expert Systems in Chemistry: Not Counting on Computers*. (Cambridge, UK: RSC Publishing, 2009)
128. N.N.Kiselyova. In *Intermetallic Compounds. Principles and Practice*. (Eds J.H.Westbrook, R.L.Fleischer). (Chichester, UK: Wiley, 2002) P. 811
129. O.Isayev, D.Fourches, E.N.Muratov, C.Oses, K.Rasch, A.Tropsha, S.Curtarolo. *Chem. Mater.*, **27**, 735 (2015)
130. O.Isayev, C.Oses, C.Toher, E.Gossett, S.Curtarolo, A.Tropsha. *Nat. Commun.*, **8**, 15679 (2017)
131. W.D.S.Motherwell. *Crystallogr. Rev.*, **14**, 97 (2008)
132. S.Chong, S.Lee, B.Kim, J.Kim. *Coord. Chem. Rev.*, **423**, 213487 (2020)
133. N.Artrith, K.T.Butler, F.-X.Coudert, S.Han, O.Isayev, A.Jain, A.Walsh. *Nat. Chem.*, **13**, 505 (2021)
134. C.J.Court, B.Yildirim, A.Jain, J.M.Cole. *J. Chem. Inf. Mod.*, **60**, 4518 (2020)
135. P.Z.Moghadam, S.M.J.Rogge, A.Li, C.M.Chow, J.Wieme, N.Moharrami, M.Aragones-Anglada, G.Conduit, D.A.Gomez-Gualdron, V.Van Speybroeck, D.Fairen-Jimenez. *Matter*, **1**, 219 (2019)
136. M.Pardakhti, E.Moharreri, D.Wanik, S.L.Suib, R.Srivastava. *ACS Comb. Sci.*, **19**, 640 (2017)
137. H.Dureckova, M.Krykunov, M.Z.Aghaji, T.K.Woo. *J. Phys. Chem. C*, **123**, 4133 (2019)
138. M.Fernandez, P.G.Boyd, T.D.Daff, M.Z.Aghaji, T.K.Woo. *J. Phys. Chem. Lett.*, **5**, 3056 (2014)
139. N.W.Ockwig, O.Delgado-Friedrichs, M.O'Keeffe, O.M.Yaghi. *Acc. Chem. Res.*, **38**, 176 (2005)
140. A.P.Shevchenko, E.V.Alexandrov, A.A.Golov, O.A.Blatova, S.Duyunova, V.A.Blatov. *Chem. Commun.*, **56**, 9616 (2020)
141. Q.Lin, T.Wu, S.T.Zheng, X.Bu, P.Feng. *Chem. Commun.*, **47**, 11852 (2011)
142. S.Thapa, D.A.Dickie, Y.Qin. *Cryst. Growth Des.*, **20**, 1598 (2020)
143. X.-R.Hao, X.-L.Wang, K.-Z.Shao, G.-S.Yang, Z.-M.Su, G.Yuan. *CrystEngComm*, **14**, 5596 (2012)
144. X.Guo, G.Zhu, Z.Li, Y.Chen, X.Li, S.Qiu. *Inorg. Chem.*, **45**, 4065 (2006)
145. B.Chen, S.Ma, F.Zapata, E.B.Lobkovsky, J.Yang. *Inorg. Chem.*, **45**, 5718 (2006)
146. D.N.Dybtsev, I.E.Sokolov, E.V.Peresypkina, V.P.Fedin. *Russ. Chem. Bull., Int. Ed.*, **56**, 225 (2007)
147. K.Barthelet, J.Marrot, D.Riou, G.Férey. *Angew. Chem., Int. Ed.*, **41**, 281 (2002)
148. A.Kawamura, A.S.Filatov, J.S.Anderson, I.-R.Jeon. *Inorg. Chem.*, **58**, 3764 (2019)
149. H.Wu, J.Yang, Z.Su, S.R.Batten, J.-F.Ma. *J. Am. Chem. Soc.*, **133**, 11406 (2011)
150. Z.-Z.Lu, R.Zhang, Y.-Z.Li, Z.-J.Guo, H.-G.Zheng. *Chem. Commun.*, **47**, 2919 (2011)
151. R.Ma, X.Guo, Y.Sun, F.Wang, S.Sun, T.Zhou, S.Liu, H.Guo, E.V.Alexandrov. *Inorg. Chim. Acta*, **496**, 119032 (2019)
152. T.G.Mitina, V.A.Blatov. *Cryst. Growth Des.*, **13**, 1655 (2013)
153. L.Carlucci, G.Ciani, D.M.Proserpio, T.G.Mitina, V.A.Blatov. *Chem. Rev.*, **114**, 7557 (2014)
154. C.T.Chen, K.S.Suslick. *Coord. Chem. Rev.*, **128**, 293 (1993)
155. A.N.Khlobystov, A.J.Blake, N.R.Champness, D.A.Lemenovskii, A.G.Majouga, N.V.Zyk, M.Schröder. *Coord. Chem. Rev.*, **222**, 155 (2001)
156. W.L.Leong, J.J.Vittal. *Chem. Rev.*, **111**, 688 (2011)
157. E.Loukopoulos, G.E.Kostakis. *J. Coord. Chem.*, **71**, 371 (2018)
158. A.Deák, T.Tunyogi, G.Pállnkás. *J. Am. Chem. Soc.*, **131**, 2815 (2009)
159. B.Grünbaum, G.C.Shephard. *Math. Mag.*, **53**, 139 (1980)
160. G.-Q.Kong, S.Ou, C.Zou, C.-D.Wu. *J. Am. Chem. Soc.*, **134**, 19851 (2012)
161. L.Han, H.Valle, X.Bu. *Inorg. Chem.*, **46**, 1511 (2007)
162. P.Pachfule, C.Dey, T.Panda, R.Banerjee. *CrystEngComm*, **12**, 1600 (2010)
163. L.Rajput, M.Sarkar, K.Biradha. *J. Chem. Sci.*, **122**, 707 (2010)
164. Y.-K.Gu, X.Li, H.Liang, X.-B.Deng. *Inorg. Chem. Commun.*, **14**, 52 (2011)
165. Y.-C.Lo, Y.-J.Chang, P.M.Chhetri, W.-J.Huang, J.-D.Chen. *Polyhedron*, **117**, 777 (2016)
166. B.Liu, H.-F.Zhou, L.Hou, J.-P.Wang, Y.-Y.Wang, Z.Zhu. *Inorg. Chem.*, **55**, 8871 (2016)
167. M.O'Keeffe, M.M.J.Treacy. *Acta Crystallogr., Sect. A*, **76**, 110 (2020)
168. Y.Liu, M.O'Keeffe, M.M.J.Treacy, O.M.Yaghi. *Chem. Soc. Rev.*, **47**, 4642 (2018)
169. Y.Liu, Y.Ma, Y.Zhao, X.Sun, F.Gandara, H.Furukawa, Z.Liu, H.Zhu, C.Zhu, K.Suenaga, P.Oleynikov, A.S.Alshammari, X.Zhang, O.Terasaki, O.M.Yaghi. *Science*, **351**, 365 (2016)
170. J.E.Mizzi, R.L.LaDuca. *Inorg. Chem. Commun.*, **70**, 4 (2016)
171. A.-L.Cheng, N.Liu, Y.-F.Yue, Y.-W.Jiang, E.-Q.Gao, C.-H.Yan, M.-Y.He. *Chem. Commun.*, 407 (2007)
172. A.-L.Cheng, Y.Ma, J.-Y.Zhang, E.-Q.Gao. *J. Chem. Soc., Dalton Trans.*, 1993 (2008)
173. G.K.Kole, A.J.Cairns, M.Eddaoudi, J.J.Vittal. *New J. Chem.*, **34**, 2392 (2010)
174. L.Liu, T.Wen, W.-Q.Fu, M.Liu, S.Chen, J.Zhang. *CrystEngComm*, **18**, 218 (2016)
175. W.Jing, Z.-G.Ren, M.Dai, Y.Chen, J.-P.Lang. *CrystEngComm*, **13**, 5111 (2011)
176. L.Zhang, W.Dou, W.Liu, C.Xu, H.Jiang, C.Chen, L.Guo, X.Tang, W.Liu. *Inorg. Chem. Commun.*, **59**, 53 (2015)
177. K.H.Park, T.H.Noh, Y.-B.Shim, O.-S.Jung. *Chem. Commun.*, **49**, 4000 (2013)
178. D.Wang, H.He, X.Chen, S.Feng, Y.Niu, D.Sun. *CrystEngComm*, **12**, 1041 (2010)
179. E.V.Alexandrov, A.V.Virovets, V.A.Blatov, E.V.Peresypkina. *Chem. Rev.*, **115**, 12286 (2015)
180. L.Öhrström, K.Larsson. *Dalton Trans.*, 347 (2004)
181. B.C.Bukowski, R.Q.Snurr. *ACS Appl. Mater. Interfaces*, **12**, 56049 (2020)
182. Y.Chen, X.Feng, X.Huang, Z.Lin, X.Pei, S.Li, J.Li, S.Wang, R.Li, B.Wang. *Chem. – Eur. J.*, **21**, 13894 (2015)
183. A.A.Lysova, D.G.Samsonenko, K.A.Kovalenko, A.S.Nizovtsev, D.N.Dybtsev, V.P.Fedin. *Angew. Chem., Int. Ed.*, **132**, 20742 (2020)
184. P.Deria, D.A.Gómez-Gualdrón, I.Hod, R.Q.Snurr, J.T.Hupp, O.K.Farha. *J. Am. Chem. Soc.*, **138**, 14449 (2016)
185. J.Wang, L.Zhou, C.Rao, G.-L.Wang, F.Jiang, A.Singh, A.Kumar, J.Liu. *Dyes Pigm.*, **190**, 109285 (2021)
186. M.O.Barsukova, K.A.Kovalenko, A.S.Nizovtsev, A.A.Sapianik, D.G.Samsonenko, D.N.Dybtsev, V.P.Fedin. *Inorg. Chem.*, **60**, 2996 (2021)
187. B.R.Saifutdinov, V.I.Isaeva, E.V.Alexandrov, L.M.Kustov. *Russ. Chem. Bull., Int. Ed.*, **64**, 1039 (2015)
188. O.A.Blatova, A.A.Golov, V.A.Blatov. *Z. Kristallogr. – Cryst. Mater.*, **234**, 421 (2019)
189. D.Bazer-Bachi, L.Assié, V.Lecocq, B.Harbuzaru, V.Falk. *Powder Technol.*, **255**, 52 (2014)
190. B.Van De Voorde, R.Ameloot, I.Stassen, M.Everaert, D.De Vos, J.C.Tan. *J. Mater. Chem. C*, **1**, 7716 (2013)
191. J.C.Tan, T.D.Bennett, A.K.Cheetham. *Proc. Natl. Acad. Sci. USA*, **107**, 9938 (2010)
192. T.D.Bennett, J.Sotelo, J.C.Tan, S.A.Moggach. *CrystEng-Comm*, **17**, 286 (2015)
193. Z.Zeng, J.C.Tan. *ACS Appl. Mater. Interfaces*, **9**, 39839 (2017)
194. D.F.Bahr, J.A.Reid, W.M.Mook, C.A.Bauer, R.Stumpf, A.J.Skulan, N.R.Moody, B.A.Simmons, M.M.Shindel, M.D.Allendorf. *Phys. Rev. B*, **76**, 1 (2007)

195. T.D.Bennett, Y.Yue, P.Li, A.Qiao, H.Tao, N.G.Greaves, T.Richards, G.I.Lampronti, S.A.T.Redfern, F.Blanc, O.K.Farha, J.T.Hupp, A.K.Cheetham, D.A.Keen. *J. Am. Chem. Soc.*, **138**, 3484 (2016)
196. J.C.Tan, C.A.Merrill, J.B.Orton, A.K.Cheetham. *Acta Mater.*, **57**, 3481 (2009)
197. M.Kosa, J.C.Tan, C.A.Merrill, M.Krack, A.K.Cheetham, M.Parrinello. *ChemPhysChem*, **11**, 2332 (2010)
198. Y.Sun, Z.Hu, D.Zhao, K.Zeng. *ACS Appl. Mater. Interfaces*, **9**, 32202 (2017)
199. S.Henke, W.Li, A.K.Cheetham. *Chem. Sci.*, **5**, 2392 (2014)
200. W.Li, A.Thirumurugan, P.T.Barton, Z.Lin, S.Henke, H.H.-M.Yeung, M.T.Wharmby, *E.G.*Bithell, C.J.Howard, A.K.Cheetham. *J. Am. Chem. Soc.*, **136**, 7801 (2014)
201. H.L.B.Boström, G.Kieslich. *J. Phys. Chem. C*, **125**, 1467 (2021)
202. Y.Yu, Q.Zeng, Y.Chen, L.Jiang, K.Wang, B.Zou. *ACS Mater. Lett.*, **2**, 519 (2020)
203. Q.Zeng, K.Wang, B.Zou. *ACS Mater. Lett.*, **2**, 291 (2020)
204. I.Beurroies, M.Boulhout, P.L.Llewellyn, B.Kuchta, G.Férey, C.Serre, R.Denoyel. *Angew. Chem., Int. Ed.*, **49**, 7526 (2010)
205. E.V.Alexandrov, A.V.Goltsev, R.A.Eremin, V.A.Blatov. *J. Phys. Chem. C*, **123**, (2019)
206. L.J.Ji, Y.Qin, D.Gui, W.Li, Y.Li, X.Li, P.Lu. *Chem. Mater.*, **30**, 8732 (2018)
207. S.Horike, D.Umeyama, S.Kitagawa. *Acc. Chem. Res.*, **46**, 2376 (2013)
208. S.L.Li, Q.Xu. *Energy Environ. Sci.*, **6**, 1656 (2013)
209. Z.Zuo, Y.Fu, A.Manthiram. *Polymers (Basel)*, **4**, 1627 (2012)
210. Z.Xu, Y.-L.Wong, R.Xiao, Y.Hou. In *Comprehensive Supramolecular Chemistry II* . (Amsterdam, Oxford, Cambridge: Elsevier, 2017). P. 399
211. R.M.P.Colodrero, P.Olivera-Pastor, E.R.Losilla, D.Hernández-Alonso, M.A.G.Aranda, L.Leon-Reina, J.Rius, K.D.Demadis, B.Moreau, D.Villemin, M.Palomino, F.Rey, A.Cabeza. *Inorg. Chem.*, **51**, 7689 (2012)
212. F.Yang, G.Xu, Y.Dou, B.Wang, H.Zhang, H.Wu, W.Zhou, J.-R.Li, B.Chen. *Nat. Energy*, **2**, 877 (2017)
213. L.Liu, Z.Yao, Y.Ye, Q.Lin, S.Chen, Z.Zhang, S.Xiang. *Cryst. Growth Des.*, **18**, 3724 (2018)
214. S.M.Elahi, S.Chand, W.-H.Deng, A.Pal, M.C.Das. *Angew. Chem., Int. Ed.*, **57**, 6662 (2018)
215. D.J.Tranchemontagne, J.L.Mendoza-Cortés, M.O Keeffe, O.M.Yaghi. *Chem. Soc. Rev.*, **38**, 1257 (2009)
216. H.Furukawa, J.Kim, N.W.Ockwig, M.O Keeffe, O.M.Yaghi. *J. Am. Chem. Soc.*, **130**, 11650 (2008)
217. M.O'Keeffe, O.M.Yaghi. *Chem. Rev.*, **112**, 675 (2012)
218. O.M.Yaghi, M.O'Keeffe, N.W.Ockwig, H.K.Chae, M.Eddaoudi, J.Kim. *Nature (London)*, **423**, 705 (2003)
219. Z.Chen, H.Jiang, M.Li, M.O Keeffe, M.Eddaoudi. *Chem. Rev.*, **120**, 8039 (2020)
220. M.O'Keeffe. *Chem. Soc. Rev.*, **38**, 1215 (2009)
221. M.J.Kalmutzki, N.Hanikel, O.M.Yaghi. *Sci. Adv.*, **4**, eaat9180 (2018)
222. O.M.Yaghi, M.J.Kalmutzki, C.S.Diercks. *Introduction to Reticular Chemistry*. (Weinheim: Wiley, 2019)
223. C.Gropp, S.Canossa, S.Wuttke, F.Gándara, Q.Li, L.Gagliardi, O.M.Yaghi. *ACS Centr. Sci.*, **6**, 1255 (2020)
224. K.E.Cordova, O.M.Yaghi. *Mater. Chem. Front.*, **1**, 1304 (2017)
225. W.Xu, B.Tu, Q.Liu, Y.Shu, C.-C.Liang, C.S.Diercks, O.M.Yaghi, Y.-B.Zhang, H.Deng, Q.Li. *Nat. Rev. Mater.*, **5**, 764 (2020)
226. H.Lyu, Z.Ji, S.Wuttke, O.M.Yaghi. *Chem.*, **6**, 2219 (2020)
227. H.Jiang, D.Alezi, M.Eddaoudi. *Nat. Rev. Mater.*, **6**, 466 (2021)
228. R.Freund, S.Canossa, S.M.Cohen, W.Yan, H.Deng, V.Guillerm, M.Eddaoudi, D.G.Madden, D.Fairen-Jimenez, H.Lyu, L.K.Macreadie, Z.Ji, Y.Zhang, B.Wang, F.Haase, C.Wöll, O.Zaremba, J.Andreo, S.Wuttke, C.S.Diercks. *Angew. Chem., Int. Ed.*, **60**, 23946 (2021)
229. D.Schwalbe-Koda, Z.Jensen, E.Olivetti, R.Gómez-Bombarelli. *Nat. Mater.*, **18**, 1177 (2019)
230. H.L.Nguyen, C.Gropp, Y.Ma, C.Zhu, O.M.Yaghi. *J. Am. Chem. Soc.*, **142**, 20335 (2020)
231. B.Zhang, H.Mao, R.Matheu, J.A.Reimer, S.A.Alshmimri, S.Alshihri, O.M.Yaghi. *J. Am. Chem. Soc.*, **141**, 11420 (2019)
232. R.-B.Lin, Y.He, P.Li, H.Wang, W.Zhou, B.Chen. *Chem. Soc. Rev.*, **48**, 1362 (2019)
233. Y.-L.Li, E.V.Alexandrov, Q.Yin, L.Li, Z.-B.Fang, W.Yuan, D.M.Proserpio, T.-F.Liu. *J. Am. Chem. Soc.*, **142**, 7218 (2020)
234. P.N.Zolotarev, M.N.Arshad, A.M.Asiri, Z.M.Al-Amshany, V.A.Blatov. *Cryst. Growth Des.*, **14**, 1938 (2014)
235. A.V.Vologzhanina, A.V.Sokolov, P.P.Purygin, P.N.Zolotarev, V.A.Blatov. *Cryst. Growth Des.*, **16**, 6354 (2016)
236. Y.Lin, X.Jiang, S.T.Kim, S.B.Alahakoon, X.Hou, Z.Zhang, C.M.Thompson, R.A.Smaldone, C.Ke. *J. Am. Chem. Soc.*, **139**, 7172 (2017)
237. R.Chakrabarty, P.S.Mukherjee, P.J.Stang. *Chem. Rev.*, **111**, 6810 (2011)
238. O.Delgado-Friedrichs, M.D.Foster, M.O Keeffe, D.M.Proserpio, M.M.J.Treacy, O.M.Yaghi. *J. Solid State Chem.*, **178**, 2533 (2005)
239. M.V.Bennett, L.G.Beauvais, M.P.Shores, J.R.Long. *J. Am. Chem. Soc.*, **123**, 8022 (2001)
240. B.Yan, H.Zhou, A.Lachgar. *Inorg. Chem.*, **42**, 8818 (2003)
241. J.Zhang, A.Lachgar. *J. Am. Chem. Soc.*, **129**, 250 (2007)
242. K.R.Dunbar, R.A.Heintz. In *Progress in Inorganic Chemistry*. Vol. 45. (New York: Wiley, 2007). P. 283
243. S.B.Artemkina, N.G.Naumov, A.V.Virovets, V.E.Fedorov. *Eur. J. Inorg. Chem.*, 142 (2005)
244. R.-Y.Li, B.-W.Wang, X.-Y.Wang, X.-T.Wang, Z.-M.Wang, S.Gao. *Inorg. Chem.*, **48**, 7174 (2009)
245. B.Saparov, D.B.Mitzi. *Chem. Rev.*, **116**, 4558 (2016)
246. M.-J.Lin, A.Jouaiti, N.Kyritsakas, M.W.Hosseini. *CrystEngComm*, **11**, 189 (2009)
247. P.V.Dau, S.M.Cohen. *Chem. Commun.*, **50**, 12154 (2014)
248. K.Oisaki, Q.Li, H.Furukawa, A.U.Czaja, O.M.Yaghi. *J. Am. Chem. Soc.*, **132**, 9262 (2010)
249. M.Eddaoudi. *Science*, **295**, 469 (2002)
250. H.Li, M.Eddaoudi, M.O'Keeffe, O.M.Yaghi. *Nature (London)*, **402**, 276 (1999)
251. S.Surblé, C.Serre, C.Mellot-Draznieks, F.Millange, G.Férey. *Chem. Commun.*, 284 (2006)
252. R.L.Martin, L.-C.Lin, K.Jariwala, B.Smit, M.Haranczyk. *J. Phys. Chem. C*, **117**, 12159 (2013)
253. O.K.Farha, A.Ö.Yazaydın, I.Eryazici, C.D.Malliakas, B.G.Hauser, M.G.Kanatzidis, S.T.Nguyen, R.Q.Snurr, J.T.Hupp. *Nat. Chem.*, **2**, 944 (2010)
254. D.A.Gomez-Gualdron, O.V.Gutov, V.Krungleviciute, B.Borah, J.E.Mondloch, J.T.Hupp, T.Yildirim, O.K.Farha, R.Q.Snurr. *Chem. Mater.*, **26**, 5632 (2014)
255. H.Furukawa, F.Gándara, Y.B.Zhang, J.Jiang, W.L.Queen, M.R.Hudson, O.M.Yaghi. *J. Am. Chem. Soc.*, **136**, 4369 (2014)
256. L.Feng, S.Yuan, J.-S.Qin, Y.Wang, A.Kirchon, D.Qiu, L.Cheng, S.T.Madrahimov, H.-C.Zhou. *Matter*, **1**, 156 (2019)
257. E.N.Zorina-Tikhonova, A.S.Chistyakov, M.A.Kiskin, A.A.Sidorov, P.V.Dorovatovskii, Y.V.Zubavichus, E.D.Voronova, I.A.Godovikov, A.A.Korlyukov, I.L.Eremenko, A.V.Vologzhanina. *IUCrJ*, **5**, 293 (2018)
258. J.J.Vittal, H.S.Quah. *Coord. Chem. Rev.*, **342**, 1 (2017)
259. M.Gupta, J.J.Vittal. *Coord. Chem. Rev.*, **435**, 213789 (2021)
260. R.F.Mendes, F.A.Almeida Paz. *Inorg. Chem. Front.*, **2**, 495 (2015)

261. W.-W.He, S.-L.Li, Y.-Q.Lan. *Inorg. Chem. Front.*, **5**, 279 (2018)
262. L.Öhrström. *ACS Centr. Sci.*, **3**, 528 (2017)
263. R.N.Devi, M.Edgar, J.Gonzalez, A.M.Z.Slawin, D.P.Tunstall, P.Grewal, P.A.Cox, P.A.Wright. *J. Phys. Chem. B*, **108**, 535 (2004)
264. D.Balestri, I.Bassanetti, S.Canossa, C.Gazzurelli, A.Bacchi, S.Bracco, A.Comotti, P.Pelagatti. *Cryst. Growth Des.*, **18**, 6824 (2018)
265. M.D.Allendorf, V.Stavila. *CrystEngComm*, **17**, 229 (2015)
266. H.Wang, X.Dong, J.Lin, S.J.Teat, S.Jensen, J.Cure, E.V.Alexandrov, Q.Xia, K.Tan, Q.Wang, D.H.Olson, D.M.Proserpio, Y.J.Chabal, T.Thonhauser, J.Sun, Y.Han, J.Li. *Nat. Commun.*, **9**, 1745 (2018)
267. O.Delgado-Friedrichs, M.O Keeffe, O.M.Yaghi. *Acta Crystallogr., Sect. A*, **62**, 350 (2006)
268. M.Li, M.O'Keeffe, D.M.Proserpio, H.-F.Zhang. *Cryst. Growth Des.*, **20**, 4062 (2020)
269. V.Guillerm, M.Eddaoudi. *Acc. Chem. Res.*, **54**, 3298 (2021)
270. D.Alezi, I.Spanopoulos, C.Tsangarakis, A.Shkurenko, K.Adil, Y.Belmabkhout, M.O'Keeffe, M.Eddaoudi, P.N.Trikalitis. *J. Am. Chem. Soc.*, **138**, 12767 (2016)
271. A.D.Volodin, A.A.Korlyukov, E.N.Zorina-Tikhonova, A.S.Chistyakov, A.A.Sidorov, I.L.Eremenko, A.V.Vologzhanina. *Chem. Commun.*, **54**, 13861 (2018)
272. J.M.Taylor, K.W.Dawson, G.K.H.Shimizu. *J. Am. Chem. Soc.*, **135**, 1193 (2013)
273. R.Li, S.-H.Wang, X.-X.Chen, J.Lu, Z.-H.Fu, Y.Li, G.Xu, F.-K.Zheng, G.-C.Guo. *Chem. Mater.*, **29**, 2321 (2017)
274. Q.Tang, Y.Liu, S.Liu, D.He, J.Miao, X.Wang, G.Yang, Z.Shi, Z.Zheng. *J. Am. Chem. Soc.*, **136**, 12444 (2014)
275. S.S.Nagarkar, S.M.Unni, A.Sharma, S.Kurungot, S.K.Ghosh. *Angew. Chem., Int. Ed.*, **53**, 2638 (2014)
276. S.Bureekaew, S.Horike, M.Higuchi, M.Mizuno, T.Kawamura, D.Tanaka, N.Yanai, S.Kitagawa. *Nat. Mater.*, **8**, 831 (2009)
277. A.Shigematsu, T.Yamada, H.Kitagawa. *J. Am. Chem. Soc.*, **133**, 2034 (2011)
278. G.K.H.Shimizu. *J. Solid State Chem.*, **178**, 2519 (2005)
279. J.A.Hurd, R.Vaidhyanathan, V.Thangadurai, C.I.Ratcliffe, I.L.Moudrakovski, G.K.H.Shimizu. *Nat. Chem.*, **1**, 705 (2009)
280. G.K.H.Shimizu, R.Vaidhyanathan, J.M.Taylor. *Chem. Soc. Rev.*, **38**, 1430 (2009)
281. W.J.Phang, H.Jo, W.R.Lee, J.H.Song, K.Yoo, B.Kim, C.S.Hong. *Angew. Chem., Int. Ed.*, **54**, 5142 (2015)
282. P.Ramaswamy, R.Matsuda, W.Kosaka, G.Akiyama, H.J.Jeon, S.Kitagawa. *Chem. Commun.*, **50**, 1144 (2014)
283. X.Zhao, C.Mao, X.Bu, P.Feng. *Chem. Mater.*, **26**, 2492 (2014)
284. S.-S.Bao, Y.-X.Wu, N.-Z.Li, L.-M.Zheng. *Eur. J. Inorg. Chem.*, 4476 (2016)
285. M.Sadakiyo, T.Yamada, H.Kitagawa. *Inorg. Chem. Commun.*, **72**, 138 (2016)
286. M.D.Allendorf, M.E.Foster, F.Léonard, V.Stavila, P.L.Feng, F.P.Doty, K.Leong, E.Y.Ma, S.R.Johnston, A.A.Talin. *J. Phys. Chem. Lett.*, **6**, 1182 (2015)
287. S.Biswas, H.S.Jena, S.Sanda, S.Konar. *Chem. – Eur. J.*, **21**, 13793 (2015)
288. A.Mallick, T.Kundu, R.Banerjee. *Chem. Commun.*, **48**, 8829 (2012)
289. M.Sadakiyo, T.Yamada, K.Honda, H.Matsui, H.Kitagawa. *J. Am. Chem. Soc.*, **136**, 7701 (2014)
290. W.J.Phang, W.R.Lee, K.Yoo, D.W.Ryu, B.Kim, C.S.Hong. *Angew. Chem., Int. Ed.*, **53**, 8383 (2014)
291. D.N.Dybtsev, V.G.Ponomareva, S.B.Aliev, A.P.Chupakhin, M.R.Gallyamov, N.K.Moroz, B.A.Kolesov, K.A.Kovalenko, E.S.Shutova, V.P.Fedin. *ACS Appl. Mater. Interfaces*, **6**, 5161 (2014)
292. V.G.Ponomareva, K.A.Kovalenko, A.P.Chupakhin, D.N.Dybtsev, E.S.Shutova, V.P.Fedin. *J. Am. Chem. Soc.*, **134**, 15640 (2012)
293. F.-M.Zhang, L.-Z.Dong, J.-S.Qin, W.Guan, J.Liu, S.-L.Li, M.Lu, Y.-Q.Lan, Z.-M.Su, H.-C.Zhou. *J. Am. Chem. Soc.*, **139**, 6183 (2017)
294. E.-L.Zhou, C.Qin, X.-L.Wang, K.-Z.Shao, Z.-M.Su. *Chem. – Eur. J.*, **21**, 13058 (2015)
295. Y.Yoshida, H.Kitagawa. *ACS Sustain. Chem. Eng.*, **7**, 70 (2019)
296. M.Inukai, S.Horike, T.Itakura, R.Shinozaki, N.Ogiwara, D.Umeyama, S.Nagarkar, Y.Nishiyama, M.Malon, A.Hayashi, T.Ohhara, R.Kiyanagi, S.Kitagawa. *J. Am. Chem. Soc.*, **138**, 8505 (2016)
297. T.Panda, T.Kundu, R.Banerjee. *Chem. Commun.*, **49**, 6197 (2013)
298. G.Zhang, H.Fei. *Chem. Commun.*, **53**, 4156 (2017)
299. S.-S.Bao, K.Otsubo, J.M.Taylor, Z.Jiang, L.-M.Zheng, H.Kitagawa. *J. Am. Chem. Soc.*, **136**, 9292 (2014)
300. S.Horike, W.Chen, T.Itakura, M.Inukai, D.Umeyama, H.Asakura, S.Kitagawa. *Chem. Commun.*, **50**, 10241 (2014)
301. T.H.N.Lo, M.V.Nguyen, T.N.Tu. *Inorg. Chem. Front.*, **4**, 1509 (2017)
302. L.Zou, S.Yao, J.Zhao, D.-S.Li, G.Li, Q.Huo, Y.Liu. *Cryst. Growth Des.*, **17**, 3556 (2017)
303. D.Umeyama, S.Horike, M.Inukai, S.Kitagawa. *J. Am. Chem. Soc.*, **135**, 11345 (2013)